

**An Investigation of Textile Sensors and Their Application in Wearable  
Electronics**

Orathai Tangsirinaruenart

Submitted for the degree of Doctor of Philosophy

Heriot-Watt University

School of Textile and Design

February 2022

The copyright in this thesis is owned by the author. Any quotation from the thesis or use of any of the information contained in it must acknowledge this thesis as the source of the quotation or information.

## ABSTRACT

Using a garment as a wearable sensing device has become a reality. New methods and techniques in the field of wearable sensors are being developed and can now be incorporated into the wearer's everyday attire. This research focuses on two types of textile based sensors – a wearable textile electrode used for ECG continuous monitoring, and a stitch sensor for monitoring body movement. These sensors were designed into a purposely engineered Smart Sports Bra (SSB) which can be regarded as a sensor itself. After a thorough investigation, two optimum textile electrodes were created; a plain electrode using cut and sew method (CSM) and a net type knitted electrode using knitting method (KM). The CSM electrode was made with conductive fabric (MedTex™ P-130) and the KM electrode was made with conductive thread (silver-plated nylon 234/34 four-ply), these materials having the lowest tested contact impedance;  $450\Omega$  and  $500\Omega$ , respectively. Both electrodes demonstrated a level of noise and baseline drift comparable with standard commercial wet-gel electrodes, which was corrected by optimising their size to 20x40 mm, holding pressure of 4 kPa (30 mmHg) and the electrode position at the 6<sup>th</sup> intercostal space on the right and left mid-clavicular, with one placed at the scapular line in the rear side (i.e. back horizontal formation) which gives clear and reliable ECG signal. These optimum electrodes were integrated directly into SSBs, in which a novel high shear, net structure, acting as a shock absorber to body movement that shows more stable electrode to skin contact by reducing the body motion artefact.

During the investigation of the stitch stretch sensor the single jersey nylon fabric (4.44 tex two-ply) with 25% spandex (7.78 tex) had the highest elastic recovery (93%). Using this fabric, the work went on to show that the stitch type 304 (Zig-zag lock stitch) using the 117/17 two-ply thread demonstrated the best results i.e., maximum working range 50%, gauge factor 1.61, hysteresis 6.25%  $\Delta R$ , linearity ( $R^2$ ) is 0.98, and good repeatability (drift in  $R^2$  is -0.00). The stitch stretch sensor was also incorporated into a sports bra SSB and positioned across the chest for respiration monitoring.

This thesis contributes to a growing body of research in wearable E-textile solutions to support health and well-being, with fully functional sensors and easy-to-use design, for continues health monitoring.

Key words: E-textiles, textile electrode, stitch sensor, Smart Sport Bra, conductive fabric, conductive thread, ECG monitoring, respiration monitoring.

## **ACKNOWLEDGEMENTS**

I would like to extend my indebtedness to the Royal Thai Government for a Ph.D. scholarship and to Rajamangala University of Technology Thanyaburi (RMUTT) Thailand for the opportunity to pursue my Ph.D.

My deep gratitude goes to my main supervisor, Professor George K Stylios, for his expertise and guidance. He encouraged me, with his expert guidance, to move forward confidently in my research work.

My sincere appreciation also goes to my colleagues and staff members of the Research Institute for Flexible Material (RIFlex), School of Textiles and Design, Heriot Watt University, UK for technical assistance and a welcoming environment.

Finally, special thanks go to my beloved husband, my dear family and also my supportive Thai colleagues at the Department of Textile, Faculty of Engineering, RMUTT Thailand.

## Research Thesis Submission

Name:	ORATHAI TANGSIRINARUENART		
School:	School of Textile and Design		
Version: <i>(i.e. First, Resubmission, Final)</i>	Final	Degree Sought:	Doctor of Philosophy

### Declaration

In accordance with the appropriate regulations I hereby submit my thesis and I declare that:

1. The thesis embodies the results of my own work and has been composed by myself
2. Where appropriate, I have made acknowledgement of the work of others
3. The thesis is the correct version for submission and is the same version as any electronic versions submitted\*.
4. My thesis for the award referred to, deposited in the Heriot-Watt University Library, should be made available for loan or photocopying and be available via the Institutional Repository, subject to such conditions as the Librarian may require
5. I understand that as a student of the University I am required to abide by the Regulations of the University and to conform to its discipline.
6. I confirm that the thesis has been verified against plagiarism via an approved plagiarism detection application e.g. Turnitin.

### ONLY for submissions including published works

7. Where the thesis contains published outputs under Regulation 6 (9.1.2) or Regulation 43 (9) these are accompanied by a critical review which accurately describes my contribution to the research and, for multi-author outputs, a signed declaration indicating the contribution of each author (complete)
8. Inclusion of published outputs under Regulation 6 (9.1.2) or Regulation 43 (9) shall not constitute plagiarism.

\* Please note that it is the responsibility of the candidate to ensure that the correct version of the thesis is submitted.

Signature of Candidate:	<i>Orathai Tangsirinaruenaert.</i>	Date:	28 February, 2022
-------------------------	------------------------------------	-------	-------------------

### Submission

Submitted By <i>(name in capitals):</i>	ORATHAI TANGSIRINARUENART
Signature of Individual Submitting:	<i>Orathai Tangsirinaruenaert.</i>
Date Submitted:	28 February, 2022

### For Completion in the Student Service Centre (SSC)

Limited Access	Requested	Yes	No	Approved	Yes	No
<i>E-thesis Submitted (mandatory for final theses)</i>						
Received in the SSC by <i>(name in capitals):</i>				Date:		

## Inclusion of Published Works

### Declaration

This thesis contains one or more multi-author published works. In accordance with Regulation 6 (9.1.2) I hereby declare that the contributions of each author to these publications is as follows:

Citation details	Xiang An, Orathai Tangsirinaruenart, and George K. Stylios. Investigating the performance of dry textile electrodes for wearable end-uses. The journal of the Textile Institute, 110(1), pp.151-158 (2019).
Author 1	Conceptualization, Methodology, Software, Validation, Formal Analysis, Investigation, Data Curation, Writing—Original Draft Preparation, Visualization
Author 2	Conceptualization, Methodology, Investigation, Validation
Author 3	Conceptualization, Resources, Writing—Review & Editing, Supervision
Signature:	<i>Orathai Tangsirinaruenart.</i>
Date:	28 February, 2022

Citation details	Tangsirinaruenart O, Stylios G. A novel textile stitch-based strain sensor for wearable end users. Materials. 12(9):1469 (2019).
Author 1	Conceptualization, Methodology, Validation, Writing—Original Draft Preparation, Visualization
Author 2	Conceptualization, writing—review and editing, supervision.
Signature:	<i>Orathai Tangsirinaruenart.</i>
Date:	28 February, 2022

Citation details	George K. Stylios, Xiang An and Orathai Tangsirinaruenart A Novel Exempt from Motion Artefact Wearable Vest for Continuous Well-being Monitoring, International Conference on the Challenges, Opportunities, Innovations and Applications in Electronic Textiles. 3-4 November 2020, E Textiles, Online, <a href="https://e-textiles-conference.com/e-textiles-2020-speakers-2/">https://e-textiles-conference.com/e-textiles-2020-speakers-2/</a>
Author 1	Conceptualization, Methodology, Resources, Writing, Supervision, Oral Delivery
Author 2	Methodology, Investigation, Software, Validation
Author 3	Methodology, Investigation, Validation
Signature:	<i>Orathai Tangsirinaruenart.</i>
Date:	28 February, 2022

# TABLE OF CONTENTS

<b>TABLE OF CONTENTS</b> .....	i
<b>LISTS OF TABLES</b> .....	iv
<b>LISTS OF FIGURES</b> .....	v
<b>LIST OF PUBLICATIONS BY THE CANDIDATE</b> .....	ix
Chapter 1 – Introduction .....	1
1.1 Background .....	1
1.2 Objectives of the research .....	10
1.3 Research focus.....	10
1.4 Thesis organisation.....	12
Chapter 2 – Literature Review .....	14
2.1 E-Textiles; Materials and Manufacturing.....	14
2.2 Wearable Textile -Based Biosensors.....	16
2.3 Biopotential electrodes .....	19
2.3.1 Gel Based Electrodes .....	21
2.3.2 Textile Dry Electrodes .....	22
2.4 Structure and impedance of human skin .....	24
2.5 The electrode-skin interface .....	25
2.6 The Electrocardiography (ECG) Measurement.....	26
2.7 Development of Wearable Integrated Electrodes-based Bio-signal monitoring	
28	
2.8 Wearable textile-based stretch sensors.....	31
2.9 Essential and desirable properties of stretch sensors.....	34
Chapter 3 – Introduction and Evaluation of the Properties of Conductive Textile	
Materials.....	37
3.1 Conductive Thread .....	38
3.2 Conductive Fabric .....	41
3.3 Skin-impedance of textile electrodes .....	42
3.3.1 Electrode Fabric used.....	42
3.3.2 Electrode structure .....	43
3.3.3 Electrode Fabrication.....	43
3.3.4 Experimental procedure.....	46
3.3.5 Results and discussion .....	49

3.4	Electrical signal transmission of textile electrodes .....	50
3.4.1	Materials selection .....	50
3.4.2	Experimental procedure .....	51
3.4.3	Results and discussion .....	52
3.5	Summary of the Results and Conclusions .....	56
Chapter 4 – Investigation, Analysis, Development and Optimisation of Textile-Based Dry Electrodes.....		58
4.1	The Influence of the Skin-electrode Impedance.....	58
4.1.1	The effect of electrode position on the skin-electrode impedance .....	60
4.1.2	The effect of electrode holding pressure on the skin-electrode impedance..	63
4.2	Investigation of textile electrodes for ECG measurement.....	66
4.2.1	ECG Electrode mounting design and electrodes placement consideration ..	66
4.2.2	Investigation of ECG Electrode Size .....	67
4.2.3	Investigation of ECG Electrode placement .....	70
4.3	Summary of the Results and Conclusions .....	74
Chapter 5 – Investigation of A Stitch-Based Stretch Sensor .....		75
5.1	Part I: Fabric-substrate based sensor .....	77
5.1.1	Materials .....	78
5.1.2	Experimental procedure .....	79
5.1.3	Experimental Results .....	80
5.2	Phrase II: Stitch Sensor Construction.....	82
5.2.1	Garment stitch structures .....	82
5.2.2	Materials .....	84
5.2.3	Experimental sample.....	85
5.2.4	Experimental procedure .....	86
5.2.5	Data Analysis Procedure.....	87
5.2.6	Experimental Results .....	90
5.3	Summary of the Results and Conclusions .....	98
Chapter 6 – Sensor Integration in a Wearable Sport Bra for Well Being Monitoring....		99
6.1	Wearable Requirement and Electronic Garment Concept .....	100
6.2	Designing of the wearable Sport Bra .....	100
6.3	Designing a Smart Sport bra with Electrodes .....	101
6.3.1	Electrode design.....	101
6.3.2	Smart Sport Bra Design .....	106
6.3.3	Garment production .....	108

6.4	Evaluation of SSBs using real ECG measurement.....	110
6.4.1	Experimental procedure.....	111
6.4.2	Experimental results .....	112
6.5	Integration of stitch stretch sensor for respiration monitoring .....	115
6.5.1	Respiration measurement.....	115
6.5.2	Respiration sensor mounting and design .....	116
6.6	Summary of the Results and Conclusions .....	119
Chapter 7 – Summary and Conclusion .....		121
7.1	Further work. ....	126
REFERENCES.....		127
Appendix A - The specification sheet of the electrode design.....		135
Appendix B - Additional Results for the effect of electrode size on the skin-electrode impedance. ....		136
Appendix C - The details of the two formations of the belt electrode.....		140
Appendix D - The computerised flat-bed knitting machine; Shima Seiki SWG091, N2 15 gauge. ....		141
Appendix E - Garment Prototypes and design development of SSBs. ....		142
Appendix F - The description and information of the SSBs.....		143
Appendix G - Garment production of SSBs. ....		148



## LISTS OF TABLES

Table 2.1 - The characteristics for textile sensors.....	35
Table 3.1- Specification of conductive threads.....	39
Table 3.2 - Properties of conductive threads.....	39
Table 3.3 - The properties of conductive fabric.....	42
Table 3.4 - Comparison between the sinusoidal and rectangular reference and measured signals.....	53
Table 3.5 - The reference signals relative to the measured signals transmissible through the thin metal plate at 10Hz, 100Hz and 1kHz frequency. ....	54
Table 3.6 - The reference signals relative to the measured signals transmissible through gel at 10Hz, 100Hz and 1kHz frequency. ....	55
Table 4.1- Standard electrode placement for 12-lead ECGs (SCST, 2022).....	66
Table 4.2 - Experimental textile electrode size.....	68
Table 4.3 - The ECG readings from the two formations of lead placement .....	73
Table 5.1 - The experimental single jerseys fabrics specification .....	78
Table 5.2 - The experimental stitch structure for sensor design. ....	85
Table 5.3 - Close-up photographs of one sample of each stitch type, relaxed and stretched. ....	91
Table 5.4 - Tabulated data from percentage resistance change vs. strain of the assembly from graph averages. Stitch two-ply uses 117/17 33 tex thread and four-ply uses 234/34 92 tex.....	93
Table 5.5 - Change in gauge factor from 2 <sup>nd</sup> to 99 <sup>th</sup> cycles. Calculated across the entire extension. ....	97
Table 5.6 - Change in relaxed percentage resistance change and R <sup>2</sup> values from 2 <sup>nd</sup> to 99 <sup>th</sup> cycles. Calculated across entire extension. ....	97
Table 6.1- Sear properties of Net and Plain fabric structures .....	106
Table 6.2 - Specifications of the experimental single jersey fabrics.....	108

## LISTS OF FIGURES

Figure 1.1 - ICD+ jacket produced by Philips [5].....	2
Figure 1.2 - Photograph of the prototype smart shirt [6]. .....	3
Figure 1.3 - The Bristol Cyber Jacket [7]. .....	3
Figure 1.4 - Koyono Black Coat Jackets with a washable textile keypad from Eleksen. .	4
Figure 1.5 - Image of the business suit made by Philips [9] the image on the right shows the embroidered keypad located under the flap on the cuff. ....	5
Figure 1.6 - NYX clothing .....	6
Figure 1.7 - The T-Qualizer and battery holder .....	6
Figure 1.8 - Moodwear [20]. ....	7
Figure 1.9 - The prototype of the BabyTex underwear [22]. ....	8
Figure 1.10 - Respiratory monitoring based on piezoresistive sensing, developed by a) Molinaro [23], b) Di Toccowe [24]. .....	9
Figure 2.1- Different kinds of textile/fabric manufacturing and treatment. (a) embroidery; (b) sewing; (c) weaving; (d) non-woven; (e) knitting; (f) spinning; (g) breeding; (h) coating/laminating; (i) printing and (j) chemical treatment [2]. ....	16
Figure 2.2 - Textile based sensors; chemical sensors and physical sensors [45]. ....	17
Figure 2.3 - Various types of body-surface biopotential electrodes. (a) Metal-disk electrode used for application to limbs. (b) A metallic suction electrode. (c) The recessed electrode with a cup structure. (d) A flexible thin-film neonatal electrode (e) 3D printed EEG electrode, and (f) Disposable ECG foam-pad electrodes.....	20
Figure 2.4 - Typical internal electrodes, hypodermic EMG Needle Electrode.....	21
Figure 2.5 - Structure of gel-based electrode. ....	22
Figure 2.6 - The skin structure. ....	24
Figure 2.7 - The electrode-skin interface model. Left: the electrical model of wet electrodes. Right: The electrical model of dry electrodes. ....	26
Figure 2.8 - The ECG measurement using 12 different perspectives records. ....	27
Figure 2.9 - Standard electrocardiogram representation of normal ECG [74]. ....	28
Figure 2.10 - LifeShirt® [ [75, 76]. .....	29
Figure 2.11- Bio-sensor of Wearable Healthcare System [ [76]. ....	29
Figure 2.12 - Adidas miCoach™ [76]. ....	30
Figure 2.13 - Device for Monitoring the Flexion Angle of Elbow and Knee.....	32
Figure 2.14 - Strain Sensor for Lower Limb Joint Position.....	32

Figure 3.1 - Conductive threads: Silver plated nylon 117/1/ two-ply (left) and Silver plated nylon 235/34 four-ply (right). .....	38
Figure 3.2 - SEM image of Silver plated nylon conductive thread: (a) 117/17 two-ply and (b) 234/34 four-ply. ....	39
Figure 3.3 - Resistance against extension in different type of silver plated nylon conductive thread: (a) 117/17 two-ply and (b) 234/34 four-ply. ....	40
Figure 3.4 - Sewing thread tensile performance during 5 cycles. (a) 117/17 two-ply; (b) 234/34 four-ply. ....	40
Figure 3.5 - Computerised flat-bed knitting machine, Shima Seiki SES 122-S 12 gauge. ....	43
Figure 3.6 - The experimental textile electrode, Top and Cross-sectional View.....	43
Figure 3.7 - The assembling materials used for the experimental electrode.....	45
Figure 3.8 - LCR Bridge meter. ....	46
Figure 3.9 - Five pairs of experimental fabric electrode types, 1 is MedTex™ P-130, 2 is Spacer knitted, 3 is Plain 1x1 woven, 4 is silver plated nylon 117/17 two-ply, and 5 is silver plated nylon 234/34 four-ply.....	47
Figure 3.10 - The experimental sample of skin dummy and a pair of electrodes. ....	48
Figure 3.11- Skin dummy test set up. ....	48
Figure 3.12 - The average skin-electrode impedance on skin dummy at 100Hz against time.....	49
Figure 3.13 - Signal generation and measurement: a signal generator (left) and an oscilloscope (right).....	51
Figure 3.14 - Electrical characteristic measurement schematic diagrams of (a) conductive electrode fabric, (b) Gel electrode. ....	52
Figure 4.1- Electrical equivalent circuit of skin [110]. ....	59
Figure 4.2 - Skin-electrode contact surface (side view).....	60
Figure 4.3 - Electrode positions on subject's forearm and assembled electrodes, front and back side. ....	61
Figure 4.4 - Skin-electrode impedance at six different electrode positions on the subject's forearm. (a) Gel electrodes. (b) Dry textile electrodes. ....	62
Figure 4.5 - The electrode holding pressure measurement setup.....	64
Figure 4.6 - The variation of skin-electrode impedance on electrode holding pressure, (a) Gel Electrodes, (b) Dry Textile Electrodes.....	65
Figure 4.7 - Standard ECG chest electrode position (SCST, 2022).....	66
Figure 4.8 - Experimental set up of ECG measurement. ....	69

Figure 4.9 - ECG signals recorded under different electrodes. (a) Small textile electrode. (b) Medium textile electrode. (c) Large dry textile electrode. (d) Commercial gel electrode.....	70
Figure 4.10 - ECG lead placements: (a) A, front horizontal formation; (b) B, back horizontal formation.....	71
Figure 4.11- The low energy wireless ECG device. ....	71
Figure 4.12 - ECG measurement processed with belt attached electrodes. ....	72
Figure 5.1 - Tensile testing set up. ....	79
Figure 5.2 - The residual extension of fabric sample after the load is removed. ....	80
Figure 5.3 - Elastic recovery values of six various nylon/spandex sample fabrics in course-wise and wale-wise direction. ....	81
Figure 5.4 - Stitch formation by interlacing of zigzag (BS 3870-1). ....	82
Figure 5.5 - Multi thread stitch; (a) Stitch type 401; (b) Stitch type 404; and (c) Stitch type 406 (BS 3870-1). ....	83
Figure 5.6 - Overlock stitch; (a) stitch type 505; (b) Stitch type 506 (BS 3870-1). ....	83
Figure 5.7 - Covering chain stitch; (a) Stitch type 602; (b) Stitch type 605 and (c) Stitch type 607 (BS 3870-1). ....	84
Figure 5.8 - Experimental setup. ....	86
Figure 5.9 - Example of resistance vs time plot. ....	88
Figure 5.10 - Example of ensemble average over 10 cycles. ....	89
Figure 5.11 - Example repeatability graph. ....	90
Figure 5.12 - Graphs of percentage resistance change vs. strain, assembly averages over the 2 <sup>nd</sup> to 11 <sup>th</sup> cycles. (a) Legend for all graphs; (b) 304: two-ply; (c) 406: two-ply; (d) 406: four-ply; (e) 506: two-ply; (f) 506: four-ply; (g) 605: two-ply; and (h) 605: four-ply. Note the different vertical axis scales. two-ply is thread 117/17, 33 tex and four-ply is thread 234/34, 92 tex. ....	92
Figure 5.13 - Conductive thread deformation ....	94
Figure 5.14 - Graphs of percentage resistance change vs. strain, for the 2 <sup>nd</sup> and 99 <sup>th</sup> cycles. (a) Legend for all graphs; (b) 304: two-ply; (c) 406: two-ply; (d) 406: four-ply; (e) 506: two-ply; (f) 506: four-ply; (g) 605: two-ply; and (h) 605: four-ply. Note the different vertical axis scales. two-ply is thread 117/17, 33 tex and four-ply is thread 234/34, 92 tex. ....	96
Figure 6.1 - Sport bras designs. (a) compression (b) encapsulation, (c) combination. .	101
Figure 6.2 - The Electrode manufactured using CSM with conductive knitted fabric. .	102
Figure 6.3 - The electrode manufactured using KM with conductive thread. ....	102

Figure 6.4 - Two types of knitted electrode designs, (a) plain knitted electrode and ...	103
Figure 6.5 - Shear measurement, (a) KES shear instrument (b) shear experimental set up.....	103
Figure 6.6 - Baseline drift of the electrode with (a) net structure, (b) plain structure. .	104
Figure 6.7 - The shear of the net structure fabric, indicating low shear rigidity G and good Hysteresis HG. ....	105
Figure 6.8 - The shear of the plain structure fabric, indicating higher shear rigidity G than the net structure fabric.....	105
Figure 6.9 - Garment information design for ECG measurement.....	106
Figure 6.10 - Electrode's interconnections in zigzag formation line of SSBs. ....	107
Figure 6.11 - CSM-SSB, (a) outer front. (b) inside front and back. ....	109
Figure 6.12 - Net structure design on the knitted sport bra.....	109
Figure 6.13 - KM-SSB. (a) outer front. (b) inside front and back. ....	110
Figure 6.14 -The ECG system and measurement.....	111
Figure 6.15 - The ECG measurement activities (a) sit position, (b) walk and (c) Arm movement.....	111
Figure 6.16 - ECG recorded from Cut & Sew SSB in the position of, (a) Sitting, (b) Walking, (c) Arm moving position. ....	112
Figure 6.17 - ECG recorded from knitted SSB in the position of, (a) sitting, (b) walking, (c) arm moving position. ....	113
Figure 6.18 - ECG recorded from commercial electrode in the position of, (a) sitting, (b) walking and, (c) arm moving. ....	114
Figure 6.19 - Abdominal circumference changes of respiration: a) inhalation and b) exhalation phase [121]. ....	116
Figure 6.20 - Design feature of SSB for respiration monitoring.....	117
Figure 6.21- Fabrication of stitch stretch sensor for respiration monitoring. ....	118
Figure 6.22 - A typical respiration signal at rest.....	119

## LIST OF PUBLICATIONS BY THE CANDIDATE

### Papers

1. An, X., Tangsirinaruenart, O. and Stylios, G.K. 2018. Investigating the Performance of Dry Textile Electrodes for wearable End-Uses. *The Journal of the Textile Institute*, 110(1), 151-158.
2. Tangsirinaruenart, O., Stylios, G.K. 2019. A novel textile stitch-based strain sensor for wearable end users. *Materials*. 12(9):1469.
3. Stylios, G.K., An, X., and Tangsirinaruenart, O. 2020. ETextiles 2020, A Novel Exempt from Motion Artefact Wearable Vest for Continuous Well-being Monitoring, International Conference on the Challenges, Opportunities, Innovations and Applications in Electronic Textiles, 3-4 November 2020, E Textiles, Online, <https://e-textilesconference.com/e-textiles-2020>
4. Tangsirinaruenart, O. and Stylios, G.K. A novel dry electrode based bra vest for continuous ECG monitoring. Submitted to Sensors,

# Chapter 1 – Introduction

## 1.1 Background

Wearable Electronic-textiles (E-textile) are textile materials that become sensors, actuators themselves and enable unobtrusive integration with small electronic devices, thus offering to users wearable computing potential and continuous monitoring of their wellbeing with good functionality and comfort. It is increasingly expected that the textile itself will be an electronic element, such as a connection or a sensor itself, and hence supporting the idea of wearable computing. Wearable E-textiles are able to carry out multiple functions in response to environmental stimuli [1] such as measuring and monitoring temperature, force, chemical reactions, radiation, magnetic and electric fields and fulfil many varied requirements [2] such as; detecting injury, protection, health monitoring, and entertainment.

Wearable technology has a huge global market. As well as the demand from the medical sector in monitoring patient's well-being and the elder, population, there is also a very large market in the sports and leisure world where people want to monitor their own vital data signals. The growing popularity of the Internet of Things (IoT) along with a technology capable population are driving the demands of this industry, the market size of which is valued at US \$32.63 billion (2019) and estimated to expand with an annual growth of around 15% until 2027; (Report ID: 978-1-68038-165-8)

E-textiles are considered as the preferred material choice for breaking new boundaries and extending the limitations of wearable applications because of their diverse properties, comfort and ease of use. Hence developments have been progressing rapidly in order to obtain a modern and convenient form of communication and interconnection technology allowing sensors to be networked together within a textile, such as garments capable of various functions, for example light-emitting, heat radiating, flexible active display screens, interactive colour change and sensitivity or in vital body monitoring such as ECG, respiration, blood pressure, movement and skin temperature.

The development of wearable e-textiles first began with studying smart textiles [3, 4]. Before 2000s, there were numerous attempts and prototypes for the integration of electronics into garments which inclined towards simply using clothing to accommodate portable devices such as in a Phillips-Levi collaboration [5]. The said product; ICD+ jacket is a combination of a mobile phone and MP3 player connected to a jacket with

special pockets to carry the electronics as shown in Figure 1.1. Electronics in the jacket are voice-activated by a microphone located in the collar and are actually separate from the jacket - in which case the garment only serves as the device holder. The mobile phone and MP3 player are connected with wires running standalone through the jacket's seams, so the jacket just carries the electronics, and the two parts are separate.

Another example of electro-textile electronic circuitry was a wearable motherboard [6] invented by Sundaresan Jayaraman, called the Smart Shirt and shown in Figure 1.2. The shirt was formed by a mix of natural fibers, thin wires, and optical fibers. The optical fibers are used to detect bullet wounds and vital signs via special sensors interconnected to monitors. The shirt could also be attached to headphones, an MP3 player, and a blood pressure monitor. The weight of electronics hanging from the shirt made it impractical to wear, and the garment part and the electronics part are separate, making this shirt heavy and cumbersome.

Figure 1.3 shows the Cyber Jacket which was developed by Randell [7]. Based on a heavy duty leisure jacket produced by Hein Gericke, which has a GPS, accelerometers, and an electronic compass all served via its internal networking computer. The jacket comes with user voice recognition and audio playback. The displays can be hand-held, mounted or worn on the sleeve, as required. This was a better attempt but again based on separation between the electronics and the garment.



Figure 1.1 - ICD+ jacket produced by Philips [5].



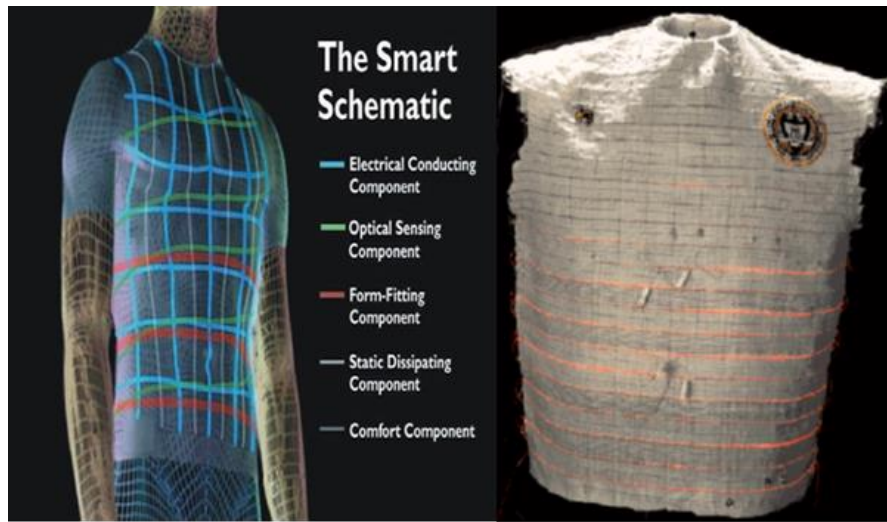


Figure 1.2 - Photograph of the prototype smart shirt [6].

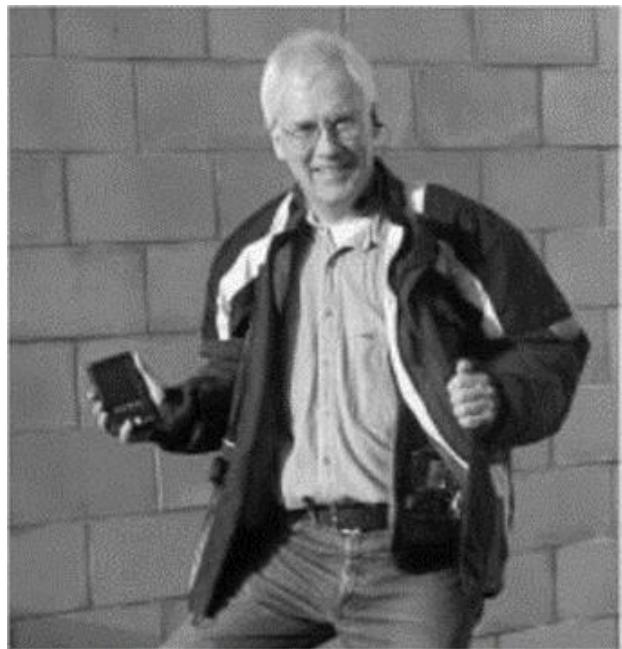


Figure 1.3 - The Bristol Cyber Jacket [7].

The partnership between Koyono and Eleksen made an experimental Black Coat MFI, in which they have integrated iPod technology using five-button textile keypads being part of the coat designed by Jay Foo, as shown in Figure 1.4. The new fabric controls of these coats allowed full functionality of an iPod without the need for removal from the coat except for the purpose of laundry or maintenance. This design shows the start of integration and the need of ubiquitous wearables. This method of integration, although primitive, was popular in the early developmental stages of smart textiles.



Figure 1.4 - Koyono Black Coat Jackets with a washable textile keypad from Eleksen.  
(<https://www.koyono.com/pages/blackcoat> 31/07/17).

The above-mentioned smart clothes were still limited to only having pockets for hiding the wires and cable connections to the actual devices, where consideration for fashion and design was abandoned in favour of the need to accommodate electronic devices.

In the 2000s, smart textiles were developed into more wearable and fashionable garments due to technological advancement, multidisciplinary approaches and the adoption of wide user-centered designs. These textiles were constructed with conductive materials which allowed them to form electrical connections, be lighter-weight, easier to wear, and being more comfortable. Wireless circuitry in those textiles were made possible with the development of conductive thread, yarn, inks, and coatings, as well as optical and metallic fibres and yarns. Therefore, the appeal of this technology increased, the number of projects and products soared, and the textile and clothing designers and companies began to develop fashionable smart textiles and garments [8]. Research and development into electro-textiles continued by Philips and their New Nomads project [9] producing a business suit, shown in Figure 1.5, which exceeded the Levi's ICD+project effort in terms of technology/garment integration. The Nomads suit contains everything a business person would require throughout their working day. Electronic items such as a mobile phone are miniaturised and are clipped onto the jacket. Under a folded flap as shown in Figure 1.5, on the cuff, they embroidered a functional keypad using conductive thread, where the idea of full integration with conductive textiles, good design, comfort and functionality became a common requirement.

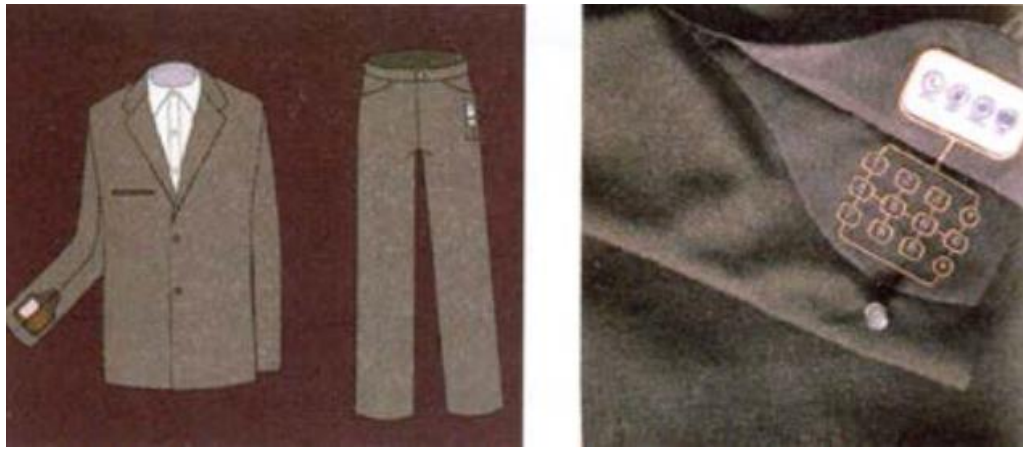


Figure 1.5 - Image of the business suit made by Philips [9] the image on the right shows the embroidered keypad located under the flap on the cuff.

At the same time, several European Commission funded projects started to be developed, focussing mostly on wearable devices for medical purposes. These projects were using smart textiles for monitoring vital body signals with embedded sensors and textile-based actuators. Some representative projects are Wealthy [10], My Heart [11], Ofseth [12], and Proetex [13] with some of them having some success in developing garments with specific health monitoring capabilities, such as ECG monitoring vests [14]. Despite some success, again there were difficulties in integration, particularly having reliable connection, between the textile with the electronic device parts. Respiratory monitoring and piezoresistive motion detection also became possible with these garments [14-17], and silicone patches containing sweat monitoring sensors were also mounted on textile fabrics with some success [18].

With the concept of using an optical fibre screen on garments [19], NYX clothing company has introduced a wide variety of customised jackets which incorporated flexible display screens that are capable of connecting with OS PDA or smart phones as shown in Figure 1.6. Later, NYX offered prototypes of their illuminated jacket, which had a microphone installed, activating a sound-to-light capability. This will respond to any voice sound or music. NYX has never commercialised this device despite promoting this idea for two years.



Figure 1.6 - NYX clothing

(<http://crunchwear.com/nyx-display-jacket/31/07/17>).



Figure 1.7 - The T-Qualizer and battery holder

([http://infosthetics.com/archives/2006/07/t-qualizer\\_equalizer\\_tshirt.html](http://infosthetics.com/archives/2006/07/t-qualizer_equalizer_tshirt.html) 31/07/17)

Figure 1.7 shows the T-Qualizer, a T-shirt based on the display of a graphic equalizer. With its sound receptor, the light on the shirt is activated on each frequency according to music beats just like a normal equalizer. The shirt does not use LEDs but it uses instead ultra-thin electroluminescent technology installed on the chest area to display a live equalizer, powered by 4 AAA batteries housed in a small battery holder located in the hem of the shirt. The display, although interesting, is not a textile fabric but a very thin vinyl-like material sewn into the shirt front, so again separation of the two materials still exists.

In 2012, Stylios and Yang [20] created a novel highly designed smart wearable garment described as ‘an emotional interactive garment with energy harvesting capability’. The design is for both men and women and it has named “Moodwear” (shown in Figure 1.8). In this research, electro-luminescent fibre optics are located in the undergarment whilst the coat has flexible and removable photovoltaic pannels that make part of the garment design aesthetic. A miniature microphone detects the user’s voice characteristics; tone, amplitude and rhythm which are analysed in a mini electronic device that they developed which works out the mood state of the user according to a psychometric chart comparison. Then the color of the garment changes by using LEDs to illuminate the fibre optic bundle ends of the garment. Bespoke electronics were carefully embedded during the garment’s construction in an unobstrusive manner making them undetectable. Therefore, “Moodwear” can immediately react to the user’s emotions by, for instance, detecting a low mood, and changing the garment colour to one that give a happy feeling such as blue or green. Another interesting feature of this research is that all energy was harvested from UV light by a series of flexible photovoltaic strips carefully blended around the collars of both men and woman’s coat garments so that they become part of its design. These solar cells are attached using snaps/poppers so they could easily be taken off and attached to a pouch to also charge a mobile phone, promoting modularity and interchangeability. These garments were of high design aesthetics, ubiquitous and surreptitious and was probably the first time that the technology was integrated with culture design in its outset.



Figure 1.8 - Moodwear [20].

Selex- Galileo/ES of Finmeccanica SA is one of the largest defense and security manufacturers in the world. They are known for their radars, their combat systems but not for anything to do with wearable vests for combat theatre use. Stylios [21] of Heriot Watt University developed a vest for the well-being of UK Army soldiers during combat. This was the first multi-sensor garment incorporating GPS, temperature, respiration, ECG and movement in a knitted wearable vest and which was tested at the MoD ranges in Colchester. The integration of these sensors in a vest was a breakthrough realising the importance of size, weight and low energy. Several prototype vests incorporating this technology were produced and deployed. Although integration between textiles and electronics was one of the priorities of this project, there were parts that needed conventional connection and some sensors/ICs had not been developed yet as small as desired.

Jakubas et al. [22] developed BabyTex underwear to monitor vital functions of infants, as shown in Figure 1.9. The prototype was made in the form of knitwear integrated with temperature, humidity and respiratory rhythm sensors, by using a smartphone. In the case of babies, the comfort level and freedom of movement should be given extra consideration. The selection and placement of the sensors in the underwear should not limit the baby's movements or cause abrasions or burns. The system must be safe to use and have a sufficiently long period of operation between charges. The microcontroller however was obstrusive to the baby's movement questioning its practical use.

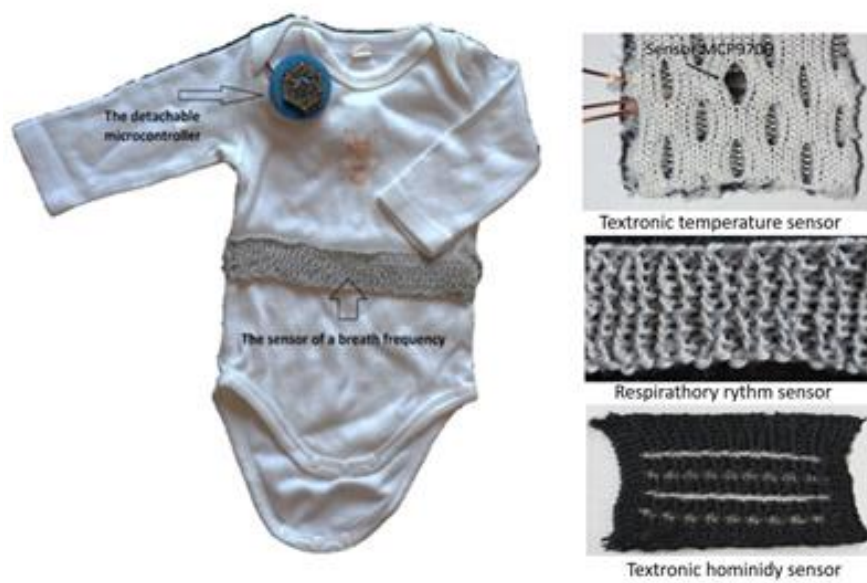


Figure 1.9 - The prototype of the BabyTex underwear [22].

Wearable systems are also becoming widely accepted for monitoring physiological parameters in many medical applications. Molinaro et al. [23] developed a smart textile for respiratory sensing based on piezoresistive elements which were stitched onto a textile and connected to one of the branches of a Wheatstone bridge circuit. The proposed system was used by placing the sensor on the torso of the body (Figure 1.10a). Similarly, in 2020, Di Toccowe et al. [24] proposed the use of two elastic bands for monitoring respiration (Figure 1.10b) using multiple cables connected to a custom designed electronic board, where bluetooth and a mobile app allow real-time monitoring of respiratory activity displayed on a smartphone. It can be noted that this system is a belt-mounted sensor and not integrated into an e-textile garment. The repeatability of sensor positioning is not as reliable as in a system that is fully integrated into a garment. This is not only because of the initial challenge of positioning the belt in the same place each time it is used, but also because the belt is prone to change position during exercising and running.



Figure 1.10 - Respiratory monitoring based on piezoresistive sensing, developed by a) Molinaro [23], b) Di Toccowe [24].

Even though E-textiles are being developed for practical applications, the products from this technology have not yet reached the maturity necessary for mass marketing, and are yet to reach full potential and end user acceptance. This restricts the benefits of E-textiles and wearable devices. The problem is the need of interdisciplinarity of textile technology,

microelectronics and garment design. There are various attempts by companies and large research groups internationally to develop this area. In the UK, this aim is realised by an EPSRC funded network called the E-Textiles network which brings all interested parties to work together [25] and reach the desired potential of this field. The research reported in this thesis and the Research Institute for Flexible Materials (RIFleX) being a founding member of the E Textiles Network, is trying to help this effort.

There is a need of developing e-textiles which when coupled with the development of wireless electronics with low energy consumption can become much more effective, functional, comfortable and easier to make and wear. Textile sensors and connections between devices are on top of the priorities of current international research efforts, so that truly wearable electronic garments can become commercially viable. Therefore the aim of this research project is to assist this effort by investigating and developing textile sensors such as textile electrodes and stretch sensors, that would be capable of being garments on their own right or part of garments, and hence add new knowledge to E-Textile devices and help in their end uses.

## **1.2 Objectives of the research**

1. To establish the requirements for and the benefits of new textile sensors.
2. To investigate and evaluate different conductive threads and fabrics to determine the optimum material for developing dry electrodes and stretch sensors.
3. To establish a dry electrode capable of replacing wet gel-type commercial electrodes, for continuous ECG wearable monitoring.
4. To study, develop, and evaluate different threads and stitch formations for establishing an optimum stretch sensor.
5. To process the development of a garment in which the E-textile sensors are part of the garment, promoting full integration for optimum performance and continuous end user monitoring.

## **1.3 Research focus**

This research is at the interface between textile and garment technology and wearable electronics. The study looks at two important sensors, a dry textile electrode and a textile stretch sensor, with the former for use in ECGs and the latter for monitoring movement. Hence investigations into development, measurement and optimisation of sewing threads, stitches and fabrics are being reported for the realisation and efficacy of those sensors,



and after establishing sensor performance they are finally incorporated into an optimum garment bra design SSB that shows their end use.

For the textile electrode, there were several investigations on five types of fabric before making prototypes for experimentation. The experiments were carried out by using dry electrodes, without chemical gels, and comparing their performance with wet gel commercial electrodes. The five fabric-based electrodes are made from two types of material. Three of them are made from conductive fabric coated in silver and two are made by knitting a fabric using a silver-plated conductive thread. Various electrode characteristics such as fabric construction, electrode size, position and holding pressure were evaluated in terms of stability and electrode impedance. All electrode measurements were performed on human skin as well as using a simulated skin dummy.

For the stretch sensor, preliminary studies indicated the importance of use of stitching and hence evaluation was carried out on four different stitch formations. These stitch structures were performed by sewing, using a silver-plated nylon conductive thread, which is also studied for efficacy. Knitted fabric substrates have also been investigated to determine the optimum elastic behaviour of the formed stitch. The results of these tests revealed the optimum stitch design and thread size for use as a movement sensor, which was later applied for respiration monitoring.

An integrated garment SSB with ECG and respiration (stretch monitoring) was then created using an optimum design process as described further, in which certain design attributes of the garment could support the functionality of sensor monitoring; such as ensuring reliable electrode and sensor body positioning while avoiding sensor movement even during exercise. All connections were made by conductive thread, so they were all part of the garment itself, for minimising disruption between garment parts. The electrode in the SSB maintains good contact with the skin, and the integration of the stretch sensor into the SSB for respiration was easy to carry out and was reliable.

## **1.4 Thesis organisation**

This thesis is organised in seven chapters as follows:

Chapter 1: This chapter introduces the general background of wearable E-textile technology. It includes research objectives; research focus of this study and an overview of the thesis organisation.

Chapter 2: This chapter is the critical review of literature on wearable e-textiles for health monitoring and textile-based wearable sensors. Background information and critique are provided to give context and understanding of this research.

Chapter 3: This chapter studies the conductive performance of textiles focusing on the development of a dry textile electrode for continuous ECG monitoring in a wearable garment. The characteristics and specifications of conductive thread and fabric were evaluated. The electrodes were created, and impedance properties were measured, the skin-electrode interface was studied, and further experiments were made by devising a skin dummy model. The optimum properties of conductive textile materials have been used to further create the design of the stretch sensor and ECG electrode.

Chapter 4: This chapter further describes the methodology and results of the research work carried out on fabric electrodes. The electrodes were investigated in various forms such as electrode size, position and pressure. All electrode measurements were performed on the human skin and body in this chapter. The electrodes were also fully implemented in a commercial ECG wearable system to show its efficacy and the test results are described and analysed.

Chapter 5: This chapter describes the methodology and results of the research work carried out on stretch sensors. The fabric substrate-based sensor is produced and tested first. Different garment stitch formations were then created, and the characteristics of the sensor, were investigated. The sensors were fabricated using conductive thread and sewn on the knitted fabric substrate. The electrical characteristics of the stitch-thread assembly was evaluated by measuring the changes of its variable electrical resistance under dynamic conditions.

Chapter 6: This chapter covers the design of an optimum SSB and the optimising/maintaining of the performance of textile sensor by virtue of its garment design. The sewing methods and knitting techniques for integration are discussed for minimising the effect of body movement and improving electrode holding pressure. The

stretch sensor was placed in the lower front part of the SSB for ease of being capable of monitoring respiration. Thus the garment prototype with sensor capability is presented in this chapter.

Chapter 7 : The general conclusion of this work and a future research discussion are presented in this chapter.

## Chapter 2 – Literature Review

The last few decades have witnessed the development of E-textiles undergoing a number of improvements in new features and functions responding to the ever-increasing demands of the marketplace. As already discussed in the introduction, the advantage of using E-textiles is in the comfort, appearance and ease of wear of textiles coupling with their good connectivity, functionality and compatibility with electronic devices. Of particular interest is the promising high-performance monitoring of wearable E-textiles in which sensors are integrated into fabrics and garments for the detection of vital signs of various well-being and health conditions; body motion, temperature, breathing, heart, blood oxygen, etc. Hence, these sensors are capable of measuring and monitoring at the same time the well-being, safety and protection of the wearer.

There are a number of research studies on the use of textile sensors fabricated from various materials, e.g., conductive yarns [26], thread [27], conductive fabrics and silicone [22, 28], for a variety of wearable applications. Investigations are being carried out with textile sensors for medical applications, such as the measurement of an electrocardiogram (ECG) [29, 30], electromyography (EMG) [29], respiration [31, 32], body temperature [33], global positioning system (GPS) antenna [34] and gyroscope [35, 36]. Despite those efforts sensor fidelity, their interconnection and full unobtrusive integration in a garment are still areas of considerable concern and hence these are the areas that are being addressed in this thesis.

### 2.1 E-Textiles; Materials and Manufacturing

E-textiles are involved with the integration of electronics and textiles, and the development of sensors made out of textiles themselves. Many regard this area as the next generation of smart textile devices which are made from fibres, yarns, fabrics and coatings as well as polymers, inks, metals and microelectronic circuits. A recent IDTechEx's [37] survey shows that the most widely developed E-textile materials for wearable applications are conductive threads, yarns, fabrics, and inks.

Conductive polymers are a key material to create an e-textile: metallic or hybrid coated polymers, which can be fine diameter metal fibres combined with primary threads or yarns, which have the flexibility required for textile production, ease and comfort of wearing. Conductive yarns are of great interest in the design of clothing-based

electronics, as the soft textile interfaces can easily be incorporated into clothing, allowing electrical connectivity and sensing. Piezoelectric fibers can generate an electric potential when they are stretched. Synthetic compounds such as polypropylene (PP) and polyethylene terephthalate (PT) have shown a good results compared with natural fibers. These fibers and materials have been proven to be the most useful in the development of wearable sensors and have been used in applications such as respiratory rate measurement, muscle movement, wrist posture and racket grip monitoring. The advancement of E- textiles has also made textiles smarter as they can perceive changes in environmental conditions or external stimuli. A comprehensive review of this area has been conducted by Ismar et al. [38].

Smart textiles have sensing and reacting functions [39]. For several years, researchers have dedicated their work to the development of responsive textile materials which can respond in a defined manner when exposed to chemical, electrical, mechanical, magnetic, heat, and light based stimuli. E-textile components have been manufactured using various techniques [2] as shown in Figure 2.1. Conductive fabrics can be produced by conductive coating or by conductive yarns. To that end, garments can be made from conductive yarns, conductive fabrics, and during the textile manufacturing process electronics can be integrated into the yarn segment by weaving [40], knitting [32, 41], braiding, or by attaching electronics onto the surface of textiles by sewing [42, 43] embroidery [44], or printing [31] and laminating techniques.

The E-textile base development roadmap for achieving wearable technologies can be classified into three generations [2]. The first generation is electronics applied directly onto the textile surface or attaching a sensor onto clothing. The second generation has added further functionality by embedding of sensors into the textile structure using conductive yarns to create a sensor switch or actuator. The third generation, which is still under development is progressing to a higher step of integrated wearables in which the garment is the sensor acting directly onto the body of the wearer, and hence the scope of E-Textiles is expanding to more diverse applications. There are now many examples of innovation associated in this field. This work deals with the third generation of E-textiles.

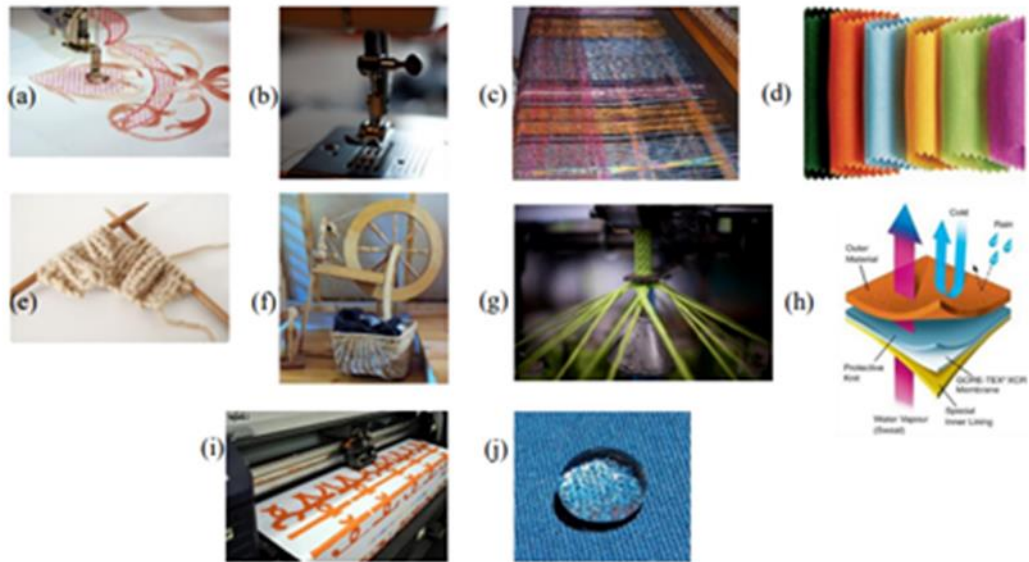


Figure 2.1- Different kinds of textile/fabric manufacturing and treatment. (a) embroidery; (b) sewing; (c) weaving; (d) non-woven; (e) knitting; (f) spinning; (g) braiding; (h) coating/laminating; (i) printing and (j) chemical treatment [2].

The large scale production of E-textiles remains difficult, with industrial engineering issues such as fabrication and the connection between flexible and inflexible conductive materials not yet having been fully addressed. This research goes some way in solving these issues and hence bringing the technology closer to being available to a wider public.

## 2.2 Wearable Textile -Based Biosensors

E-Textiles have been shown to be an optimum material for the construction of wearable biosensors, capable of detecting physical signals (i.e. body movements, vital signs, stretching and temperature) and chemical signals (i.e. biological fluids such as sweat) produced by the human body [45]. The integration of electrical devices into conventional garments for the purpose of monitoring vital bio-signals, transforms that ordinary garment into a smart garment. Some examples of E-textile based sensors such as a belt, glove, bandages, and vests, can be seen in Figure 2.2.

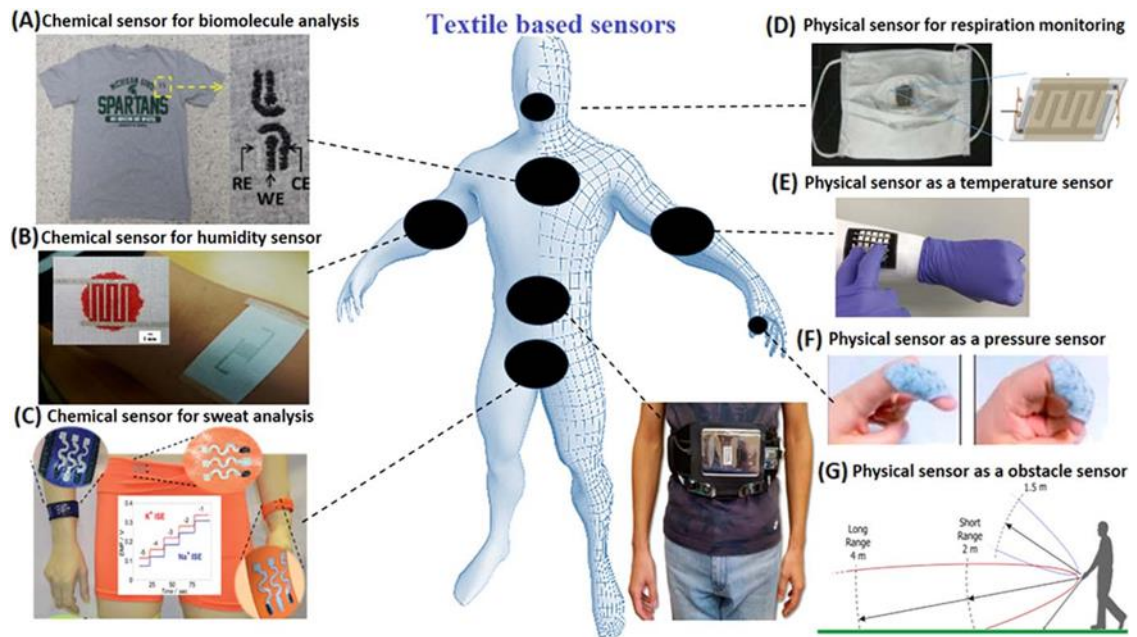


Figure 2.2 - Textile based sensors; chemical sensors and physical sensors [45].

These sensors are used for monitoring human activity, for example body temperature, which is one of the common measurements particularly useful for identifying physiological conditions and well-being [46]. Boano et al. [47] demonstrated a wireless body temperature monitoring system that can be worn for a long period of time. Measurement of the heart rate is a well-established method of monitoring this main organ that plays a crucial role in health, wellbeing and sport activities. This signal provides information about the physiological state of the heart, identifying changes in the cardiac cycle. Respiration rate is an essential physiological parameter in patient observation. It detects symptoms of respiratory ailments such as asthma and sleep apnea. Respiration rates can be measured by identifying the expansion and contraction of the ribcage by means of fabric strain or pressure using sensors [48, 49].

Skin perspiration is not a clinical parameter, rather it is a physiological signal used to analyse the reaction of humans in various situations. Skin sweat is widely used in sports to monitor physiological signs of the sportsperson. Flexible textile-based sensors are having an advantage because of a large, constant contact with the skin. Zhao et al. [50] proposed a sweat biosensor based on carbon-based conductive yarn and used for the detection of lactate and sodium in perspiration during exercises. The sweat biosensor is integrated into the headband and can monitor human sweat wirelessly. Two drawbacks to this design are that the integrated connector uses an electronic cable and the biosensor patch assembly moved and vibrated during the entire testing process.

Blood pressure is an important cardiopulmonary parameter, indicating the pressure applied by blood on the walls of blood vessels. Blood pressure provides indirect information on blood flow when the heart contracts (systole) and relaxes (diastole). Wu et al. [51] designed a cuff-based blood pressure monitoring system by sewing conductive fabric into the arm of a sitting chairs and connected to the circuit board by shielded wire. The subject was asked to sit on the chair so that the blood pressure could be measured. It can be seen that a major disadvantage to this system is it's immobility. The patient is always required to go to the measuring device rather than taking the measuring device to the patient.

ECG is used for people with chronic heart problems. The ECG signal is used in the diagnosis of cardiac illnesses and provides a useful information of the heartbeat regulation. The analysis of the ECG waveform patterns (named P, Q, R, S, T, U), plays a major role in the diagnose of cardiovascular diseases. Ag/AgCl electrodes (gel electrodes) are commonly used in ECG. However, during longer periods of signal acquisition, the gel dries, resulting in a reduction of the contact between the electrode and the skin. As textile electrodes do not use any gel, this problem does not exist with their use.

In the field of medical rehabilitation, human body movement or kinetic analysis is also widely used to examine and assess human rest and routine daily activities. This helps to assess movement and gives an aid to improving exercise technique, maximising recovery in patients. Body-worn wearable sensors play an important role in monitoring physiological parameters due to the connection between the sensor and the body [52]. A huge benefit to the end user of wearable sensor technology is the elimination of the necessity of carrying external monitoring equipment.

With the increasing number of sensory systems and applications, there is a need for more studies on the integration of these sensors with an interactive communication network which is nowadays wireless and of low energy (Sensors, actuators, computers and power sources) [53]. In addition to functionality and ease of fabrication, it is important to take into consideration the user mobility, comfort, aesthetics and the cost of the proposed wearable sensor garment.



### 2.3 Biopotential electrodes

In order for the electrode potentials and current in the body to be measured and recorded, it is important to provide an interface between the electronic measuring apparatus and the body. Biopotential electrodes are used to perform this interface function which can be classified into three types: dry, wet, and non-contact electrodes. Numerous forms of electrodes have undergone development for different types of biomedical measurements [54] as illustrated in Figure 2.3. Conventionally, the metal-plate electrode is used for body-surface biopotential sensing electrodes. It is made of a metallic conductor with electrolyte gel covering the surface and is attached to the body with a tape or rubber strap as illustrated in Figure 2.3 (a). The electrode is made of nickel brass (nickel-silver alloy). A terminal is positioned on its outer surface at one end and is used to attach the lead wire to the electrocardiograph.

Suction electrodes, floating electrodes, and flexible electrodes are illustrated in Figure 2.3(b), (c), and (d). Each electrode type has its own method of achieving stability and so reducing motion artefacts. However, these types of electrode can only be used for a short period of time due to skin irritation caused by the pressure and suction of the contact surface against the skin. Textile electrodes do not cause skin irritation as they do not need any gel or pressure because they are part of the garment.

In addition, dry electrodes with 3D-printed fingers as shown in Figure 2.3 (e) are also used to make a good contact with the skin. Even though this technology has certain advantages, as they do not require gel and skin preparation, the mechanical stability of the interface between the skin and the electrode is inadequate to prevent motion artefact in monitoring during body movement. Figure 2.3(f) presents a disposable electrode with electrolyte-impregnated sponge or a silver-silver chloride interface. This is the most widely used body-surface electrode. Before placing these electrodes, the patient's skin should be thoroughly cleaned and dried. There are many commercial variations of these electrodes available, each offered in a range of sizes.

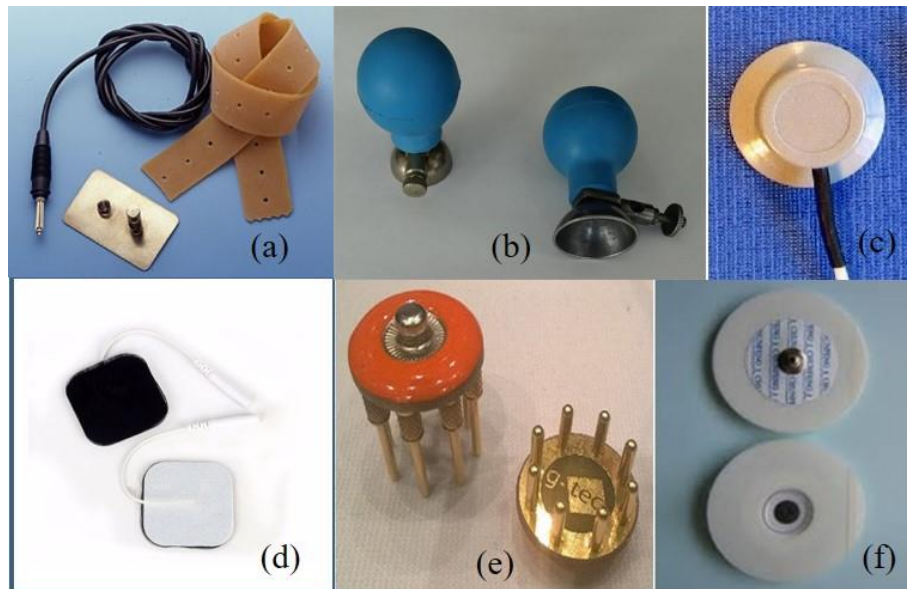


Figure 2.3 - Various types of body-surface biopotential electrodes. (a) Metal-disk electrode used for application to limbs. (b) A metallic suction electrode. (c) The recessed electrode with a cup structure. (d) A flexible thin-film neonatal electrode (e) 3D printed EEG electrode, and (f) Disposable ECG foam-pad electrodes.

Unlike body surface electrodes, there are electrodes which are fully internal with an implanted electronic circuit, in the form of a needle and fine-wire connected to hypodermic needles as illustrated in Figure 2.4. These internal electrodes differ from typical body-surface electrodes in that they are invasive. The needle creates a hole in the skin, required for insertion and the electrode wire is fed inside. In addition, the needle electrode has a lower impedance compared to the surface electrode due to being in direct contact with the sub-dermal tissue. The needle electrodes consist of fine insulated wires placed in such a way that their tips are in contact with the skin, which reduces the interface and noise (artifacts), caused due to electrode movement during the measurement of EEG, EMG etc. There are further reviews giving more detail on hypodermic electrodes [54, 55].



Figure 2.4 - Typical internal electrodes, hypodermic EMG Needle Electrode.

(<https://www.technomed.nl/product/disposable-hypodermic-emg-needle-electrodes>  
06/06/2021)

Electrode properties play a crucial role in determining the types of materials and apparatus to be used for biopotential monitoring. There has been an increasing use of pre-gelled, disposable electrodes with self-adhesive properties. These types of electrode can be readily placed on the patient's skin and disposed of after use. As a result, the amount of time associated with the use of these electrodes is minimised. Nonetheless, there are certain limitations associated with them, as explained in section 2.3.1

### **2.3.1 Gel Based Electrodes**

Silver-silver chloride (Ag/AgCl) electrodes are usually used for electrical biopotential and non-invasive physiological measurements. Changes in electrical charges naturally present in skin have been found to be the main cause of motion artefact, according to studies on gel electrodes [56, 57]. Body cells act like salt water transmitting the current to the skin surface. A hydrogel is used to improve the electrical properties of the interface between the skin and the electrode, as well as aiding attachment of the electrode to the skin surface. The hydrogel decreases electrode impedance to facilitate better charge transfer.

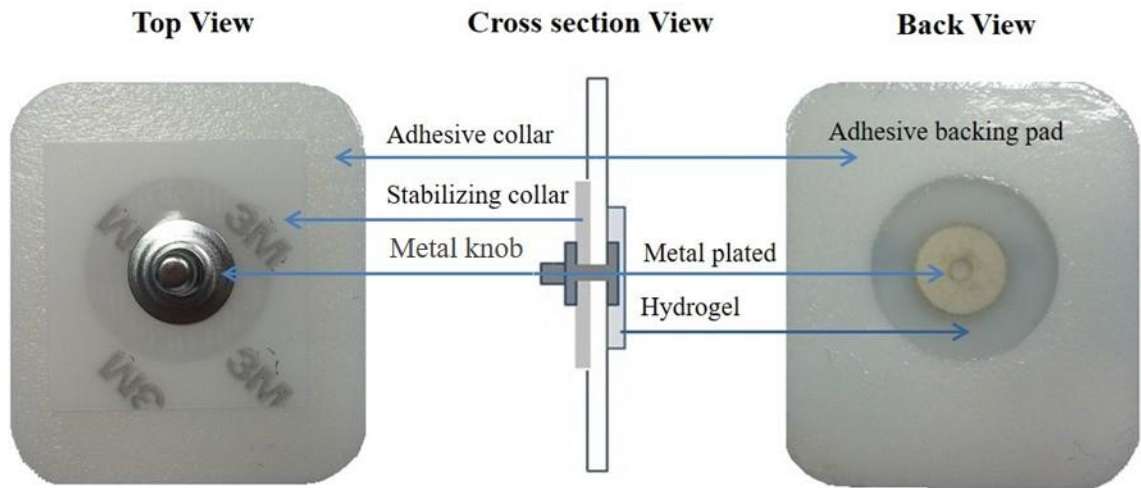


Figure 2.5 - Structure of gel-based electrode.

Figure 2.5 illustrates standard gel-based electrodes. At the top there is a metal knob attached to the cable. It pierces through the other layers to the bottom, where it is embedded in a conductive media, often a hydrogel or a gel. In between, there is a layer of paper or plastic disc serving as a stabiliser and an adhesive collar fastened to the skin.

Despite their popularity and ease of use, gel-based electrodes can induce skin irritation and also lead to potential measurement error during long-term cardiac monitoring, due to the drying of gel which cannot last longer in standard conditions [58]. This is also experienced during our investigation as we will report later in the thesis. Thus, the disadvantages of gel-based electrodes are that they can only be used for a short period of time and for one-time usage only. Due to these limitations, this study has attempted to seek alternatives in order to develop electrodes that would meet the requirements of long-term monitoring for wearable end uses.

### 2.3.2 Textile Dry Electrodes

Different types of textile electrodes have been developed to cope with a variety of biopotential measurement requirements. Various fabrication processes have been examined and much effort has been made to enhance their performance. Overall, gel-less or “dry” electrodes are known to have comparable or better than gel-based performance. In general any contact electrode, is reliant on the charge flow between the conductive electrode and the skin, emitted when there is a direct physical contact, and it can be intensified by sweat and moisture. The difficulty of positioning and setting electrodes on

the skin and the motion artefacts remains a problem for the further development of dry textile electrodes. A comprehensive overview of this matter has been made by Xu et al. [59].

A standard for wet electrodes “Disposable ECG Electrodes - ANSI/AAMI EC12:2000/(R) 2010” has been approved by the American National Standard Institute (ANSI). The test methods and performance requirements for disposable ECG electrodes are described within the standard. However, there is no standard yet for dry electrodes such as an electro-conductive textile electrode testing.

Measuring the biopotential using electrodes has been studied since 1903 [60], when the string galvanometer for ECG recording was first created. The advancement of ECG recording techniques enables many types of electrodes to be designed for meeting various requirements. In 1997, a textile-based electrode was originally introduced for ECG monitoring by Ishijima [61]. He used a bed sheet made of electrically conductive yarns, which acts as electrodes to monitor the subject’s ECG while sleeping. Since then, a number of researchers have been studying numerous textile electrode types.

Various unique features of textile electrodes depend upon the type and structure of materials used. Different investigations have been carried out on the properties of electro-conductive textile electrodes such as biocompatibility, skin-electrode impedance, skin response [62, 63], detectability of ECG waves [64], and signal-to-noise ratio [65]. In comparison to disposable wet Ag/AgCl electrodes, textile dry electrodes are more flexible and breathable. There has been some research suggesting that dry conductive electrodes display a better performance in long-term end use [66]. It has also been reported that they have good performance in terms of EMG or ECG signal measurements, even after being repeatedly washed [59, 67]. Having said that textile electrodes still suffer limitations as they are unable to hold gel or fluid, and are required to be used for repeated and continuous monitoring. This is a crucial factor that obstructs the circulation of electron ions around the skin-electrode interface, which has an influence on the electrode impedance and electrode polarization. In this work, we have set out to investigate solutions to the questions of electrode impedance, electrode size, holding pressure and electrode position of textile electrodes to achieve optimum stability without the need for using any gel. During this research, signal noise and common mode noise have also been investigated. The optimisation of the textile electrode investigated had to be capable of continuous cardiac monitoring.

Moreover, the absence of conductive gel means that the skin-electrode impedance of textile electrodes is much higher and more unstable than in wet electrodes. This is especially true when the skin is with no moisture or when the user makes sudden movements [68]. This can result in signal noise, which is a result of the transformation of the common-mode noise existing in the monitoring system, due to displacement currents between electrodes and the human body [69].

## 2.4 Structure and impedance of human skin

There are a number of important factors on which the impedance value depends upon. These factors are the current path, the duration of current flow, temperature, skin hydration level and stratum corneum thickness. In order to obtain the bio-signal by an electrode, the current must pass through the human skin and body electrolyte to arrive at the electrode. Hence, the conductivity of the skin is crucial for this procedure since the impedance of body electrolyte is significantly lower than the skin.

The skin is a multipart structure, composing of three main layers as shown in Figure 2.6. The epidermis and the dermis vary in terms of thickness on different body regions. The outer layer of the epidermis, called stratum corneum, plays a key role in the electrode-skin interface and determines the impedance of the skin at low frequencies.

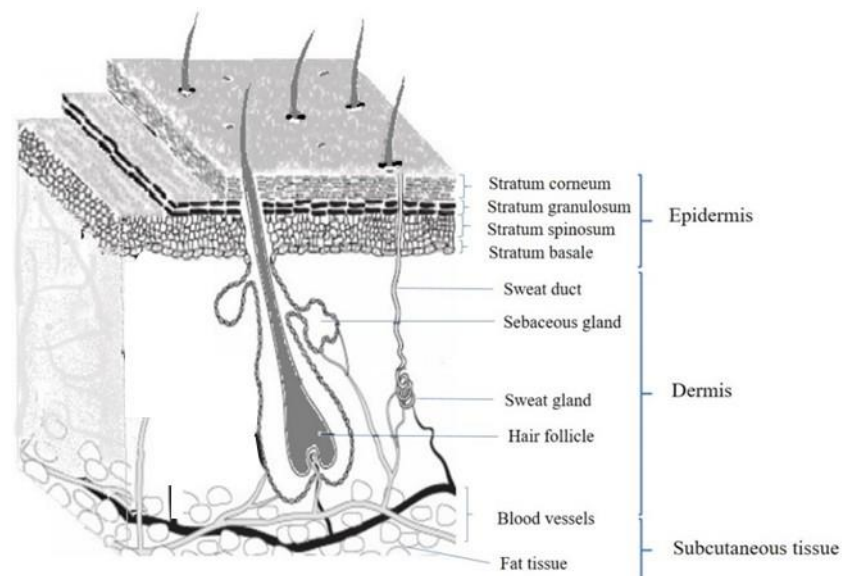


Figure 2.6 - The skin structure.

The thickness of stratum corneum may range from 0.01 mm to 0.04 mm. It can be considered as a solid-state electrolyte as it is a substance in solid-state, not necessarily containing liquid water, but its moisture content depends upon the humidity of the surrounding air. The impedance decreases as the hydration increases [70], therefore a wet gel electrode is often applied before conducting an ECG test in the hospital in order to raise the hydration level.

The study has shown that skin cleaning is not necessarily required for textile electrodes. The measurements conducted on dry skin usually lead to unwanted noise caused in most cases, by the high impedance of the skin [57, 58]. For example, muscle contractions and respiration effects cause a change in the electrode potential, however; the electrode-skin interface can be challenging to examine, as the primary source of the impedance disparity is the skin properties which vary among individuals [59]. In this study, to eliminate errors caused by the variation in skin properties among individuals, a skin dummy model was devised and used as a test rig.

## **2.5 The electrode-skin interface**

Dry and gel-based electrodes are subject to motion artefact, and noise interference at different levels. The origins of the motion artifact are explained by Talhouet and Webster [71]. They described that the effect of skin deformation causes an alteration in the current pathways, in addition to the skin stretching, resulting in variation in its electrical properties. However, the effect of impedance changes on motion artifact is smaller than the changes in epidermis potential [56].

A typical electrode-skin interface is illustrated in Figure 2.7. The gel-based electrode, portrayed on the left, is in contact with a gel which present as a conductor between the electrode and the skin. The gel electrode is very stable against vertical and lateral changes and so body motion does not have much impact on the electrode-skin interface. For dry electrodes, as shown in the model on the right, occasional air bubbles between the electrode and the skin can be detected and the galvanic connection is mainly realised only through the sweat and humidity on the skin. The presence or absence of sweat, in this case, makes a huge difference. In addition, the contact area may alter considerably with pressure and applied motion, and thus have an impact on the electrical properties of the electrode-skin interface [72]. Dry electrodes are greatly affected by motion artifacts. However, the time taken for perspiration to fill the skin-electrode gap is short, and

consequently less noise is detected from dry electrodes immediately after the onset of skin moisture compared to the wet electrodes [73]. Wet electrodes have the distinct disadvantage in that they can only be used for short periods of time and the wearer is required to stay still and not moving at all during measurement.

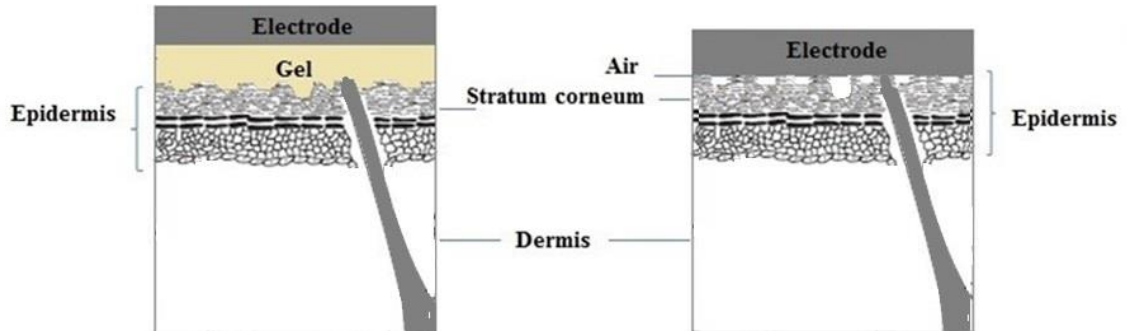


Figure 2.7 - The electrode-skin interface model. Left: the electrical model of wet electrodes. Right: The electrical model of dry electrodes.

## 2.6 The Electrocardiography (ECG) Measurement

Electrocardiography (ECG) is a widely-accepted medical technique used to monitor the electrical activity of the heart and to analyse heart conditions. Conventionally, an electrocardiogram uses electrodes placed on the skin, usually around the limb and chest areas, to monitor the biopotential differences on the body. There are various electrode positioning systems which can be represented by the number of leads, for example, 3-lead, 5-lead, or 12-lead ECGs. 3-and 5-lead ECGs are usually monitored simultaneously and are displayed on the monitoring device screen. Figure 2.8 shows a test consisting of 10 electrodes connected to record 12 different perspectives of the heart's electrical activity. The electrode wires are connected to display the image through an external device.



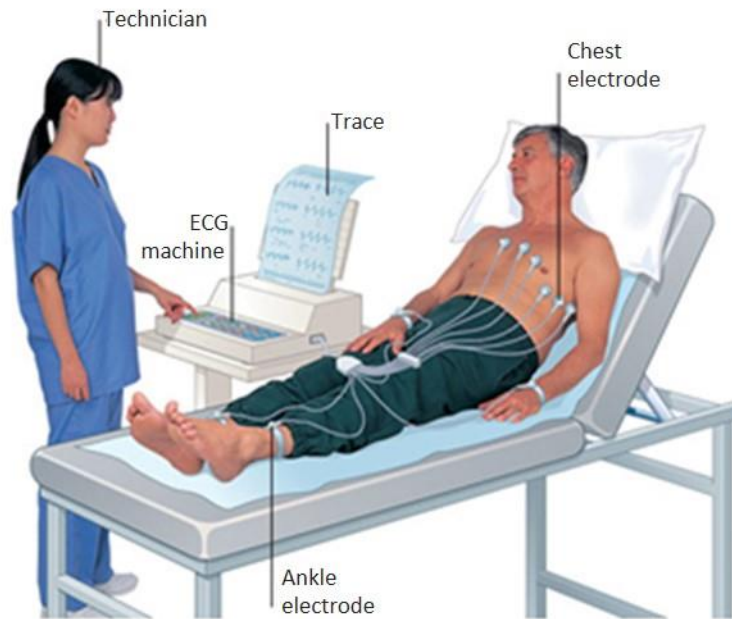


Figure 2.8 - The ECG measurement using 12 different perspectives records.

(<https://www.medicalequipment-msl.com/htm/medical-equipment-news/ECG-Machine-Fault-and-six-solutions.html> 06/06/2021)

The conventional ECG often refers to a system consisting of multiple sensors and many wires connecting the electrodes with the measuring devices. These wires will greatly limit patient movement and increase the level of discomfort. Therefore, monitoring devices using wearable technology have received widespread attention in the healthcare field. This is an additional driving factor for studying textile electrodes.

### ***ECG Signal Characterisations***

The ECG signal consists of a series of waves whose morphology and timing provide information necessary for diagnosing diseases. The wave formation is determined by the heart's electrical activity, so any disturbances in that electrical output show clearly as irregular wave patterns. The 'typical' or 'normal' ECG signal contains a common wave pattern and can be classified into four main sections. Figure 2.9 illustrates a normal ECG tracing of the cardiac cycle consisting of a P wave, a QRS complex, a T wave, and a U wave. However, the U wave typically goes unrecognisable in most ECGs as it is masked by the T wave and an upcoming new P wave.

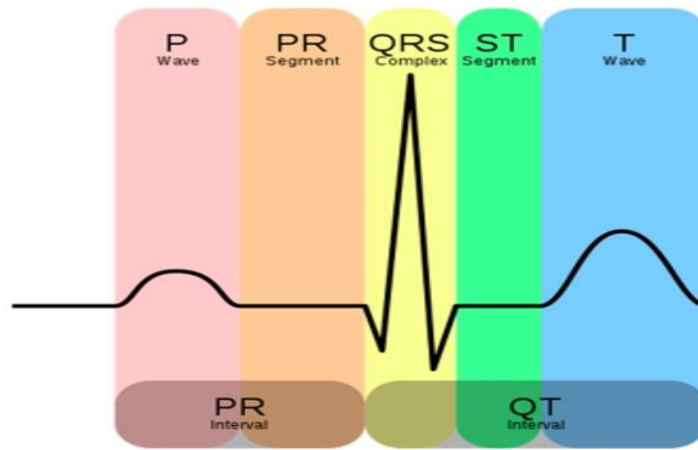


Figure 2.9 - Standard electrocardiogram representation of normal ECG [74].

## 2.7 Development of Wearable Integrated Electrodes-based Bio-signal monitoring

With regard to enhancing quality of life, it can be said that wearable technology is a great new innovation, in that it has the ability to benefit both individuals and society in many applications and markets. New products are encouraging self-responsibility, helping people to take more care of themselves and their own health, especially with an increasing elderly population. The wearable capability as a sensor device that can collect user data, offers users a virtual assurance and assistance to help them make better decisions for achieving their goals.

Body monitoring is an excellent and exciting direct application of wearable technologies. New wearable devices are aimed to enhance the functionality of garments, apparels, and accessories such as belts, bracelets, arm and head bands. Smart sensors within garments offer the best option for the collection of physiological data from the wearer, especially for long term monitoring.

In the case of specific health monitoring on garments, LifeShirt® [75] from VivoMetrics Incorporation is one example of such wearable health-monitoring systems based on a vest, which includes ECG sensors in the garment, as well as an analytic software and hand-held device operated with a PC. In this system standard, ECG electrodes were threaded into gaps in the material to come into contact with the wearer's skin. The effort is good, however, no matter how well integrated, the sensors remain separate from the garment and are reliant on cables and wires to achieve connectivity with the recording device as shown in Figure 2.10.

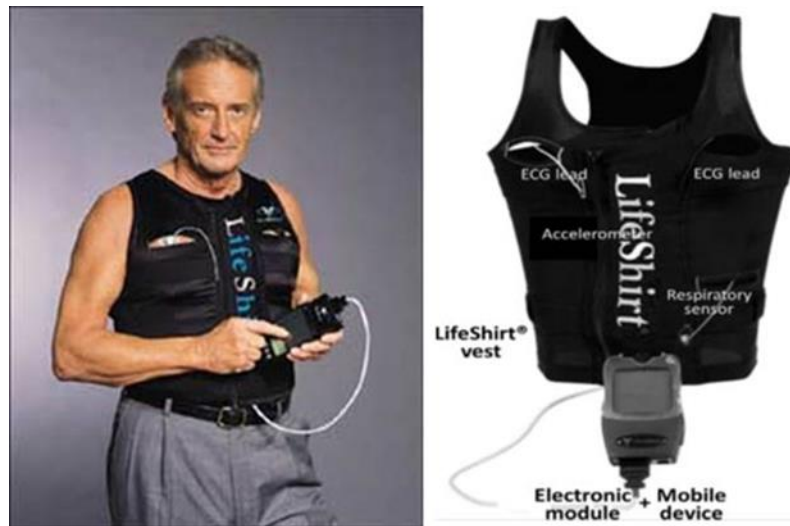


Figure 2.10 - LifeShirt® [ [75, 76].

The use of biosensors incorporated into the textile itself has greatly increased user convenience. The Wearable Healthcare System [76] is a garment that contains ECG electrodes and has an electronic device for data collection and software for data analysis. The ECG electrodes are created by winding two very fine stainless-steel wires around the yarn. The data from the electrodes is sent to a small device concealed within the garment itself. A hydrogel membrane allows the ECG electrodes to achieve better contact with the wearer's skin as shown in Figure 2.11. As mention earlier, some users find the application of hydrogel inconvenient, uncomfortable and the device can look untidy.

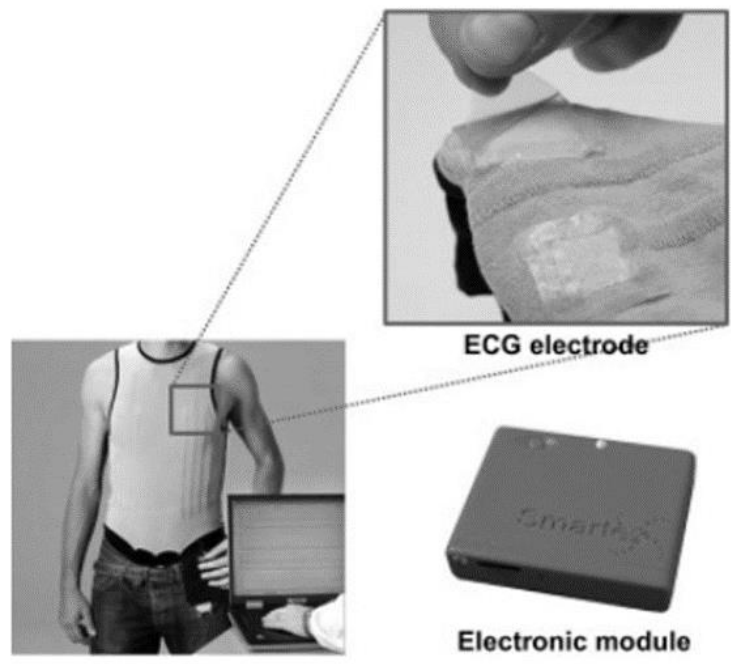


Figure 2.11- Bio-sensor of Wearable Healthcare System [ [76].

With consideration to flexibility and comfort, there is a mixture of permanent and removable sensors/electronics as in the miCoach sport bras produced by Adidas-Textronics (NuMetrex) as shown in Figure 2.12. The bra has user pulse sensing capability by knitting conductive fibres onto the textile itself. However, the chest belt, with its attached electrodes, is not compatible with standard ECG leads. In order for the collected data to be transmitted to a receiver – such as a smartphone, a cardio monitor or a sports watch – an Electronic Module has to be attached onto the bra front. In this case the module is not small or light enough to be considered unobtrusive (37mm x 65mm / 19g), compared to the module used in this study, which is designed with user convenience in mind (30mm x 37mm / 9g). However, while the NuMetrex device is showing relevant advancements, it still has limitations. It is only able to monitor the heart rate and is not able to transfer information relating to ECG measurement.



Figure 2.12 - Adidas miCoach™ [76].

It may be noted that many efforts have been made to maintain and enhance the performance and function of these smart garments. The given examples in this literature highlight design and material issues towards achieving efficient SMART textiles for continuous monitoring physiological data from the wearer. In this effort textile and garment integration has been poor. Some E-textiles are not fully integrated with or are only part of the garment. For example, the research by Arquilla [42] shows good results with their textile based electrodes. However, without full integration in the garment it is difficult to achieve consistent positioning.

To enhance the experience of wearing a properly integrated smart textile garment with excellent monitoring capabilities, a new design of sensor coupled with a suitable garment design are required.

## **2.8 Wearable textile-based stretch sensors**

Besides the importance of heart condition, body movement, acceleration and sensor position, and respiration are also important for health and well-being. A comfortable, simple and low-cost wearable sensor is an important requirement of this field. The development of textile-based sensors has been presented in numerous research projects [40, 77, 78]. In many approaches, strain sensing is more practical using textile sensors. It can allow custom-made sensors to be designed for specific applications and for different parts of the human body. Sensing techniques can be achieved by using different conductive materials and textile structures.

Several studies have been conducted to show the practicality and wearability of a textile sensor as a sensor device. It can be used to detect the user's large body movement of joint bending [79], or small movements such as breathing [80]. Garment integrated conductive elastomers have been presented by many researchers as sensors with the real capability to recognise and detect postures, gestures, and movement. Shyr [40] developed the gesture sensing device to monitor the flexion angle during elbow and knee movements. A stainless steel yarn was used as the electrode connected with the elastic conductive webbing. The non-elastic webbing was connected with an elastic conductive webbing in order to pull the elastic conductive webbing during the flexion-recovery movement. The elastic conductive webbing has a good linear relationship between flexion angle and resistance during the flexion-recovery cycles within 30% strain. However, the gesture bands are bulky and can be prone to slipping. The instability and bulkiness of this device does not lend itself to being convenient or reliable as a monitor for all-day wearing as shown in Figure 2.13.

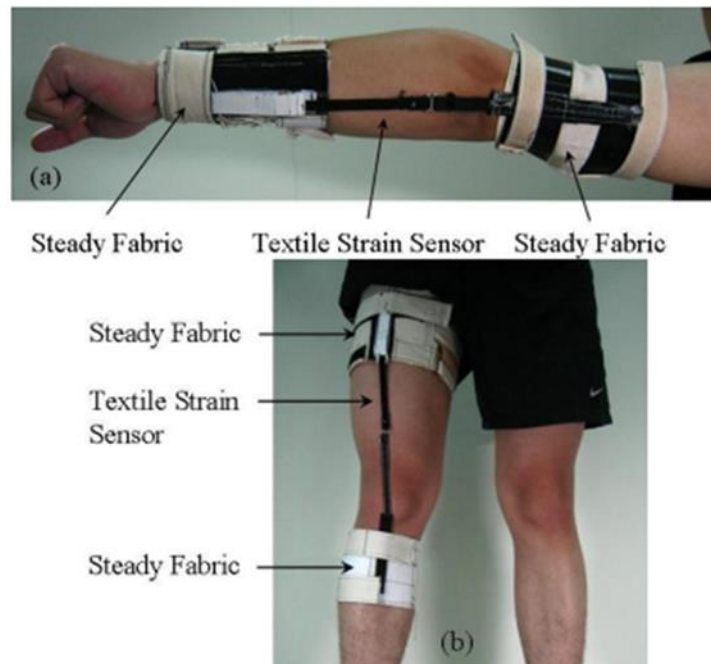


Figure 2.13 - Device for Monitoring the Flexion Angle of Elbow and Knee.

Likewise, in sports, textile sensors can be used to measure an athlete's performance by monitoring their body's physiological response to any exercises, as well as to detect abnormalities, design training plans and tactics, or to prevent them from getting injured. Totaro et al. [81] developed the Electrolycra Strain Sensor to track knee and ankle movements, shown in Figure 2.14. A capacitive sensing element that combines conductive textile and elastic polymers, was integrated with commercial knee and ankle braces, together with a detachable wireless electronic reading system. The stretchable capacitive sensor exhibits a good performance in the ~30% stress range.

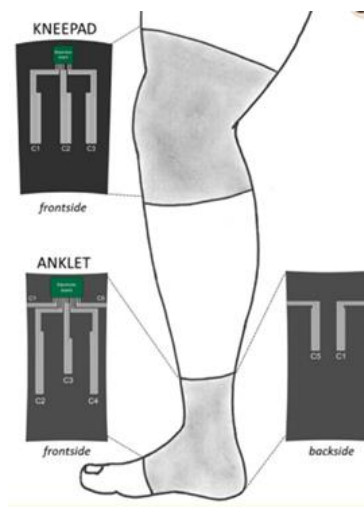


Figure 2.14 - Strain Sensor for Lower Limb Joint Position.

Gioberto and Dunne [79] explore a stretch sensor and implement a looped-conductor technique through the use of an industrial coverstitch machine to create a stretch sensor. In that work it was found that the useable range for the stretch sensor was around 19% of the sensor length and then later [82] they presented a garment-integrated stitched stretch sensor, used to sense joint movement. The 75mm long stitched stretch sensors were repeatedly stretched and relaxed for about 25% of their length. The stretch sensor was attached to the trouser leg, over the front of the knee. The trouser mounted stretch sensor was then tested on a running mannequin. It was noted that a large error in knee angle prediction of 8.39 degrees was experienced.

Coated conductive polymers and composite yarn are considered suitable to create resistive sensors. Atalay [83] developed a soft strain sensor by incorporating silicone with a conductive-knit textile used to monitor knee joint movements. The sensor is mounted onto an elastic, knitted fabric which is held tight using Velcro when worn by the subject. The sensor showed high linear ( $R^2 = 0.99$ ) and fast response (i.e. 50ms). However, this strain sensor is not integrated into any garment. It is rather a sensor strip that is fixed to the leg separately from the trouser.

Guo [84] evaluated carbon-filled silicon sensors and conductive thread sensors to determine their operating range according to the performance requirements of different applications. The test results show that the carbon filled silicon coated stretch sensor shows the optimum performance and is reliable. However, thread stretch sensors made with woven or knitted structures can be greatly improved with more careful design. In a subsequent work, Guo [16] reported clothing for respiratory monitoring designed using flexible conductive coated straps for the chest and abdomen. One major limitation found in this design was the inability to effectively eliminate motion artefact, in the sensor performance. In this system, the mounting unit with all electronic components and a wireless transmission (Bluetooth) device is designed to be placed on the waist at the back of the garment. The data collection device is rather large and heavy to be considered as a truly wearable and wearer friendly system.

The sensors mentioned above are of the piezoresistive type, which respond to body movements such as joint movements, breathing, and foot pressure. However, these types of stretch sensors has inherent problems that need to be overcome before brought to the market for end use. Issues affecting the practical use of these sensors, such as the limited working range, hysteresis and lack of sensitivity need to be carefully considered and

solutions to overcome them must be put forward. A review of the materials and the relative properties suitable for establishing a stretch sensor are presented as follows.

## **2.9 Essential and desirable properties of stretch sensors**

Sensors are devices that change their electronic properties to produce differing values in relation to static and dynamic movement. Thus, the sensors can offer electronic signals capable of being measured, recorded and analysed by appropriate devices [85]. Wearable sensors are primarily used for sensing and monitoring body parameters as the textile sensor comes into contact with the body. It means that the monitoring process can take place on several locations on the body. For example, these sensors can be used to monitor heart rate, blood pressure, respiration, and movement.

Empirical investigations on the relationship between the elongation of stretch sensors and the electrical resistance have been conducted by many researchers [79, 82, 86-90]. The characteristics and optimum range of measurement in a textile sensor, can be seen in Table 2.1.

As shown in Table 2.1, the desired characteristics of stretch sensors for textile applications include being highly flexible, durable, and stretchable. Additionally, high sensitivity, and fast response/recovery time are crucial for the detection of real-time activity [75, 91]. The applicability of wearable sensors can be enhanced under deformation (e.g. stretching), which can be conducted electrically and mechanically, as we will see later in this investigation.



Table 2.1 - The characteristics for textile sensors.

<b>Name</b>	<b>Definition</b>	<b>Units</b>	<b>Ideal sensor</b>
Maximum measurable strain	The elongation as a fraction of the original length.	% strain	High. 50 times [86].
Working range	The range over which the device is useful as a sensor.	% strain	Wide [88].
Monotonic	A function with a gradient of constant sign.		Want monotonic [86]
Linearity	The proportionality between resistance and strain (or other measurements).		Linear [79, 86, 88].
Gauge factor /sensitivity	Sensitivity of sensor resistance to strain. $(\Delta R/R)/(\epsilon)$ .	%/% (technically unitless).	High sensitivity [82, 86-88]
Baseline resistance	The initial unstretched resistance or the resistance at zero extension.	Ohms	[82, 87]
Peak-to-peak	Difference between minimum and maximum output for each cycle.		[82, 87]
Repeatability/drift	Drift in other characteristics with increasing cycle numbers.	[unit of changing characteristic] / number of cycles (at a specified % strain)	Highly repeatable, i.e. low change with cycling [82, 87, 88].
Hysteresis	The difference in the output between loading and unloading.	% , Ohm.mm	[82, 87, 88]
Response to step input	Dynamic response of resistance changes to step change of strain input.	Overshoot: % Recovery time: sec	Low overshoot and fast recovery time [86].
Response/delay time	a period of time between the onset of the stimulus and the beginning of the response.	ms	Low delay time [86, 88].
Creep	The slow continuous deformation under a constant load.	Percent at specified strain	Low [86].
Sensitivity to other deformations	Change in resistance to twisting, compression etc.		Low [86].
Sensitivity to environment	Change in other characteristics to temperature, humidity, composition of gases etc.		Low [86].
Stiffness	How much the sensor itself affects strain, e.g. if the sensor is completely rigid it would affect how much the fabric stretches.		Low [79, 82].
Ease of manufacture	Including being compatible with existing manufacturing processes.		Easy [79, 87, 88].
Comfort	Including weight, size, permeability, stiffness.		Light, small, permeable, flexible [79, 82, 87].
Aesthetics	Physical itself with appearance, design presentation.		Attractive [79, 82]
Simplicity	Including manufacturing, easy setup, ease of uses.		High [88]

### ***2.9.1 Design feature of the textile material for its suitability as wearable stretch sensor***

There are new developments of several types of textile conductive materials that offer distinct wearable sensor design and integration into fabrics and garments. Sensors made of electrically conductive components, such as stainless steel, copper, silver or carbons have already been incorporated into fibres or fabrics for optimal conductive performance. The sensors used to measure strain based on the deformation-induced electric resistance change under external force are considered as an important topic for investigation and development. Conventionally, the working principle of textile-based stretch sensors is reliant upon the traditional metal-based strain gauge principle. However; because of the inherent properties of textile structures, textile-based stretch sensors introduce a higher level of elasticity into the materials than conventional sensors, which have rigid mechanical properties [92].

The capability of using textile-based sensors is reported in numerous research projects [83, 84, 93, 94]. Several researchers investigated and developed polymers and textile-substrate based sensing to determine the optimal properties of the materials to be used as stretch sensors. The substrate material choice is essential in achieving good sensor stretch and recovery characteristics.

In a knitted sensor, functional yarns are part of the structure, so sensor placement and orientation within the garment are limited because the conductive yarn must follow the pattern of the wale and course direction [16]. In this work, the best stitch-thread architecture was found to be the most reliable method, which can be applied directly onto the textile substrate. A Stitch-thread type sensor can be used more flexibly than a knitted or woven sensor and offers easy integration in the garment, without any directional or positioning limitations. The sensor size can easily be adjusted, which provides an opportunity to develop the integration of functionality in many wearable garment products

In this research, the textile electrodes were investigated, produced and optimised, with emphasis being placed on the measurement of skin-electrode impedance. As it will be seen later in the thesis, in order to reduce the electrode impedance, materials with good conductivity and electrical properties should be used, and their size and holding pressure should be optimised e.g., low electrode impedance when being placed on the skin. This is a primary consideration of textile-based electrodes in the context of this study.

## **Chapter 3 – Introduction and Evaluation of the Properties of Conductive Textile Materials**

This chapter investigates the suitability of conductive textiles as sensors and it assesses their performance for continuous physiological monitoring such as ECG and body movement. In the field of monitoring well-being and medical diagnostics, most techniques are generally based on the monitoring and recording of bioelectrical phenomena. To that effect the values of electric potential serves as a means of electronic assessment of the heart, via a measurement of the ionic current flowing through the human body.

The interaction between ions in the body and electrons in the electrodes can significantly influence sensor performance, requiring that are met in the material and the application. This technique is widely used in ECG signals, received from the heart's electrical activity for the diagnosis of disturbances in cardiac rhythm, the EMG used in the diagnosis of neuromuscular diseases, and the EEG use in identification of brain dysfunction, as well as evaluating sleep quality. Other biopotential electrode methods are also used in the monitoring of body movement by using gyroscopes and GPS sensors. In recent years there is a demand towards textile based sensors in all of those applications and their unobtrusive integration in wearable garments for continuous monitoring.

As mentioned in the literature, the electrical properties effecting the skin–electrode interface vary in different parts of the body due to a difference in the layers of the skin. The structure of human skin is multi-layered and the properties of human skin vary for each individual. Skin conductivity varies according to the properties of the stratum corneum, sweat glands and sweat ducts. Particularly, the impedance variation in dry electrodes increases in response to the changes in skin moisture, pressure, and time. To find out how such electrical characteristics affect the recording performance of textile-based sensors, this research evaluates the variation and stability of skin-electrode interface aiming at reducing the properties of human skin disparity for each individual. To that effect a skin dummy made from agar is used for impedance measurement. This method does not only allow the electrical properties of textile electrode to be investigated, but also the contact performance between skin and electrode to be evaluated as well.

Effort was made to find and choose materials so that electrodes were made from standard conductive threads and fabrics which are commercially available, for continuity of

standard supply of materials with the same properties. Two types of conductive thread and five types of fabric to develop the electrode were investigated. To that effect further research is taken place to ascertain the transmissivity of electrical signal fed through the textile electrode by comparison against commercial gel electrodes (wet electrodes).

### 3.1 Conductive Thread

Conductive threads have been used previously for the development of measurement and sensing applications [95-98]. Various types of conductive thread are summarised by Martínez-Estrada [99]. A number of conductive threads suitable for sewing were considered according to their specifications (flexible, softness, conductivity and sewability). Silver coated thread is conductive on the outside surface of the thread and is recommended for sewing and embroidering [100] because as the thread overlaps itself, it increases the conductive surface and maintains its electrical properties [101]. In addition to this, it is suitable for medical environments where strict hygiene is required when used. Based on these advantages and preliminary trials, two conductive threads were chosen, as shown in Figure 3.1, Silver plated nylon 117/1/ two-ply and 235/34 four-ply, Statex Productions & Vertriebs GmbH, Kleiner Ort 11 28357 Bremen, Germany, which had good conductivity and stability and suited our end-use requirements. Their electrical specification is given in Table 3.1 and their properties in Table 3.2. Both threads are commercial and they have also been used by other researchers [26, 102-105].



Figure 3.1 - Conductive threads: Silver plated nylon 117/1/ two-ply (left) and Silver plated nylon 235/34 four-ply (right).

Table 3.1- Specification of conductive threads.

<b>Conductive thread</b>	<b>Thread size (Tex)</b>	<b>Linear resistance (<math>\Omega</math>)</b>
Silver plated nylon 117/17 two-ply	33	500 $\Omega$ /meter
Silver plated nylon 234/34 four-ply	92	50 $\Omega$ /meter

Table 3.2 - Properties of conductive threads.

<b>Conductive Thread</b>	<b>Maximum Load (N)</b>	<b>Energy at Break (N)</b>	<b>Extension at Break (mm)</b>	<b>Elongation (%)</b>	<b>Tenacity (N/Tex)</b>
Silver plated nylon 117/17 two-ply	10.78	10.77	65.25	26.1	0.4
Silver plated nylon 234/34 four-ply	46.27	45.88	113.17	45.27	0.36

Silver-plated nylon conductive threads has been available in the market for several years. These threads are lightweight, soft, flexible, strong, durable, and do not suffer permanent deformation after being bent. The structure and metallic coating in the surface of the thread can be seen in Figure 3.2. This enables these threads to be ideal for standard textile manufacturing processes such as knitting and weaving, and for creating fully functional conductive pathways, while being capable to withstand the stresses and strains of machine sewing for typical garment operations.

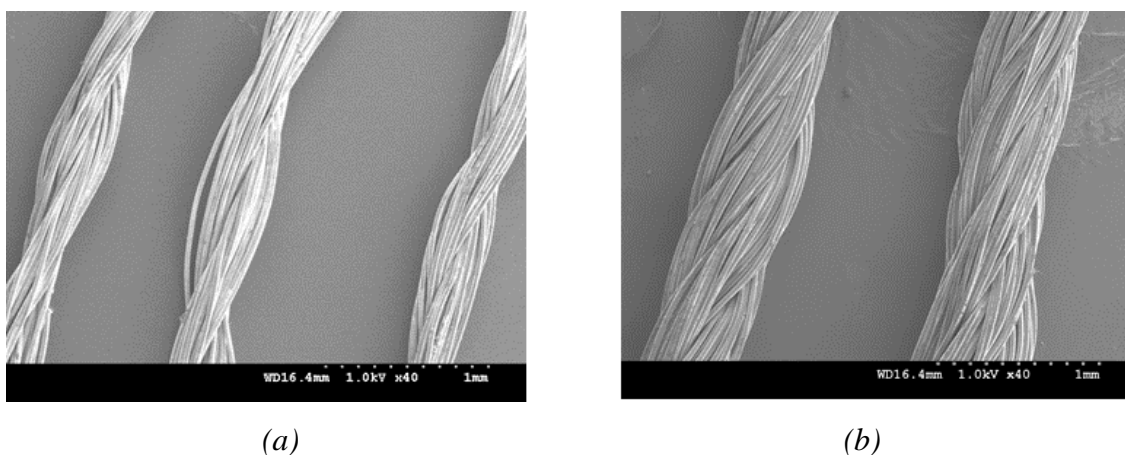


Figure 3.2 - SEM image of Silver plated nylon conductive thread: (a) 117/17 two-ply and (b) 234/34 four-ply.

To consider these threads for suitability for the development of textile-based sensors in wearable electronic devices, their electrical performance was examined. Cyclic tensile testing has been performed based on the British Standard BS EN 14704-1:2005 test method. During this testing the conductive thread is connected to digital multimeter probes (DMM Agilent U1273A/U1273AX, Agilent Technologies, Inc. Santa Clara, CA 95051 USA) for recording the electrical properties of the thread. The electrical resistance of the two threads, 117/17 two-ply and 234/34 four-ply show baseline resistance at  $215\Omega$  and  $24\Omega$  respectively. Figures 3.3 and 3.4 show that the electrical resistance response of both threads is increasing to  $441\Omega$  and  $69\Omega$  respectively with elongation (loading) and decreasing when relaxing (unloading) to  $215\Omega$  and  $24\Omega$  respectively, and having good stability over time at 400sec and 600sec respectively. This good overall electrical behavior with only a minimal delay in unloading renders them suitable for wearable applications.

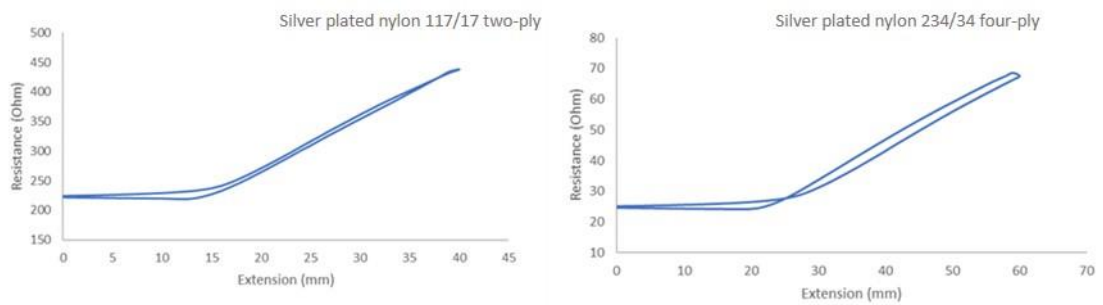


Figure 3.3 - Resistance against extension in different type of silver plated nylon conductive thread: (a) 117/17 two-ply and (b) 234/34 four-ply.

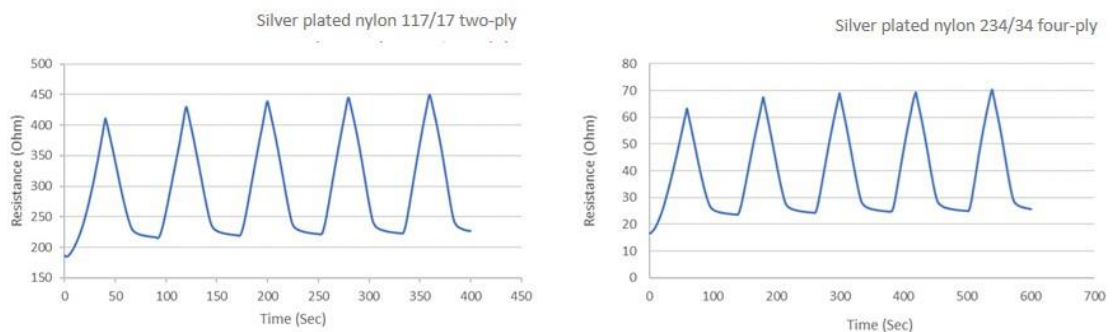


Figure 3.4 - Sewing thread tensile performance during 5 cycles. (a) 117/17 two-ply; (b) 234/34 four-ply.

Conductive thread compatible strain sensors can be produced by integrating loop structures in a textile fabric such as by knitting and stitching. The resistance of those strain sensors changes from the changes in contact resistance between loops of the conductive yarns during stretching.

The good electrical performance of silver-plated nylon 117/17 two-ply and 234/34 four-ply threads can provide functions such as interconnections, circuits and conductive tracks that can be both flexible and stretchable, which allows custom-made sensors to be designed for specific applications for different parts of the human body.

Further experiments were carried out to develop textile sensors in which the conductive thread was knitted and stitched in different structures and patterns. A knitted fabric electrode will be investigated in chapter 3 and 4, a stitch stretch sensor will be presented in chapter 5, and integration of stitch stretch sensor into a SSB garment for respiration monitoring is presented in Chapter 6.

### **3.2 Conductive Fabric**

Conductive fabrics have been produced using various methods, either using conductive yarns in fabrics or coating the fabric or yarn with electrically conductive materials, such as copper, carbon, silver, or nickel. Conductive fabrics are mostly used in devices that require a flexible, soft, and occasionally washable circuit. They are ideal where solid conductive materials are not suitable, and hence suitable for wearable electronics and garments.

In this research, silver was chosen as the conductive material, as it is harmless to human skin, electrically stable and antibacterial [106]. Hence, for the construction of the electrodes in this investigation, five fabrics of different structure have been used manufactured from 99% silver-plated knitted and woven fabrics. These types of fabric do not only have a high electrical conductivity, but are also comfortable and friendly to skin. All fabric electrodes were examined to determine their performance at the skin-electrode interface for using them as sensors. Therefore the skin-electrode impedance was investigated and the optimum design and fabrication of the textile electrodes described.

### 3.3 Skin-impedance of textile electrodes

#### 3.3.1 Electrode Fabric used

Five electrodes are made from standard commercial conductive threads and fabric which were made from silver-plated nylon, as described in sections 3.1 and 3.2. The experimental electrode fabric samples in this work were developed from those different types of material and different knitted fabric structures. Fabric electrodes 1,2,4,5 are knitted whilst fabric 3 is made of woven fabric, all electrodes were tested and compared for fabric performance. The experimental conductive fabrics are shown in Table 3.3. Three electrodes (Electrode 1, 2 and 3) were made from conductive fabrics (MedTex™ P-130, Spacer knitted and Plain 1x1 woven respectively). The other two electrodes (Electrode 4 and 5) were made from the conductive thread (silver plated nylon 117/17 two-ply and 234/34 four-ply) that we tested previously. This ensured that the beneficial properties of the threads were incorporated into knitted textile sensors and further examined for efficacy, using a Shima Seiki SES 122-S 12 gauge computerised flat-bed knitting machine, shown in Figure 3.5. The conductive threads and fabrics used are commercially standard products from Statex Shieldex, USA.

Table 3.3 - The properties of conductive fabric.






Electrode No.	Image	Components	Structure	Weight (g/m <sup>2</sup> )	Thickness (mm)	Fabric density	
						Couses per mm	Wales per cm
1		78% Nylon 22% Elastomer	Single jersey knitted	130	0.45	30	28
2		94%Ag/Nylon 6% Elastomer	Spacer knitted	349	2.35	28	17
3		Silver plated nylon fabric	Plain 1x1 woven	72	0.10	42 (weft/cm)	61 (warp/cm)
4		Silver plated nylon 117/17 two-ply	Single jersey knitted	240	1.0	12	8
5		Silver plated nylon 234/34 four-ply	Single jersey knitted	528	1.25	8	7





Figure 3.5 - Computerised flat-bed knitting machine, Shima Seiki SES 122-S 12 gauge.

### 3.3.2 *Electrode structure*

Figure 3.6 shows the structure of the experimental electrode, in which the middle square area illustrates that the conductive fabric is being surrounded by the non-conductive fabric on the outside. The conductive fabric is connected with a metal snap. Between the conductive fabric and the non-conductive electrode base, there is a textile filler placed to provide a good support to the electrode as a pad [107, 108]. The detailed specification of the electrodes is given in Appendix A.

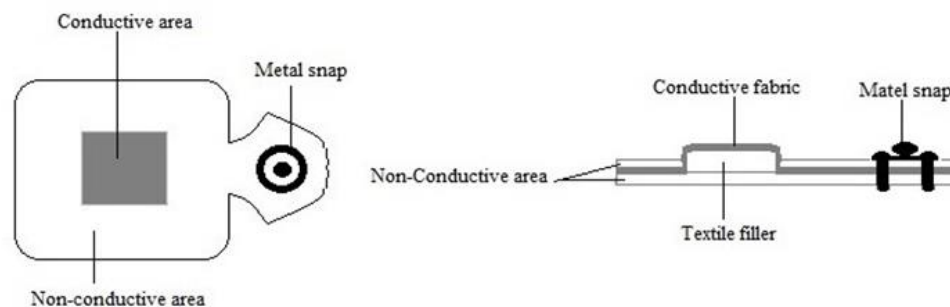


Figure 3.6 - The experimental textile electrode, Top and Cross-sectional View

### 3.3.3 *Electrode Fabrication*

In fabricating the electrodes, it was essential that a reliable electrical connection be made between the base of the electrode which will be in contact with the skin, and the top of the electrode which will be connected to the recording instrument. In metal-based electrodes, soldering is used to make this connection, but that is not possible in fabric-

based electrodes because they get damaged by heat from soldering/connecting. To overcome this problem, the connection was made using a metal snap.

A snap punch machine was used to attach size 16 metal snaps onto the electrodes. Double-sided PU thermoplastic adhesive was used to function as the electrode base. A Non-woven fabric  $70\text{g/m}^2$  was used as insulation covering the top of the electrode. The materials and components used for producing the electrode are shown in Figure 3.7.

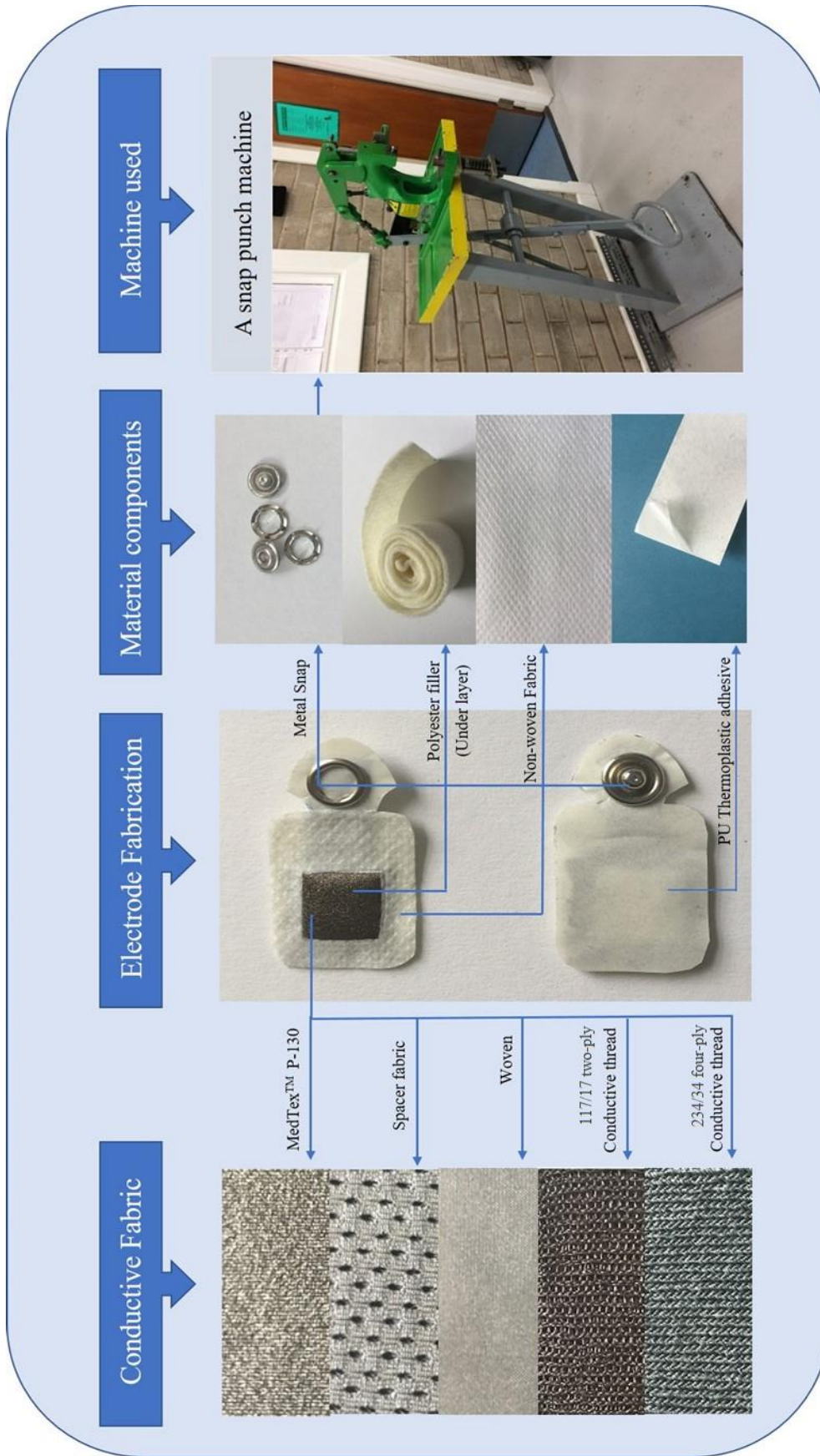


Figure 3.7 - The assembling materials used for the experimental electrode

### 3.3.4 Experimental procedure

The fabric-electrodes discussed above were used to evaluate the skin-electrode interface. The electrical properties of five different fabric electrode-substrates (Table 3.3) were measured, and the stability and interface impedance were considered by the use of a skin dummy made of agar.

The investigation and measurements were performed in a standard conditioned laboratory. The room temperature was controlled at  $20\pm 2^{\circ}\text{C}$  and the relative humidity at  $65\pm 2\%$ . A high-precision LCR-Bridge meter HM8118 (HAMEG instruments from Germany) as shown in Figure 3.8 was used to measure the skin-electrode impedance with the test sinusoidal signal being set to 100Hz in order to provide very accurate data over a relatively wide range of frequencies [109].



Figure 3.8 - LCR Bridge meter.

To study the influence of the skin-electrode impedance, five different textile-electrodes were created as shown in Figure 3.9, and the performance of their electrical properties was examined. Figure 3.9 illustrates a typical experimental sample of fabric-electrodes. The skin-electrode impedance investigation was carried out on the skin dummy made of agar-agar ( Figure 3.10), which consists of salt and distilled water. The salt was mixed with distilled water to achieve a conductivity of  $29.3 \mu\text{S}/\text{cm}^{-1}$  [110]. Then the solution was mixed with 7g agar-agar /100ml to achieve good stability as shown in Figure 3.10. This gives a conductivity property similar to that of wet skin tissue, which then provided very accurate data.

The stable properties of the dummy are necessary for the measurements to be reproduced several days later. Sweating skin can be simulated through the humid dummy surface. In this way, all electrodes will become slightly moist as they come into contact with the dummy.

A pair of electrodes is placed on the top position of the skin dummy at a distance of 10 mm between each of the five fabric electrode pairs (Conductive fabric in Table 3.3). The skin contact area of 15mm x 15mm is the same for all textile electrode samples, which is identical to the conductive area of commercial electrodes. In order to control the electrode pressure, a fastening elastic band was used to hold the electrode onto the skin dummy with the contact force of 0.7 kPa (5mmHg). The pressure applied was measured by a compression sensor (PicoPress) as show in Figure 3.11. The skin-electrode impedances were recorded every 20 seconds for 30 minutes.

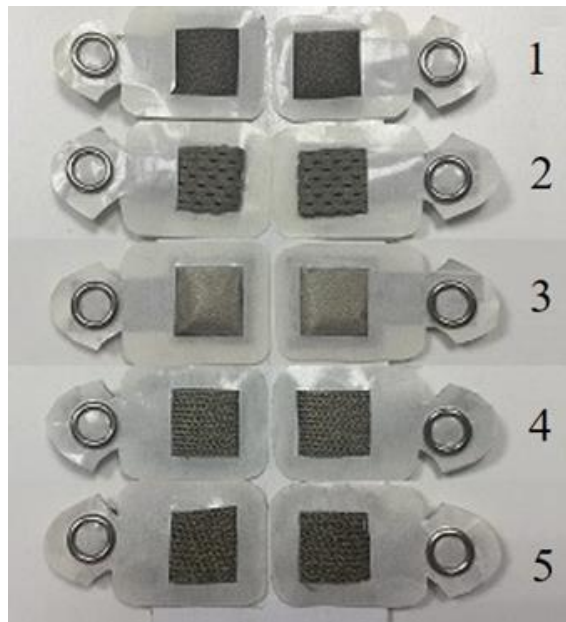


Figure 3.9 - Five pairs of experimental fabric electrode types, 1 is MedTex™ P-130, 2 is Spacer knitted, 3 is Plain 1x1 woven, 4 is silver plated nylon 117/17 two-ply, and 5 is silver plated nylon 234/34 four-ply

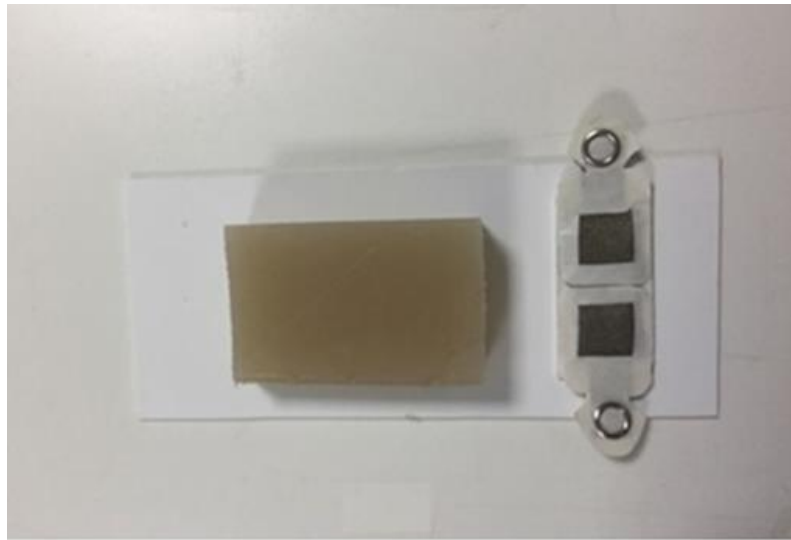


Figure 3.10 - The experimental sample of skin dummy and a pair of electrodes.

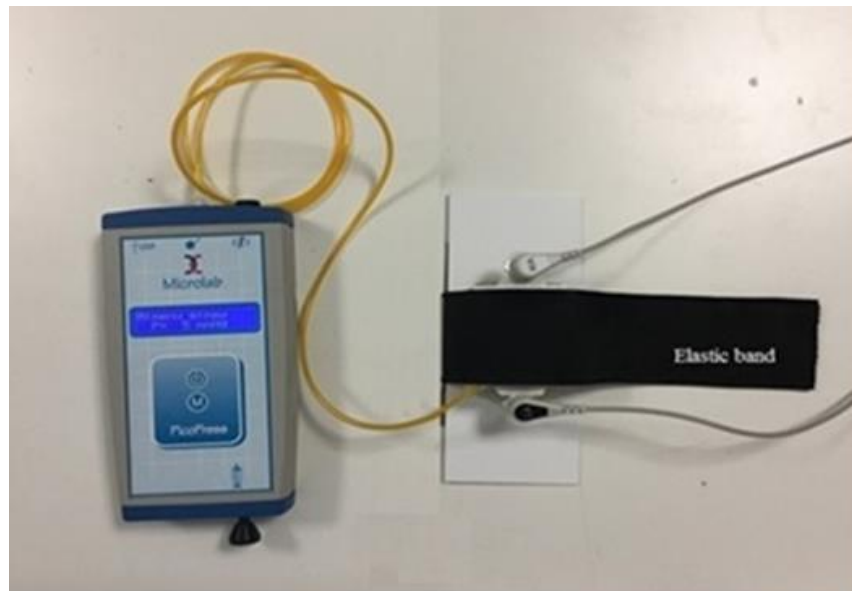


Figure 3.11- Skin dummy test set up.

### 3.3.5 Results and discussion

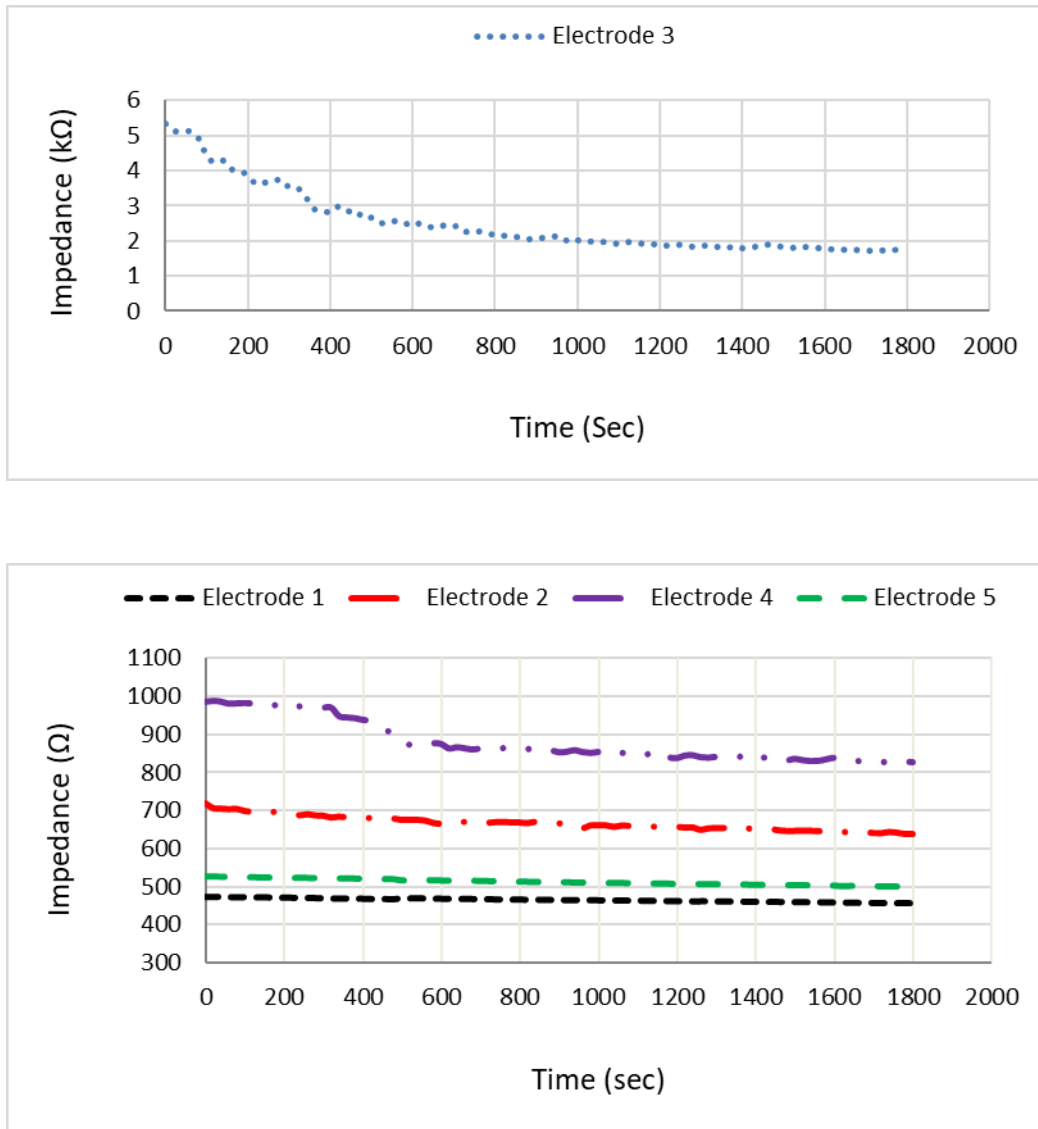


Figure 3.12 - The average skin-electrode impedance on skin dummy at 100Hz against time

Figure 3.12 shows the averaged impedance change with time of five different electrode pairs attached onto the skin dummy. The impedance data record has shown a similar trend across all electrodes. The impedance declined over time, maintaining a steady value after approximately 25 minutes. However, the absolute values of impedances for all five electrode materials vary considerably.

The variation in impedance values is a result of different surface structures that the electrodes have. The impedance values of electrode 3 are notably high, being 5-10 times higher compared to the other electrode materials. The fabric structure of electrode 3 is

made of woven fabric. Since the surface layer of such fabric is non-stretchable, the electrode does not maintain a good conductive connection between electrode and the skin, resulting in higher contact impedance. The conductivity of this fabric is much lower than the conductivity of the knitted fabrics used in all other electrodes.

The other four electrodes (Electrode 1, 2, 4, 5) have relatively smaller contact impedance (between 450  $\Omega$  and 1000  $\Omega$ ) compared to electrode 3 (5.2 k $\Omega$ ), with electrode 1 having the lowest contact impedance (450 $\Omega$ ). The variations of the contact impedance of the electrodes can be explained by differences in fabric manufacturing and in the fabrication of the electrodes. Not only is the manufacturing procedure important for contact impedance, but the property of the conductive part also plays a crucial role. Electrode 2 is made of open structure spacer fabric, leading to lack of conductivity because there is a smaller amount of silver per unit area, the surface layer is not highly conductive and hence the contact impedance increases to approximately 700  $\Omega$ .

Electrodes 4 and 5, which are knitted electrodes, differ in terms of yarn properties i.e. number of filaments and thickness. Electrode 5 has low contact impedance (500  $\Omega$ ) due to a larger number of filaments. More filaments contribute to a higher amount of silver, and thus, better conductivity.

This experiment shows that the two electrodes made from single jersey fabric (MedTex™ P-130), electrode 1, and silver plated conductive thread 234/34 four-ply, electrode 5 have low contact impedance of 450 $\Omega$  and 500 $\Omega$ , respectively. These two fabric electrodes are used in further experiments.

### **3.4 Electrical signal transmission of textile electrodes**

#### **3.4.1 Materials selection**

Textile-based electrodes for use in wearable devices, have their conductive pads (conductive area) to measure the electrical signal which is then passed through the textile to the processing circuit board.

In order to find the electrical signal transmission performance of these conductive textile materials, three electrodes were chosen, two fabric electrodes performing best in the experimental skin-electrode interface; electrode 1 which is made from MedTex™ P-130, single jerseys knitted fabric and electrode 5 which is knitted from silver plated



conductive thread 234/34 four-ply. The third is a commercial (3M, 2228, USA), wet type electrode with a thin metal plate and electrolyte or gel internally embedded. This electrode was compared with the textile electrodes.

After choosing the optimum conductive electrode to transmit a signal, the reference signals (sinusoidal and rectangular) for the three types of electrodes are generated using a signal generator at an amplitude and frequency of 1-V<sub>pp</sub> and 10Hz, respectively, for determining how signals can be transmitted along fabric electrode (Conductive fabric) and gel electrode. In the experiments, electrical signals are fed through the electrodes and measurements are taken with an oscilloscope.

### 3.4.2 Experimental procedure

Initially, the reference sinusoidal and rectangular signals were generated with a signal generator (the left side item in Figure 3.13) at 1-V<sub>pp</sub> amplitude and 10Hz frequency for all three experimental electrodes. In the experiments, electrical signals are fed through the electrodes prior to measurements taken on the opposite side with the oscilloscope (item on the right in Figure 3.13) and compared with the reference signals.

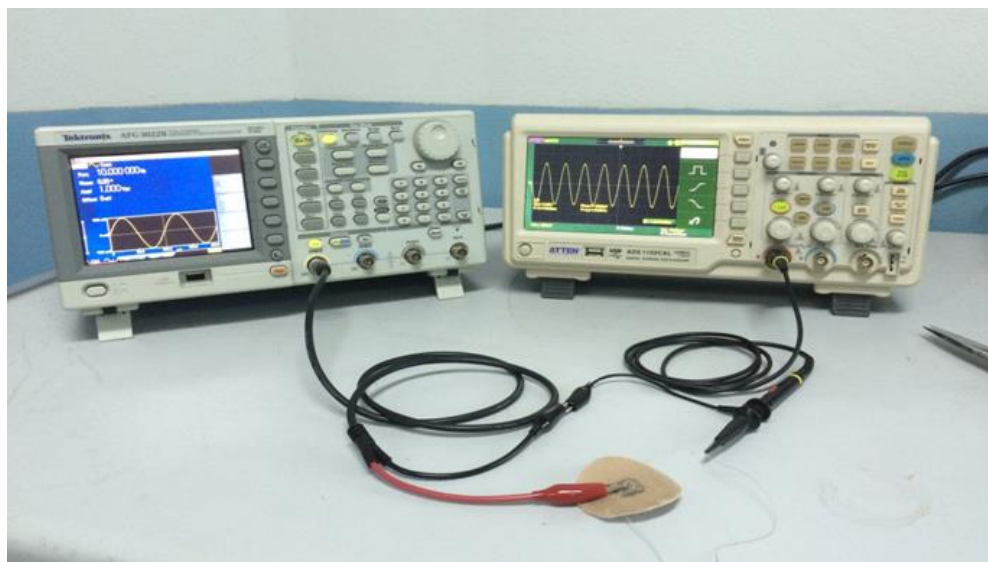


Figure 3.13 - Signal generation and measurement: a signal generator (left) and an oscilloscope (right).

### 3.4.3 Results and discussion

Table 3.4 presents the comparative results between the reference signals (sinusoidal and rectangular) and the measured signals for all four experimental electrodes. It is observed that the transmissivity of the textile-based electrodes (i.e. the conductive fabric) was a good response, whereas an offset was detected for the commercial electrode.

A typical signal diagram of electrode elements that causes this phenomenon is shown in Figure 3.14. After passing through the conductive fabric, the signal remains at the same voltage levels as when it was generated, as shown in Figure 3.14a. However, after passing through the gel electrode, the signal axis becomes higher (shown as the dotted line in Figure.3.14b) than in the generated signal (shown as the solid line).

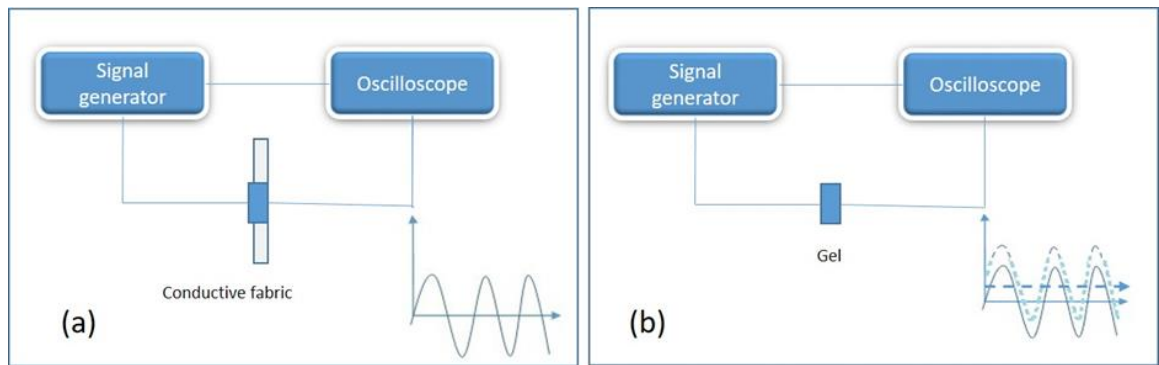
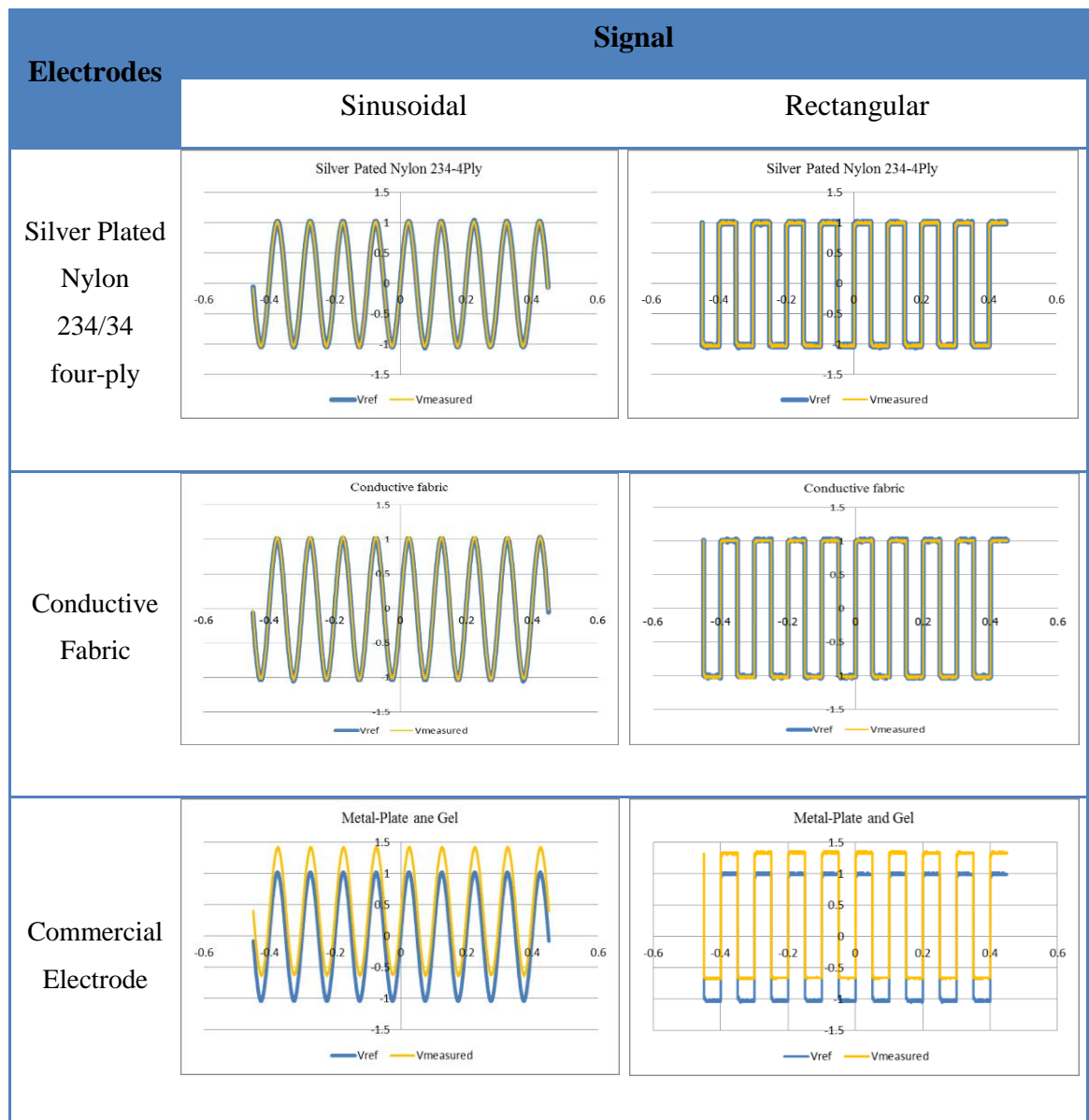


Figure 3.14 - Electrical characteristic measurement schematic diagrams of (a) conductive electrode fabric, (b) Gel electrode.

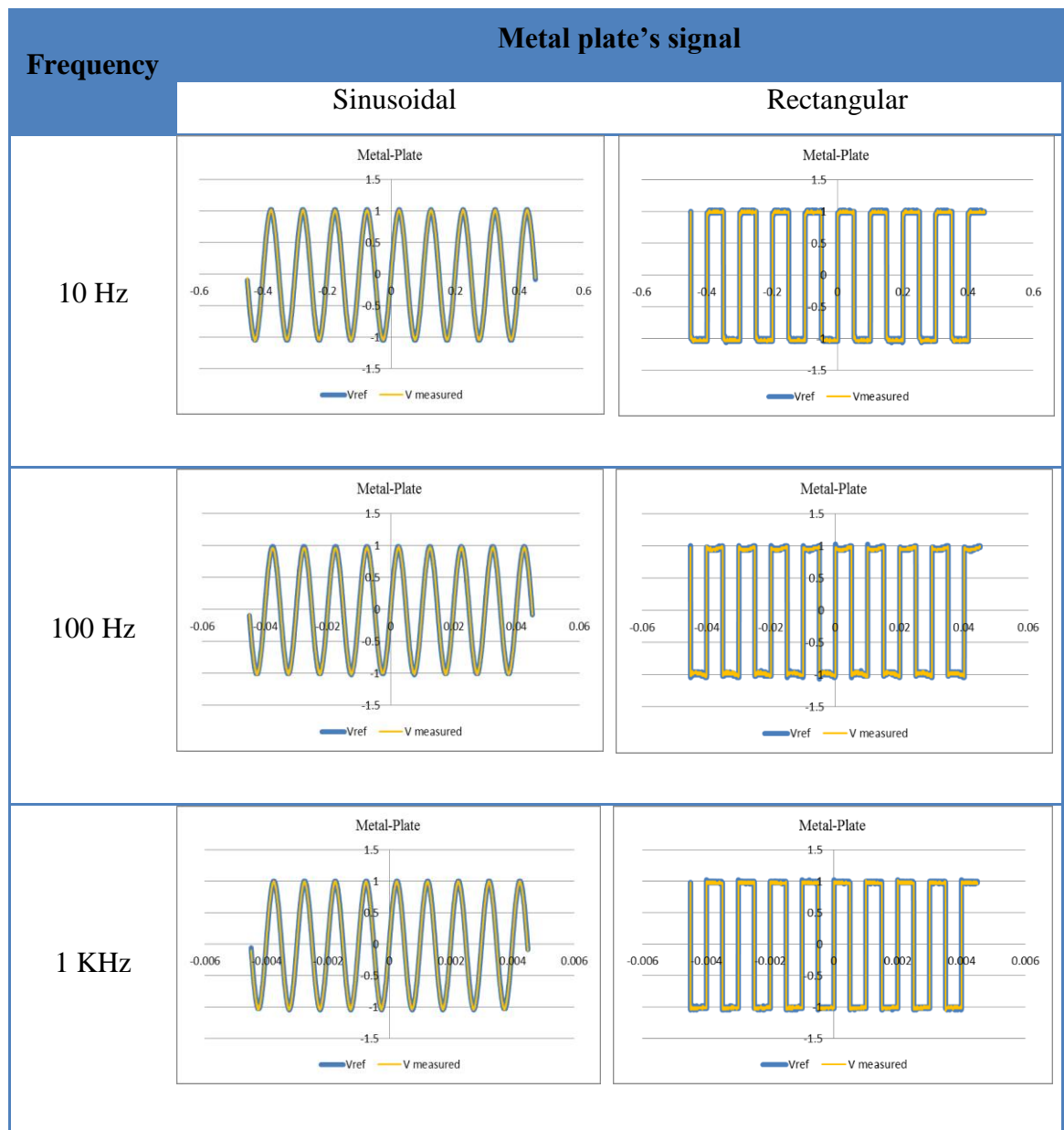
To identify the cause of the offset, the wet electrode was investigated further by varying the signal generator's frequency from 10Hz to 100Hz and then to 1kHz to obtain additional sets of reference signals. Next, electrical signals were fed through either the thin metal plate or gel individually prior to measurements taken on the opposite side with the oscilloscope.

Table 3.4 - Comparison between the sinusoidal and rectangular reference and measured signals.



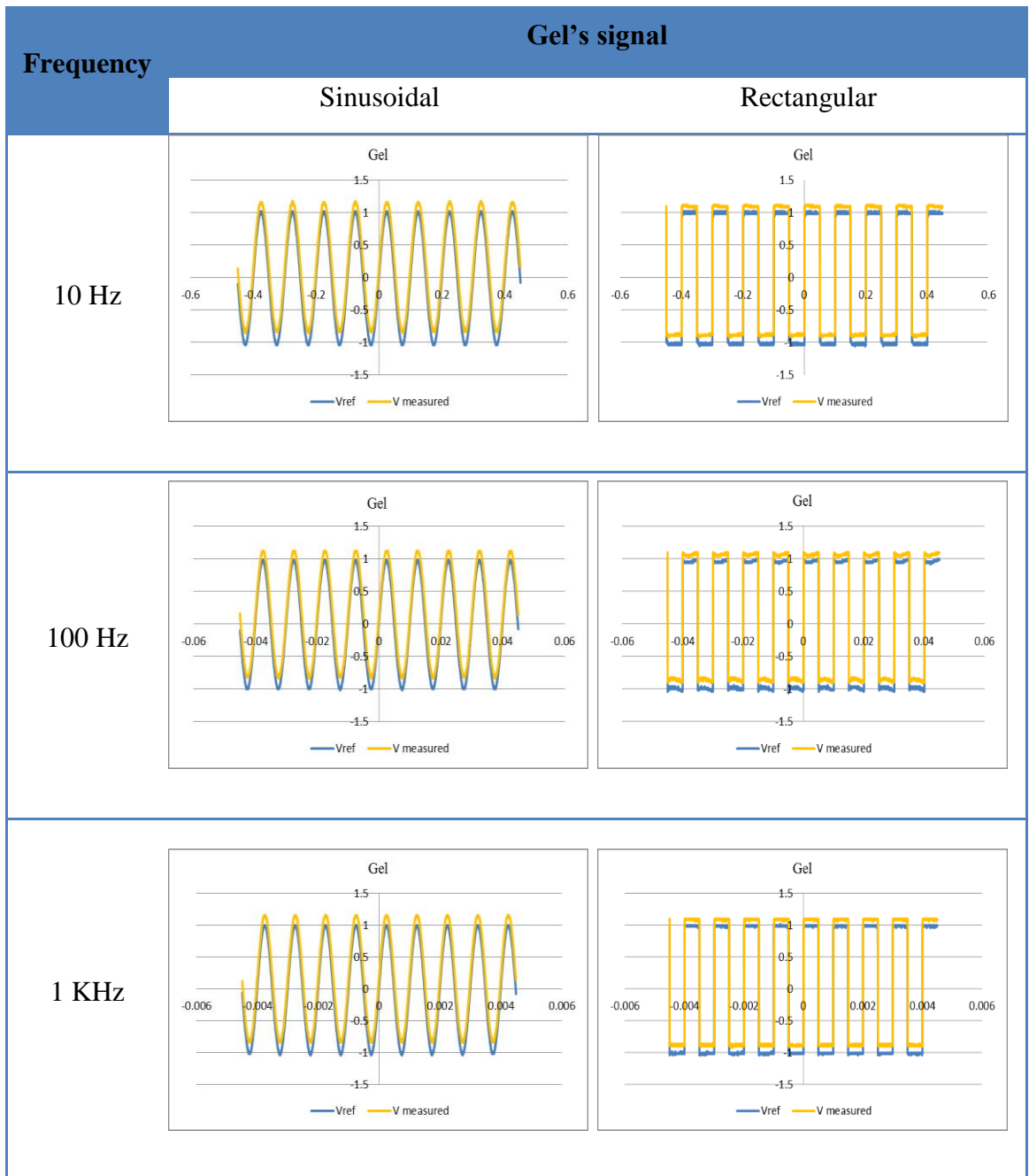
In the experiments with the thin metal plate at three different frequencies of 10Hz, 100Hz and 1kHz, it was observed that the measured results are identical to the reference signals; in other words, no offset is detected as shown in Table 3.5. On the contrary, the experimental results with gel produce an offset for all three frequencies as shown in Table 3.6.

Table 3.5 - The reference signals relative to the measured signals transmissible through the thin metal plate at 10Hz, 100Hz and 1kHz frequency.



As we can see in Table 3.6, most of the properties of the transmissivity signal of the gel electrodes (period, range, amplitude, and frequency) are the same as reference signals (sinusoidal and rectangular), but the axis of the transmissivity of the gel electrodes shifts upwards from 1.0V (reference signal) to 1.2V. Gels are typically referred to as hydrogels composed of an elastic cross-linked network of both solid and liquid electrolytes which is soft and wet [111, 112]. The viscosity of this material is considered in the conductivity mechanism in which the gel electrolyte contributed to the offset associated with the relaxation time of the polymer gel [113].

Table 3.6 - The reference signals relative to the measured signals transmissible through gel at 10Hz, 100Hz and 1kHz frequency.



### 3.5 Summary of the Results and Conclusions

These investigations confirmed the ability to use textile-based conductive materials for well-being and health monitoring devices and applications. The need for different materials that are suitable for designing textile-based electrodes and sensors for wearable garments were considered. It was shown that two conductive threads were examined and the skin-electrode impedance of five conductive fabrics were investigated. Moreover, the electrical transmission of a number of fabric electrodes was measured.

During these studies conductive threads are investigated by a cyclic test and both types of thread, Silver plated nylon 117/1/ two-ply and 235/34 four-ply, have shown a slight delay in returning to the fully unloaded relaxed state. The overall electrical performance was good and proved suitable for wearable applications. The performance of conductive thread is crucial in the design of a stretch sensor. Using the Silver plated nylon 117/1/ two-ply and 235/34 four-ply, that demonstrated the good performance in cyclic tests, we are also able to create a stitch stretch sensor. Chapter 5 shows how it can be successfully integrated into any garment for monitoring physical movement in the human body, such as leg articulation and respiration.

Using a skin dummy to test the performance of electrodes provides a foundation for detailed investigation of the changes in contact impedance of textile electrode properties. In this investigation, the results show that the skin-electrode impedance varies with time and the different material manufacturing processes have an influence on the contact impedance of the textile electrodes. The greatest performance of the experimental fabric electrode surface was electrode 1 which is made from MedTex™ P-130, single jersey knitted fabric. This is closely followed by electrode 5 which is knitted from silver plated conductive thread 234/34 four-ply. As can be seen, the knitted materials have better contact impedance values than a woven (electrode 3), because the knitted fabric is softer and more flexible than the woven fabric, which allows it to easily follow the curvatures of the body, and to have better contact with the skin.

Having conducted the electrical signal transmission investigation, it was observed that the conductive thread, fabrics, and metal plate electrodes have more uniform characteristics with the reference signals. The results show that conductive-textile materials are ideal for wearable end uses. On the other hand, the signal transmission of the conventional electrode which is created from metal-plate and surrounded with gel exhibited an offset between the measured signals and the reference signal due to the

relaxation mechanism occurring in the polymer gel. Based on the findings of this chapter, further investigation of textile electrode development and of a textile stretch stitch type sensor were carried out and presented in the following chapters.

## **Chapter 4 – Investigation, Analysis, Development and Optimisation of Textile-Based Dry Electrodes**

In recent years, wearable devices for health and wellbeing are becoming important, when the use of electrodes enables measurement of body functions such as the health of the heart ECG, or the health of the brain EEG, acting as sensors. Therefore, textile electrodes have drawn a great deal of attention in recent years. In the previous chapter, the behaviour of skin-interface textile electrodes on skin dummy was established. The electrodes which are made from conductive threads and conductive fabric presented an optimum contact impedance and their properties proved suitable for wearable applications.

This chapter aims to investigate the mechanical interaction of textile electrodes and their properties such as electrode size, electrode-holding pressure, and electrode position so that an optimum dry sensor can be established. This chapter presents those measurements carried out on the human skin. To this end, ECG monitoring using dry electrodes is investigated and compared with commercially available gel electrodes, to establish their efficacy on user performance.

### **4.1 The Influence of the Skin-electrode Impedance**

The skin-electrode impedance is a prominent parameter used to evaluate the performance of an electrode, because any imbalance in skin-electrode impedance will transform the common noise into differential noise, causing signal disruption. The ideal performance is that all electrodes should exhibit the same skin-electrode impedance. However, due to the variation of the impedance in the human skin, it is difficult to ensure the same skin-electrode impedance across different body areas. Hence, it is not realistic to completely exclude differential noise. But because wearable textile electrodes are suitable for continuous monitoring over a long period of time, they do not require any skin preparation and conductive gel. As described fully in Chapter 3, the characteristics and specifications of conductive thread and fabric, in relation to skin-electrode interface values was investigated to find the optimum material for ECG electrodes.

There are many challenges in the measurement of skin-electrode impedance, mainly because of the electrical interaction with the properties of the human skin such as skin position, temperature, humidity, and time. Researchers such as Rosell et al. [114] noticed that the skin impedance is significantly varied among the subjects who use the same



electrodes under “identical” standard conditions. This observation implies that the results of the measurements on different subjects are very low in comparability. Therefore, it is necessary to examine the behaviour of textile electrodes in order to optimise the skin-electrode interface and any discrepancies that needs addressing.

The electrode size has been found to have a significant impact on skin-electrode impedance and on the quality of ECG signals. Puurtinen et al. [115] examined different sizes of textile electrodes and discovered that the skin-electrode impedance increases as the electrode size decreases. Marozas et al. [102] noticed that a contact area of textile electrodes smaller than 4 cm<sup>2</sup> could cause distortion in the low frequency spectrum of the signal. However, electrode size cannot be infinitely large, not only due to the limitation of skin area but also because of its impact on the spectrum of the ECG signals.

The electrode holding pressure is also discussed, according to the commonly recognised electrical equivalent circuit, as shown in Figure 4.1, the skin morphology is highly linked with impedance. The application of electrode-holding pressure can lead to the deformation of the skin structure, thereby causing change in skin-electrode impedance. Furthermore, the electrode-holding pressure can also induce the deformation of electrode contact surface due to the mechanical properties and the surface structure of the textile electrode as illustrated in Figure 4.2. Therefore, it is essential to conduct a study on the dry textile electrode structural properties, in order to understand and optimize their performance during signal monitoring, hence two preliminary experiments for the effect of position and holding pressure were investigated and presented here.

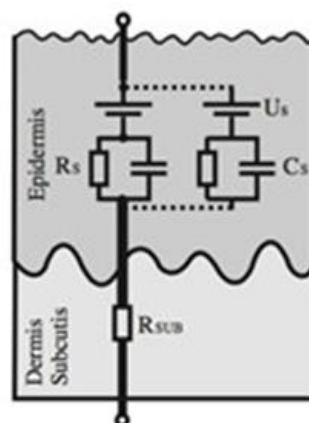


Figure 4.1- Electrical equivalent circuit of skin [110].

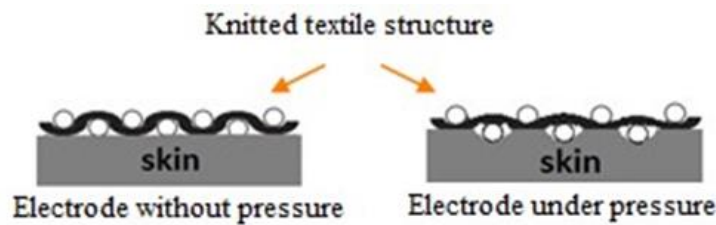


Figure 4.2 - Skin-electrode contact surface (side view).

#### ***4.1.1 The effect of electrode position on the skin-electrode impedance***

In order to study how electrode position influences the skin-electrode impedance, the preparation of textile electrodes were carried out using the same conductive fabric, MedTex™ P-130 (Electrode 1) which showed good results for electrical impedance in previous experiments in Chapter 3. A female volunteer is used as a test subject and all measurements were conducted on the inner surface of the subject's left forearm without skin preparation. Six electrodes were placed on the inner side of the subject's left forearm as shown in Figure 4.3. All 15mm x 15mm electrodes are assembled together in a precisely positioned array by using a whole piece of self-adhesive fabric, in order for the six electrode pairs to be placed in the right position. The 15mm x 15mm size was chosen as it is the same size as the gel electrode and it allowed room for 6 pairs to be fixed to the forearm.

To ensure that the pressure was consistent in each experiment, the electrodes were held onto the skin with adhesive tape. The measurements were conducted after 30 minutes, to allow settling time of the skin-electrode interface. Over the course of 10 days, this measurement was repeated and recorded ten times. In order for the influence of skin-electrode impedance to be compared, commercially disposable Ag/Ag Cl electrodes (3M, 2228, Minnesota, USA) were also assessed using the same method under identical standard conditions.

The experimental setting and the environmental conditions were identical to those of the skin dummy experiment. The laboratory atmosphere of the experiment was controlled at  $20\pm 2^{\circ}\text{C}$  and the relative humidity at  $65\pm 2\%$ . The subject remained in the conditioning lab for one hour before the start of the experiment to provide skin conditioning and to adapt to the measuring environment. A high-precision LCR Bridge meter HM8118 (HAMEG instruments, Germany) was used to measure the skin-electrode impedance.

The results show very clearly that electrode positioning affects skin-electrode impedance, even in a small area such as this.

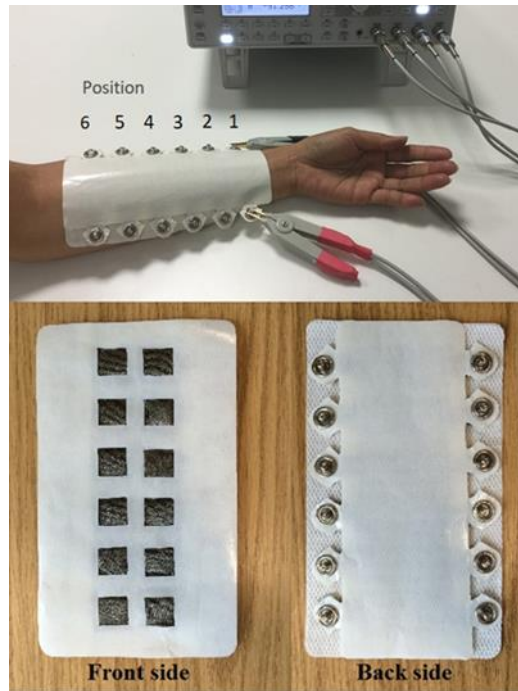
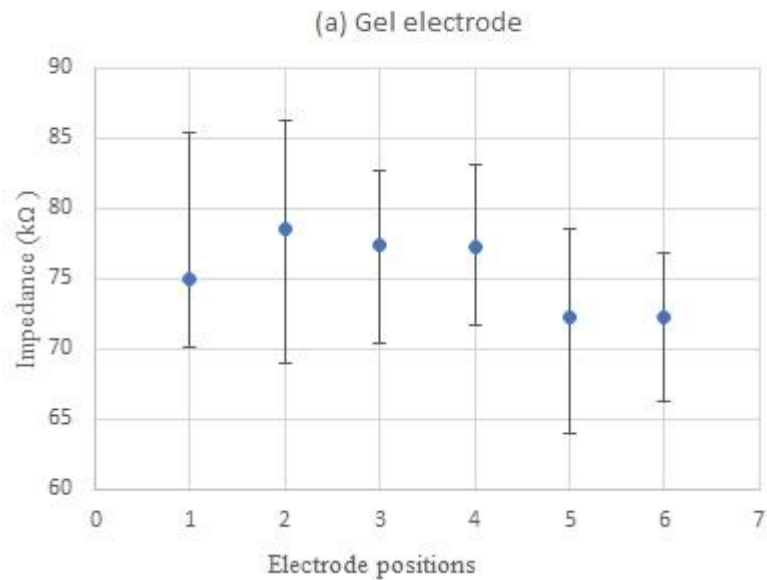


Figure 4.3 - Electrode positions on subject's forearm and assembled electrodes, front and back side.



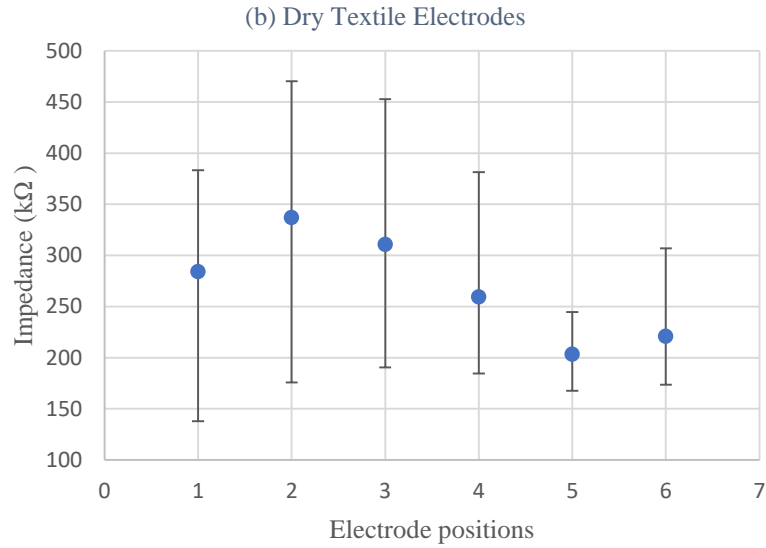


Figure 4.4 - Skin-electrode impedance at six different electrode positions on the subject's forearm. (a) Gel electrodes. (b) Dry textile electrodes.

Figure 4.4 displays the average value of skin-electrode impedance and the range of variation measured at six different electrode positions over the course of 10 days. For gel disposable electrodes, the difference in average impedance is relatively small with less than 7 kΩ at these six different electrode positions. The highest average impedance of 78 kΩ is shown in position 2, while positions 5 and 6 have the smallest value of 72 kΩ. The variation range of the gel electrodes is also relatively small with the value less than 18 kΩ and the standard deviation (SD) of the same electrode position is less than 7 kΩ. In contrast to gel electrodes, the results of the textile electrodes have large impedance variations. For the electrode at position 2, the impedance variation range of 300 kΩ and the average impedance value of 337 kΩ is the largest over the course of 10 days, as shown in Fig 4.4(b). In contrast, the electrode position 5 has the smallest impedance variation range of 77 kΩ and the smallest average impedance value of 203 kΩ. It is clear that different electrode positions lead to large differences on the average impedance value of textile electrodes, which could be as large as 133 kΩ, as shown in positions 2 and 5. Even at adjacent positions, impedance differences occur and could reach differences of 56 kΩ which can be seen in positions 4 and 5.

The results shown in Figure 4.4 highlight that the skin-electrode impedance alter with time and is specific to electrode position. Compared to the gel electrodes, the dry textile electrodes are more sensitive to position and also alter significantly with time. For textile

electrodes, these variations in the impedance caused by positioning cannot be ignored. The impedance variations caused by electrode positioning could be errors attributed to differences in electrode properties. To solve this, consistent electrode positioning can be achieved by designing and developing electrode-holding apparel such as a belts, bras or sleeve. If the garment is a close fit to the person and not affected by body movement, then the electrode will be positioned accurately in the same place each time it is worn.

#### ***4.1.2 The effect of electrode holding pressure on the skin-electrode impedance***

It is necessary for electrodes to be held tightly onto the skin in order to reduce the disruption in the skin-electrode interface and to ensure signal stability. Normally electrodes are being held in position by the use of adhesive foams, clamps, and suction bulbs. However, end user wearable requirements dictate that textile electrodes can be fixed in position by using pressure from garments. Ideally, a high electrode-holding pressure can lead to a steady and tight contact between the skin and the electrode. But higher holding pressure is not always better, as comfort needs to be considered as well.

Hence, an investigation was set up to identify the optimum, and comfortable electrode-holding pressure to the body. It has been determined that any garment pressure over 6 kPa [116] could result in discomfort for the wearer and influence the blood flow through the skin. Consequently, the electrode holding pressure selected in this experiment was ranging from 0.7 kPa (5mmHg) to 6 kPa (45 mmHg). A pair of textile electrodes measuring 15mm x 15mm was used to investigate the skin-electrode impedance under different electrode-holding pressures, adjusted using an elasticated band with Velcro strap. The electrode-holding pressure was measured using a PicoPress compression measurement system (Microlab Electronica, Italy) as shown in Figure 4.5. The skin-electrode impedances were measured at 100 Hz by the LCR Bridge meter (HM8118, HAMEG instruments, Germany) after the electrode stabilisation period of 3 minutes.

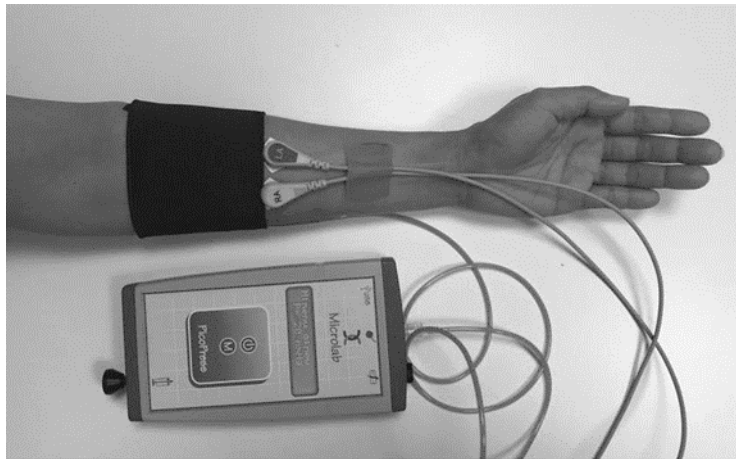


Figure 4.5 - The electrode holding pressure measurement setup

This experiment used two different electrodes; commercial disposable gel electrodes (2228, 3M, Minnesota, USA) and dry textile electrodes using the same conductive fabric, MedTex™ P-130 (Electrode 1). The performance of gel electrodes and dry textile electrodes under altered electrode-holding pressure were found to be very different. Figure 4.6 illustrates the relationship between skin-electrode impedance and electrode-holding pressure. The increase in the holding pressure of textile electrodes results in a very clear decline in the skin-electrode impedance. Also, the average impedance was reduced from 195 k $\Omega$  at 5 mmHg to 151 k $\Omega$  at 45 mmHg, while the impedance variation caused by those pressure changes is almost 45 k $\Omega$ . Likewise, the variation range of the textile electrodes was also reduced from 56 k $\Omega$  at 5 mmHg holding pressure to 21 k $\Omega$  at 45 mmHg holding pressure. In contrast to textile electrodes, the gel electrodes were insensitive to pressure changes with a slight fluctuation of approximately 0.5 k $\Omega$ . One of the reasons for this could be the presence of conductive gel on the wet skin-electrode. Therefore, the electrode-holding pressure is more important for dry textile electrodes than for gel electrodes. Increasing the textile electrode-holding pressure can lower skin-electrode impedance, as well as diminish the impedance imbalance among two electrodes.

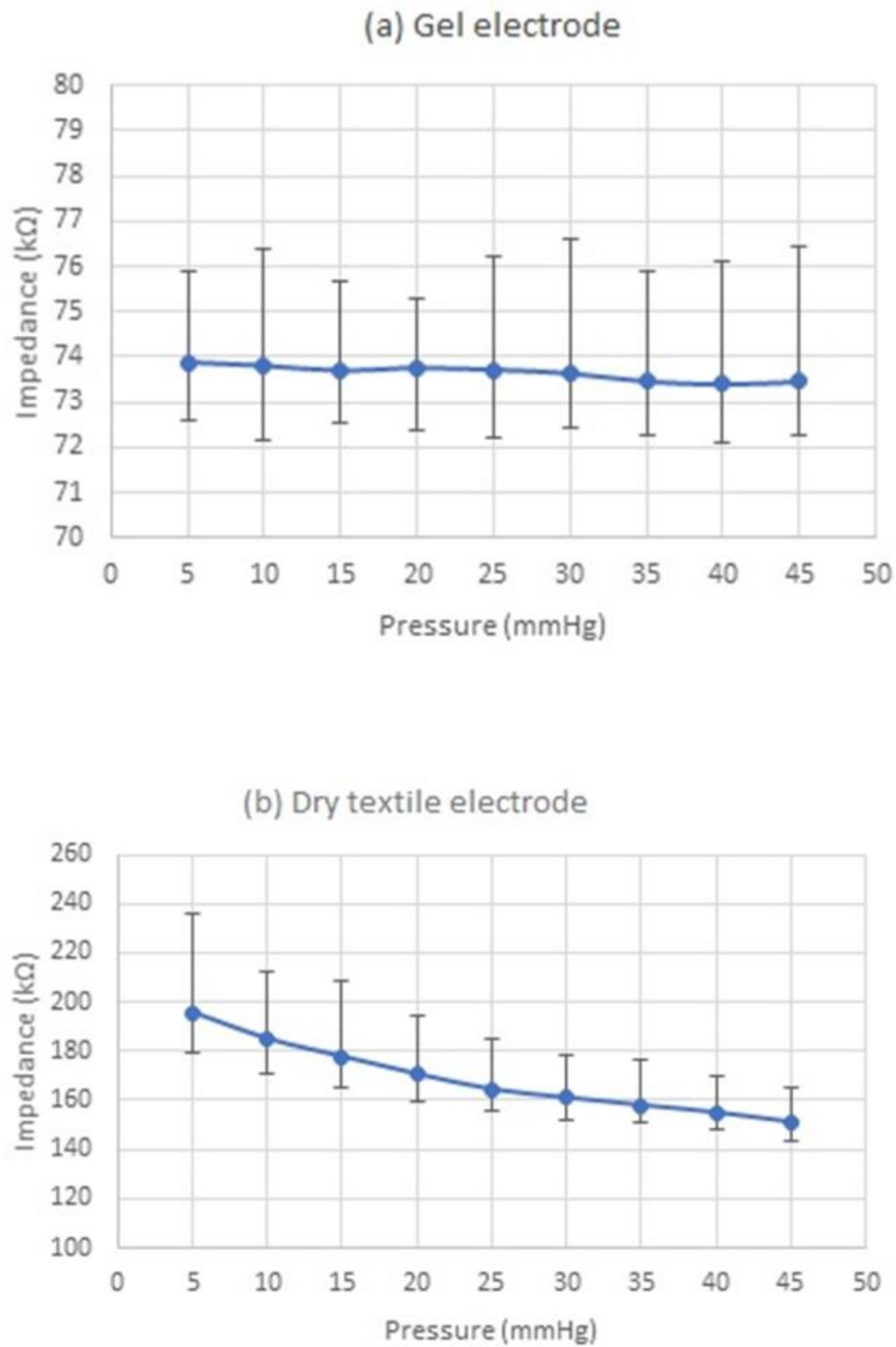


Figure 4.6 The variation of skin-electrode impedance on electrode holding pressure, (a) Gel Electrodes, (b) Dry Textile Electrodes

As a result, to achieve body sensory comfort and low skin-electrode impedance, 30 mmHg (4 kPa) was selected as an optimal electrode-holding pressure for further investigations. This is because the subject starts to feel uncomfortable at a pressure of over 30 mmHg (4 kPa), while the decrease in impedance appears to be insignificant.

## 4.2 Investigation of textile electrodes for ECG measurement

### 4.2.1 ECG Electrode mounting design and electrodes placement consideration

It is essential that consideration is given to the most appropriate positioning of the electrode within the garment. Based on the ECG measurement, there are various electrode positioning systems as mentioned in section 2.6. The body guidelines of standard electrode positioning of 12-lead ECGs by the Society for Cardiological Science & technology (SCST), 2022 is detailed in Table 4.1 and the performance of ECG electrode placement around the limb and chest area have been defined with the relevant anatomical landmark as shown in Figure 4.7.

Table 4.1- Standard electrode placement for 12-lead ECGs (SCST, 2022)

Electrode	Colour	Standard position
<b>V1</b>	Red	4 <sup>th</sup> intercostal space on the right sternal border
<b>V2</b>	Yellow	4 <sup>th</sup> intercostal space on the left sternal border
<b>V3</b>	Green	Exactly midway between V2 and V4
<b>V4</b>	Brown	5 <sup>th</sup> intercostal space on the left midclavicular line
<b>V5</b>	Black	Same horizontal plane as electrodes V4 and V6 on the left anterior axillary line
<b>V6</b>	Purple	Same horizontal plane as electrodes V4 and V5 on the left midaxillary line

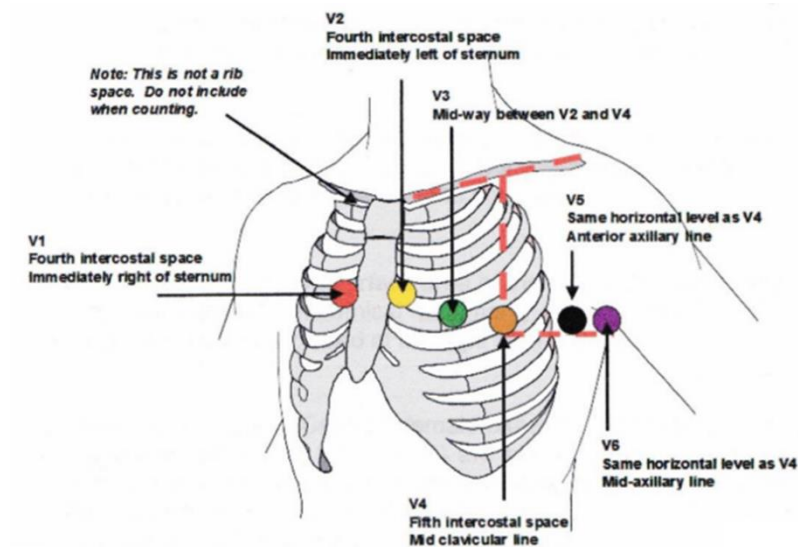


Figure 4.7 Standard ECG chest electrode position (SCST, 2022)



There are various studies relating to the optimum placement of ECG electrodes. Steijlen et al. [117] improved the diagnostic process with the design of a home-use 12 lead ECG system. The design had many features making it easy to use- including pre-formed arm straps, a system involving rollers for the easy movement of the wires and the replacement electrodes being incorporated into stickers which were provided on a sheet.



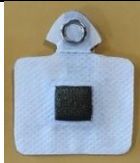
Crawford and Doherty [118] recommend that chest leads V4, V5 and V6 be placed underneath the breasts. For women with large breasts, it is important that the sensors are located under and not on top of the breasts to minimise the movement of the electrode, so giving a more stable signal. Kligfield et al. [119] also recommend that electrodes should be placed under the woman's breast and the horizontal level through V4 is placed at the fifth intercostal interspace. V5 is at midway between V4 and V6 which is conducive to offering good reproducibility. V6 should be the midaxillary line as extending along the middle of the thorax.

Based on the requirements for ECG measurement, 3-Electrode ECGs is a minimum number of electrodes to record the full PQRST wave [120]. In this study, in order to avoid motion artifact in the ECG signal, the area under the breast, as recommended was chosen, because the muscle movement is quite stable there and it does not cause undue disruption to the sensor under skin contact. Subsequently, electrode size and 3-lead electrode positioning has been investigated by testing two different formations, as described in Section 4.2.2 and 4.2.3 respectively.

#### ***4.2.2 Investigation of ECG Electrode Size***

Following the experiments on electrode positioning and pressure, the research moved on to investigate the textile electrodes for ECG monitoring. In this section, the ECG measurements were taken by comparing the textile-based electrodes in different sizes. It is known that the skin-electrode impedance is decreased when there is an increase in the electrode size. In addition, increasing the electrode size can also result in low noise being detected. In order to assess real performance on ECG measurement, sizes of the three textile electrode pairs were further investigated as shown in Table 4.2. The detailed specification of the electrodes are presented in Appendix A.

Table 4.2 - Experimental textile electrode size.

Size of electrode	Large Textile Electrode	Medium Textile Electrode	Small Textile Electrode
Shape of Electrodes			
Electrode Area (cm <sup>2</sup> )	8	4.5	2.25
Electrode Dimension (WxL,mm)	20x40	15x30	15x15

The experimental electrode 1 is of silver plated knitted conductive fabric (MedTex™ P-130, Statex shieldex), as already discussed. The same conductive fabric was chosen as reported in chapter 3, and the commercial or wet electrode (2228, 3M, Minnesota, USA) with a thin metal plate and electrolyte or gel internally embedded were used to measure the actual ECG signal. The Texas Instruments ADS1292ECG-FE demonstration kit, with only the 50 Hz notch filter active was used to filter out unwanted noise. All other filters on the instrument were switched off. In adults, the diagnostic information is contained below 100Hz [119]. Hence, a signal of 500Hz was used as the sample rate.

In order to avoid displacement of the electrode in breast, the electrode placement is chosen to be on the 6<sup>th</sup> intercostal space instead of the 5<sup>th</sup> intercostal space which are the electrode positions of V4, V5, V6. All electrodes were placed on the human body in the horizontal line of 6<sup>th</sup> intercostal, with the pressure of the elasticated band set at 4 kPa (30 mmHg), as illustrated in Figure 4.8. Prior to starting ECG recording, the skin-electrode interface stabilisation period of three minutes was followed.

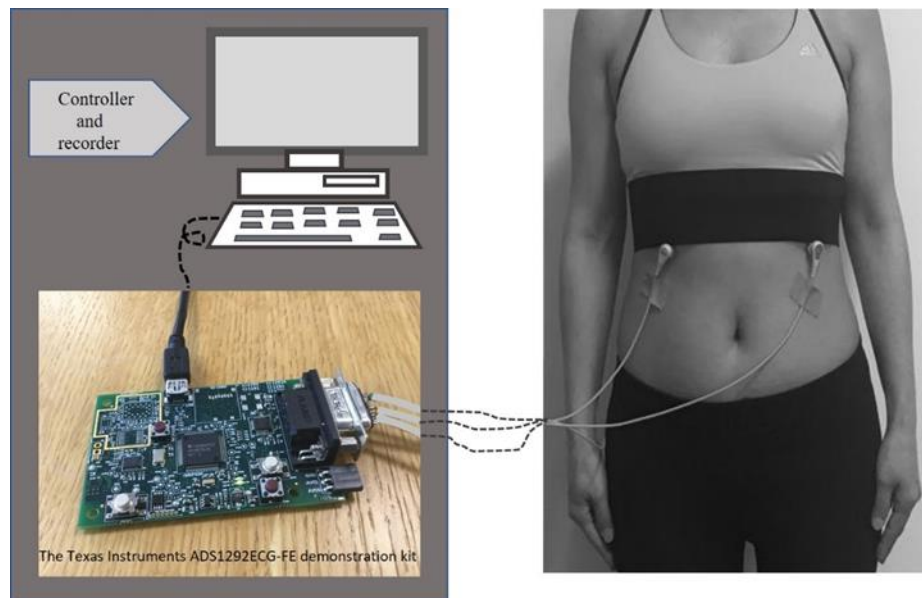


Figure 4.8 - Experimental set up of ECG measurement.

Figure 4.9 shows the recorded ECG signals obtained from three pairs of dry textile electrodes and one pair of commercial gel electrode. Baseline drifts can be seen in all ECG signals. This is due to body respiration which affects the change in body volume, causing skin potential imbalance. Apart from the baseline drift, noise can also be detected in all graphs because of the existing electromagnetic field in the subject's vicinity. As shown in Figure 4.9 (a), the small-size dry textile electrodes produced higher-frequency noise than the larger electrodes due to their high skin-electrode impedance. The ECG signal showed that dry textile electrodes produce more interference compared to wet electrodes. However, by increasing the electrode size, the quality of the ECG signal of the large-size is as good as the gel electrode in terms of low noise, as shown in Figure 4.9 (c) and (d). This reconfirms the results obtained in our preliminary test of the effect of electrode size on the skin-electrode impedance as presented in Appendix B. The results show that the skin-electrode impedance decreases when the electrode size increases, which is consistent with theory. It can therefore be seen that optimisation in dry electrode size is vital and hence the electrode size of 20mm x 40 mm was chosen as optimum.

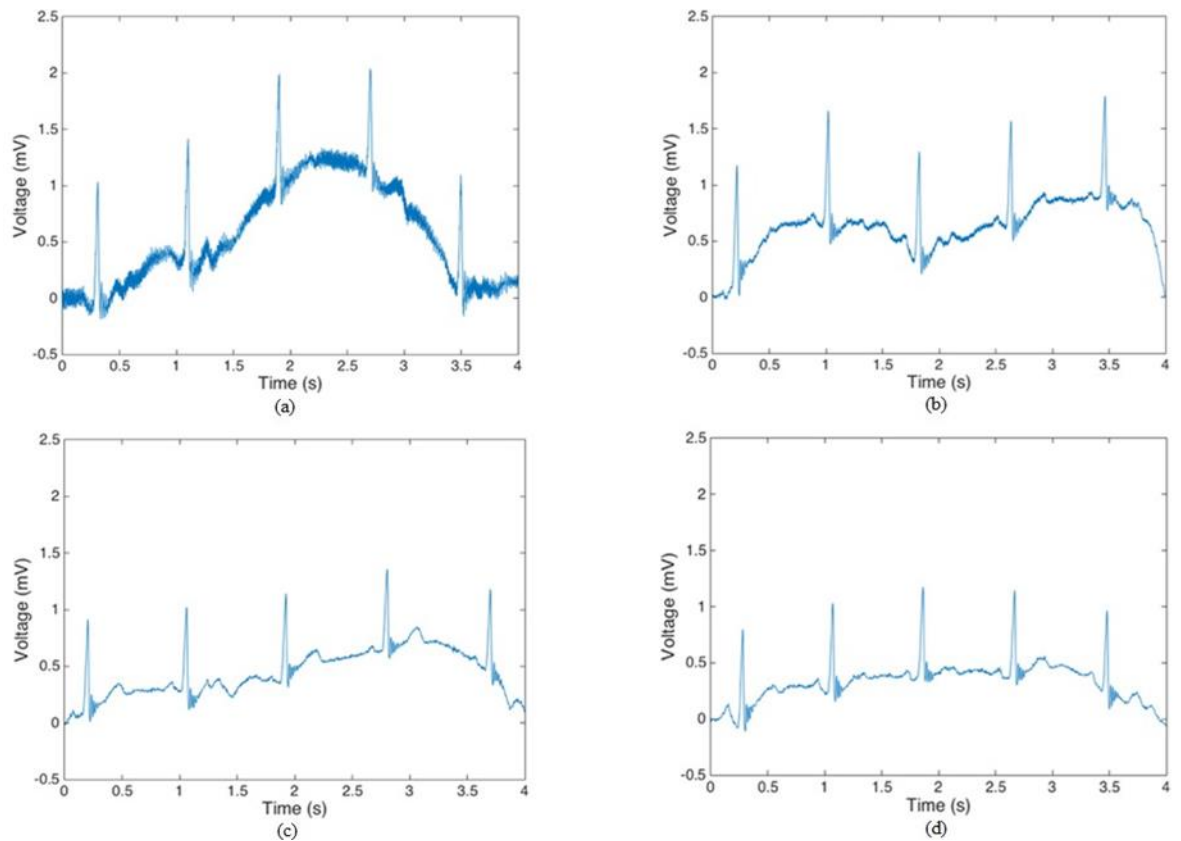


Figure 4.9 - ECG signals recorded under different electrodes. (a) Small textile electrode. (b) Medium textile electrode. (c) Large dry textile electrode. (d) Commercial gel electrode.

### 4.2.3 Investigation of ECG Electrode placement

In preliminary studies we investigated the ECG signals from various chest electrode positions were compared with two formations of 3-Electrodes configuration. Figure 4.10 shows the schematic drawings of two formations of 3-lead configuration in the horizontal level in front (Figure 4.10a) and back (Figure 4.10b) lead placement, in which, three electrodes are attached to the human torso, two of which act as the positive and negative poles while the third is a ground connection .

Figure 4.10(a) show the horizontal level in front (A), two electrodes are attached at the costal margins along the 6<sup>th</sup> intercostal space on right and left mid-clavicular line while the ground (G) electrode is placed at the epigastric region. (i.e. front horizontal formation). Figure 4.10(b) shows the horizontal level in back (B), two electrodes are placed along the 6<sup>th</sup> intercostal space on the right and left mid-clavicular, with one placed at the scapular line in the rear side (i.e. back horizontal formation).

The investigations were conducted with low support activity i.e. sitting, walking, jogging on flat ground and then walking and jogging up and down a 15 step staircase.

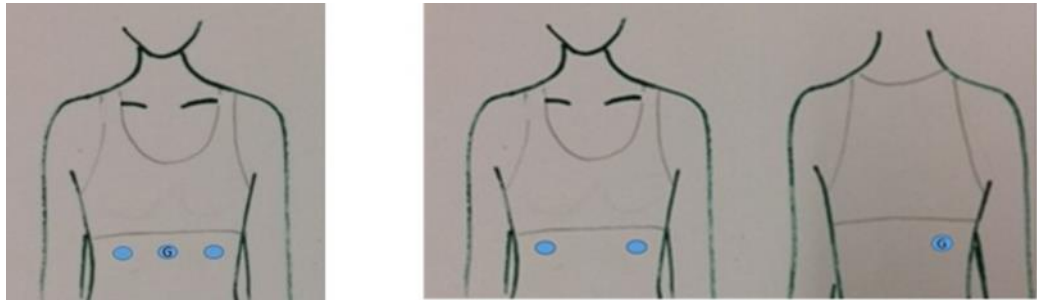


Figure 4.10 - ECG lead placements: (a) A, front horizontal formation; (b) B, back horizontal formation.

In the experiment, silver plated nylon conductive fabric, MedTex™ P-130 (Electrode 1) was used and three electrodes of previously determined optimum size 20mm x 40 mm were attached on an elastic belt fitted with the specifically designed electrodes to be worn around the costal margin (the chest's lower edge). The belt was of single jersey knitted fabric 50mm in width with fastening velcro straps on both ends. It was adjustable for different chest girths and was equipped with three metal snaps (in circle) for connecting to an ECG device, as can be seen in Figure 4.11. The detailed specification of the belt electrodes in these two formations is presented in Appendix C.

In this work, the prototype was made with the electrodes connected to a wireless Bluetooth Low Energy wearable ECG device [21]. It's light weight (only 9grams) and small size (30mmx37mmx5mm) and is connected to three ECG electrodes. The ECG signals are acquired, and the data is then transmitted wirelessly to a smartphone where further analysis of the ECG is carried out by a software app pre-installed on the phone, in which the ECG waveforms are displayed.

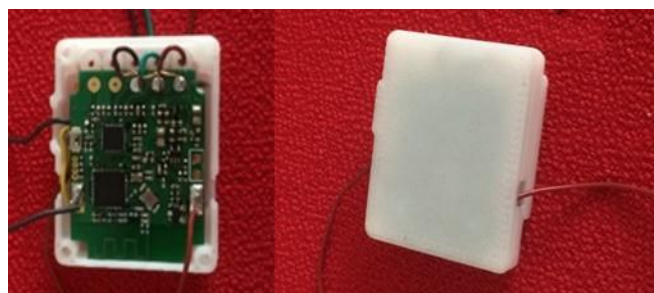


Figure 4.11- The low energy wireless ECG device.

The signals gathered by the electrodes are sent to the ECG device attached to the elastic belt which in turn wirelessly transmits the data to a smart phone in which a pre-installed app carries out analysis and shows the processed data in the form of PQRST waveform with corresponding values, as shown in Figure 4.12. The electrodes were fixed onto the selected locations around the respective body part (A and B formation,) with a pressure of 4kPa (30 mmHg).

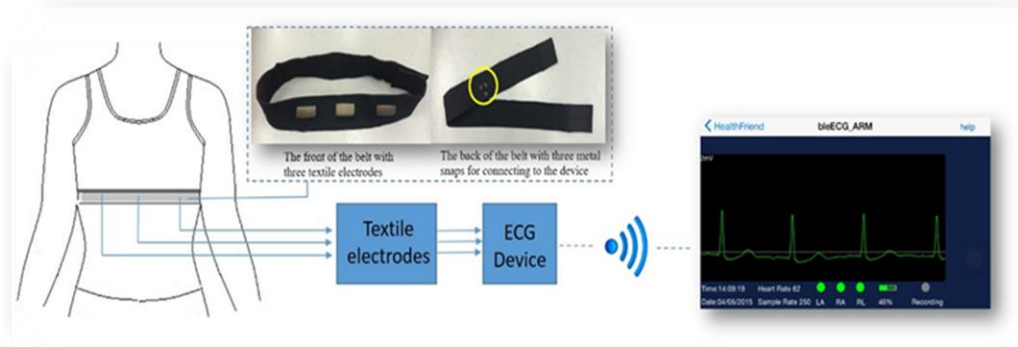


Figure 4.12 - ECG measurement processed with belt attached electrodes.

Having established the performance and optimum properties of the electrodes, further experiments were carried out to find the optimum design of the sports bra, which will be fully discussed in Chapter 6, and also questioning the ideal position of the electrodes. The resultant ECG waveforms are subsequently compared to determine the optimum positioning of the electrodes. The ECG readings from the two formations of electrode placement are provided in Table 4.3. For all activity types, the electrode potentials of the recorded ECG readings were within a 2mV range. Hence, the ECG measurement tests conducted produced high-quality signals for static postures that can be used to detect heart function. However, it was observed that in all activities, the ECG signal of electrode position B was more stable with less artefacts than electrode position A. The performance of the contact impedance of the ECG signals from electrode position A and B can be explained by the body changes in circumference during respiration [121]. In electrode position A (Figure 4.10a ), all electrodes are located on the front of the body, with a large amount of movement in the chest wall and abdomen, leading to a significant level of motion artefact [122]. Whereas, in electrode position B (Figure 4.10b ), much less movement occurs during respiration, resulting in negligible motion artifacts and the ECG

signal is better, with more consistent contact between the electrode and the wearers skin than position A.

Table 4.3 - The ECG readings from the two formations of lead placement

Activity	Lead placement	
	A	B
Sit		
Walk		
Jogging		
Walk Up-down stair		
Run Up-down stair		

### 4.3 Summary of the Results and Conclusions

In this chapter, the effects of skin/electrode mechanical interaction were evaluated and established by measuring ECG signals on the human body. These studies show that the skin-electrode impedance can be effectively reduced by increasing the electrode size in which the largest electrode-skin interface area, 20mm x 40mm had a better ECG signal performance and the electrode-holding pressure, 4kPa (30mmHg) was determined as giving optimum body comfort with low skin-electrode impedance. A three-minute electrode stabilization period is required before any signal recording is performed, in order to reduce electrode imbalance.

Another notable aspect found in this study was that the impact of electrode position on skin-electrode impedance is important. Frequently, researchers measure different types of electrodes on the subject's leg or forearm, and then compare the result of skin-electrode impedance differences. In this study, testing on the subject's inner forearm shows that the average impedance variation between two electrodes positioned 10mm apart can be as large as 56k $\Omega$ . This shows that high variations in skin impedance can occur even between two positions on the body that are very close to each other. The failure to determine whether the impedance variation is influenced by the electrode position, or whether the impedance variation is caused by the electrical properties of the skin or by the electrode properties, can lead to an error in the analysis and comparison of different electrode types. The work concludes that ECG measurement is influenced significantly by electrode position and it was determined that the back horizontal formation (Figure 4.10b) gives clearer and more reliable signal data than the front horizontal formation (Figure 4.10a).

In conclusion, this research has revealed that flexible and wearable textile dry electrodes are suitable for monitoring ECG signals, under optimum conditions and without skin preparation. Uniform electrode positioning has been achieved using close fitting electrode-holding apparel, which is further investigated in Chapter 6. Consistent skin properties prior to testing can be achieved by having a suitable stabilisation period of three minutes. The optimum electrode size is 20x40mm, and the optimum holding pressure 4 kPa (30 mmHg). The work concludes that the results from the textile electrode are as good, and in some cases better than the gel electrode, while at the same time achieving much better flexibility, comfort and user convenience, and more importantly continuous measurements that the wet electrodes cannot.



## Chapter 5 – Investigation of A Stitch-Based Stretch Sensor

Textile-based sensors are deemed to be practical and desirable to wearable end uses because of their flexible, comfortable, and non-obstructive properties. One of the fascinating applications of a stretch sensors is their ability to change their mechanical properties under strain/stress deformation. Several researchers investigated and developed polymers and others textile-substrate based sensing to determine the optimal properties of the materials to be used as stretch sensors. Compared to other types of fabrics, Kim et al. [123] and Wu et al. [124] suggested that elastic textile composites are suitable to be used as a stretch sensor for large deformation. Others reported that the best wearable material for creating a good stretch-sensor is a knitted fabric [123, 125-128], because of its elastic properties and its flexible structure that can fit closely to the human body. Despite these efforts, however, a systematic study is needed to assess the interacting properties to the efficiency of stretch sensors and to focus on structural requirements that may progress the replacement of IC type sensors with E-textiles. In this respect the stitching structures and their efficacy has been investigated as they are so closely related in the making up of wearable sensing garments. It is important also to consider that the properties that constitute these materials have a significant impact in the fabrication and performance of a stretch sensor.

Primarily, a stretch sensor is used for sensing and monitoring body movement parameters. As the textile comes into contact with the skin, its compressibility and flexibility is capable to take up the full body curvature following its geometry as it can drape and wrap around it. Other studies on stitched stretch sensors have been performed [79, 87, 103, 129, 130] showing that many sensors still have practical limitations such as lack of sensitivity, large hysteresis and small working range. The operating range of the substrate material is also an additional and important parameter that affects the performance of the sensor.

This work is therefore carried out to present new knowledge in the field as it focuses on establishing a novel textile stretch sensor capable of being used in any garment and having good performance; sensitivity, small hysteresis, repeatability and working range. The sensor types we have investigated here are focusing on wearable end uses where sensors are part of a body sensor network in a garment, which acquires, processes information and transmits it wirelessly.

In this chapter, the key objective is to explore the development of a textile stretch sensor for wearable devices. The optimum design of such a sensor is investigated in different types of stitch structures, along with its flexibility and elastic properties, and its ability to measure strain deformation and electromechanical properties. In order to understand the electrical properties and performance necessary to develop stitch-based stretch sensors, the suitability and reliability of various sewing stitches has been examined, in particular, stitches with a good stretching ability, such as the zigzag stitch, the multi thread chain stitch, the overlock stitch and the cover stitch. Simplicity and low cost are also taken into account as well as ubiquitous and unobtrusive good wear and comfort. Conductive threads are used to construct the sensor by sewing them directly onto a suitable knitted fabric acting as a substrate. The experimental methodology can be divided into two phases: Phase I and Phase II as illustrated in the following:

Phase I: A fabric-substrate used for the sensors was examined and measured. The elasticity and recovery of knitted nylon fabrics containing different amounts of Spandex was investigated. In order to determine their performance, the evaluation of ideal elastic property of the fabric substrate was established, taking into consideration its extended and relaxed states, and its linear response to stress/strain loading/unloading cycles. The experimental results examining the stretching and recovery properties were compared in terms of coefficient of determination ( $R^2$ ) and then used to assess the suitability of the materials to be used as a textile-substrate-based sensor, with which a stitch stretch sensor will be constructed.

Phases II: This phase is dealing with the physical evaluation of the usability and performance of the sensor which is made of conductive thread (the fabrics were stitched together). Four elastic garment stitches were carefully studied by examining their conductivity and sensitivity. Three of the stitch types were tested with two thread types each, and one stitch type was tested with only one thread type (seven samples in total). The basic properties of these threads are already reported in Chapter 3. They are easy to work with, flexible and strong for normal stitching and having good electrical performance.

The tested stitch types were: 304 (used one thread type), 406 (used two thread types), 506 (used two thread types), and 605 (used two thread types). The conductivity of the stitches was examined by using cyclic testing which investigates the change in electrical resistance by mechanical strain.

## 5.1 Part I: Fabric-substrate based sensor

The ideal features of a stretch sensor for wearable applications were investigated by combining the composite material with either Spandex or Lycra fabric [41, 77, 94, 131]. It was concluded that Lycra as a core yarn has a high resilience and low strength, compared to core yarns containing other types of textured filaments [132]. Gioberto and Dunne [103] compared the sensor response of two different fabric-substrate sensors: fabrics with elastomer and without elastomer. The results showed that elastomer-coated fabric exhibits a smaller change in the sensor responses than the knitted fabrics with no elastomer. However, the amount of elastomer composition was not determined. Scilingo et al. [133] produced stretch sensing fabrics by using polypyrrole and carbon loaded rubbers to coat Lycra/cotton fabrics. These stretch sensing fabrics showed a strong variation of strain-resistance with time, as well as a high response time to the mechanical stimulus.

Guo et al. [84, 94] designed knitted fabric sensors for breathing applications by using PA/Lycra to enhance the elasticity and recoverability. It claims that these capabilities reduced plastic deformation, and hence the hysteresis of sensors is reduced. Campbell et al. [134, 135] concluded that Polypyrrole-coated Nylon-Lycra is suitable for use in a fabric substrate which, in a wearable device, can be used to measure movement of the body, such as the limbs and respiration movements. Lorussi et.al. [136] explained that the characteristics of metal coated Lycra polyurethane-coated fabrics demonstrate piezoresistive effects, and therefore is suitable to be used as wearable sensors.

This work is more comprehensive than studies carried out by others on stretch-sensors, in that it explores in more depth the importance of choosing the optimum textile substrate before the conductive stitch is sewn in, and then it goes on to test seven different stitch structure types on that optimum substrate, giving conclusive results based on much wider data collection than in others works. The findings of the materials' relative properties suitable as a stretch sensor are as follows.

### 5.1.1 Materials

To qualify a textile for use as a fabric substrate-based sensor, the physical fabric properties should be closely related to sensor properties. If textiles have low resilience, they cannot recover back to their original state, and hence they are not suitable for sensing. Although there are many studies on the physical properties of textiles blends with Spandex, there has been little research regarding the properties of fabrics containing different percentages of spandex yarns in relation to sensing.

Weft knitted single jersey fabric is considered for use as the textile substrate because it has high stability and high elasticity which have been proved by many researches [136]. The intertwined characteristic of the knitted loops gives the fabric a high degree of stability, stretch and tensile strength. This structural feature of the intertwined loop avoids the dimensionally weak and unstable characteristic associated with most other types of fabric which do not employ this intertwined loop feature.

Hence, preliminary studies on the suitability of fabrics were performed to find the ideal base fabric. The fabric properties in relationship to elasticity and recovery properties were examined. Six fabric samples made of Nylon fabric containing spandex were knitted. Two Nylon yarns count 4.44 tex/two-ply and 7.78 tex/two-ply were knitted with three spandex yarns of 2.22, 4.44, and 7.78 tex respectively. Nylon/Spandex fabrics were knitted into a single jersey structure using a 28-gauge circular knitting machine. Pacific Knitting Factory Co., Ltd, Thailand supported this work by producing the fabrics for this study. The fabric specification is shown in Table 5.1.

Table 5.1 - The experimental single jerseys fabrics specification

Nylon Yarn count (Tex)	Fabric Sample	Spandex Yarn count (Tex)	Content Nylon/Spandex (%)	Weight g/m <sup>2</sup>	Thickness mm.	Yarn density per cm	
						Courses	Wale
4.44 / two-ply	A	2.22	91/9	212	0.60	24	34
	B	4.44	88/12	223	0.60	23	33
	C	7.78	75/25	260	0.55	20	39
7.78 / two-ply	D	2.22	94/6	286	0.65	19	33
	E	4.44	93/7	313	0.65	19	36
	F	7.78	83/17	323	0.60	18	33

### 5.1.2 Experimental procedure

To examine the performance of knitted fabrics used for substrate-based sensors, a tensile test was conducted to investigate the mechanical properties of the fabrics based on British Standard BS EN 14704-1:2005, to determine the elasticity of the fabric. In order for the elastic modulus to be in line with the human body movement, the extension and recovery by 50% is used for each specimen to simulate human movement in elastic fabrics or garments – which are undergoing 10-45% stretching caused by movement of different body parts [137].

The experimental setup used an Instron tensile tester that vertically stretches the fabric sample, the fabric specimens were cut in both the course and wale directions 50mm x 250 mm. The specimens were individually held in place 50 mm away from either end of the sample, leaving the middle section of 150mm gauge length free for measurement as illustrated in Figure 5.1. To determine the relationship between force and extension, the 150mm-long fabric specimens were subjected to a tension load (stretching) until their elongation reaches 225 mm. Then, the stretched specimens were gradually unloaded (retracting) until getting back to their original position. The cycle (stretching and retracting) is repeated 100 times at the rate of 200mm/min, a rate which is comparable to typical human body movement [105]. The experiment was conducted at a room temperature of  $20^{\circ}\pm 2^{\circ}\text{C}$  and with relative humidity of  $65\% \pm 2\%$ .

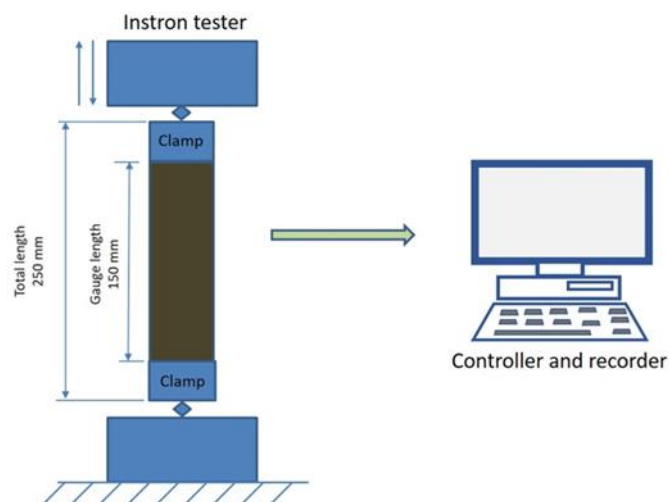


Figure 5.1 - Tensile testing set up.

### 5.1.3 Experimental Results

In order to study the tensile properties and elastic recovery, ER (%) of knitted fabrics, six different nylon/spandex sample fabrics were investigated. Dynamic loading is used to investigate the stress strain behaviour of the fabrics, as the extension is caused by fabric loading. When the load is applied onto a fabric, part of that energy will deform the yarn loop and part of that energy will stretch the yarn.

Fabrics containing Spandex are expected to behave like a spring – meaning that they should have a tendency to recover to their original size and shape when the tension is released. Nevertheless, it is known that textile fabrics do not have complete recovery and that their behaviour is nonlinear. During the experimental testing, all fabrics were stretched until they reached their ultimate extension (50%) and then the load is removed for the fabrics to recover. The fabrics did not immediately return to their original dimensions –hysteresis caused by friction- as illustrated in Figure 5.2. The reason for this phenomenon is because the fibres in the sheath of the weft yarn exert transversel pressure on the spandex core, causing friction to increase and hence preventing the total recovery of the yarn [138]. The results of ER (%) of the six fabrics under investigation in both walewise and coursewise directions are displayed in Figure 5.3.

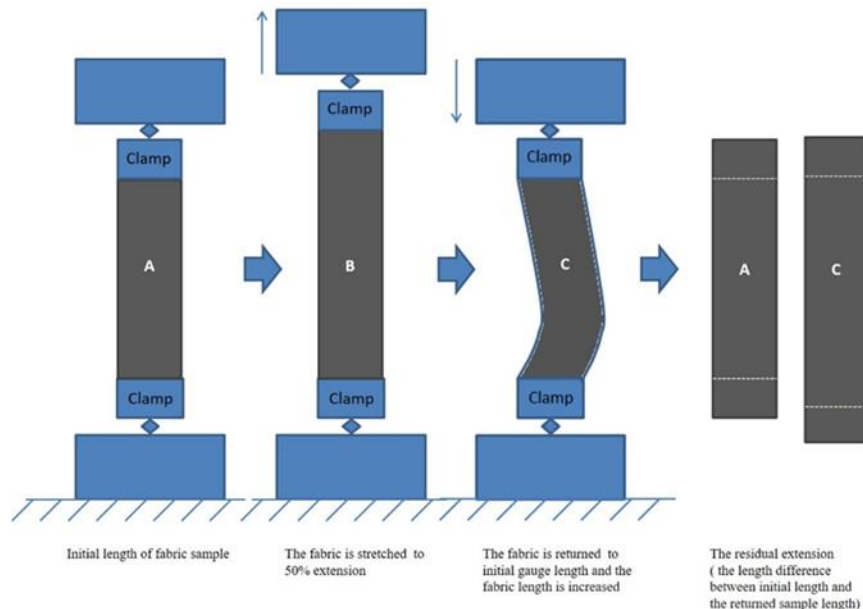


Figure 5.2 - The residual extension of fabric sample after the load is removed.

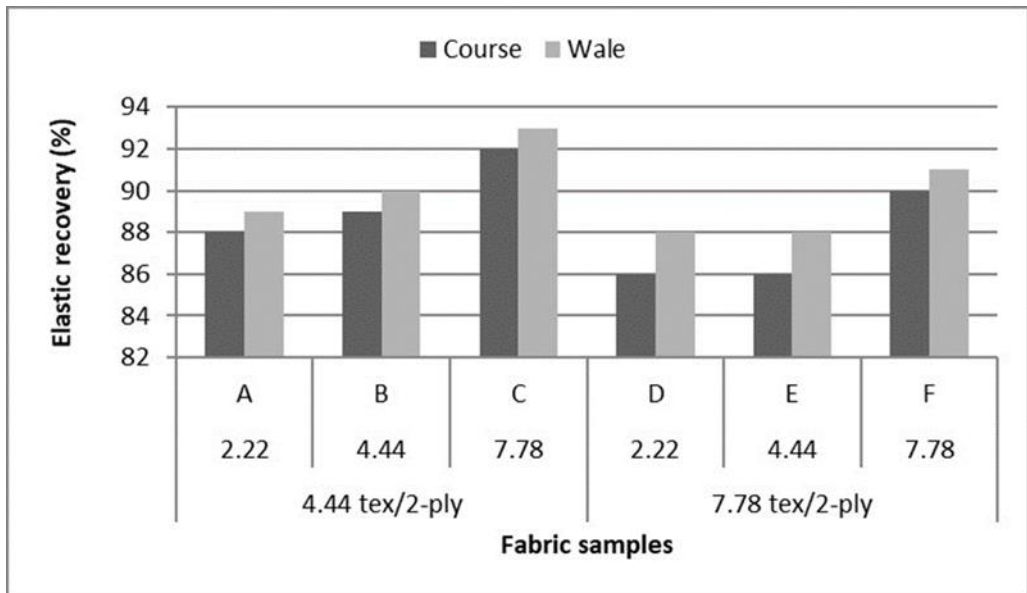


Figure 5.3 - Elastic recovery values of six various nylon/spandex sample fabrics in course-wise and wale-wise direction.

Results of the recovery behaviours of fabrics have presented a positive correlation between spandex content and elastic recovery. The tensile load is proportional to the strain within 50%, with coefficients of determination ( $R^2$ ) being in the range of 0.86~0.93, for all of the samples. It can be seen that fabric recovery is increasing with the increase in spandex content, which is consistent with previous study [139]. Fabric sample C is exhibiting the highest ER value during these experiments ( $R^2=0.92$  and  $R^2=0.93$  in course and wale direction respectively), followed by fabric sample F which is also showing high ER value ( $R^2=0.90$  and  $R^2=0.91$  in course and wale direction respectively). In case of samples A and B the ER values were higher than samples D and E, with the latter exhibiting similar values.

Overall, it could be deduced that the spandex substrate fabric had an effect on improving stretch and recovery property of fabrics. The results show that fabric recovery is dependent on spandex content, which is to be expected since we are increasing the fabrics elastic behaviour. It can therefore be concluded that a higher elastane content in the yarn corresponds to a higher recovery rate, as expected [140]. Hence a single jersey of Nylon 4.44 tex two-ply with Spandex 7.78 tex and weight of 260 g/m<sup>2</sup> (Fabric C from Table 5.1) was used based on its superior performance in our experiments. It is selected because it has a high elasticity and recoverability (93%), as seen in Figure 5.3 and hence is most suitable for use as a fabric-substrate based sensor in this experiment.

## 5.2 Phrase II: Stitch Sensor Construction

Conductive materials and sensors have been researched and developed in accordance to their application. A stretch sensor for wearable monitoring requires a sensor, whose shape can change with body movement, to produce a repeatable electrical resistance, ideally in a linear manner. For the manufacturing of stitch stretch sensors, the primary focus is to establish a stitch that has good elastic properties. To fulfil these requirements, the following stitches were investigated which are widely met in garment design and production.

### 5.2.1 Garment stitch structures

#### (a) Stitch class 300, stitch type 304 Zigzag stitch

The stitch class called lockstitch is formed by interlacing the two threads. One thread is called needle thread (upper thread) and the other bobbin thread (lower thread). Figure 5.4 illustrates how the threads are passed through the fabric from needle thread (1) to bobbin thread (2).

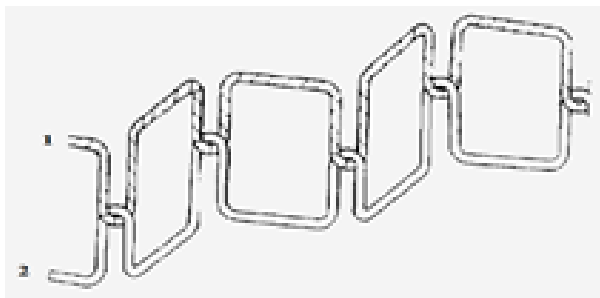


Figure 5.4 - Stitch formation by interlacing of zigzag (BS 3870-1).

The Zigzag stitch type 304 is a member of the lockstitch family, which is mostly used for stretchable garments such as for sportswear and underwear. This type of stitch is extendable and has higher strength and stability in fabric structures, thus allowing flexibility and comfort. The zigzag stitch, is also easy to produce.

#### (b) Stitch class 400, Multi thread chain stitch

This stitch class is called multi thread chain stitch, consisting of three types: 401, 404 and 406, mainly used for its increased elastic properties in waist bands and for decorative stitching on belts. This stitch is formed with two or more sets of thread. One set known



as a needle thread which passes through the fabric, while another set called double chain is secured by interlacing with the thread loops as illustrated in Figure 5.5.

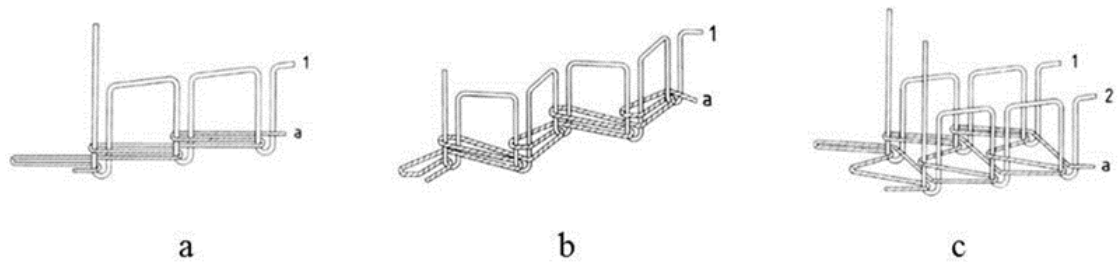


Figure 5.5 - Multi thread stitch; (a) Stitch type 401; (b) Stitch type 404; and (c) Stitch type 406 (BS 3870-1).

(c) Stitch class 500, overlock stitch

This stitch class, known as overlock, is formed from loops with one or more sets of thread cones that cover the edges of fabric within the seam. The intersection of one or two needles retains the thread in place on both sides of the seam. This stitch is used for the fabric edges, which have been cut off by the machine knife and hence stitches can overlock and cover the cut fabric edge. Figure 5.6 shows how the thread loop forms the seam. The overlocking stitch has a smooth surface, and is extensible and versatile. The members of this stitch class 500 are overlock stitch types 505 and 506, which are mostly used for seaming, hemming and edging in a variety of mainly knitted fabrics.

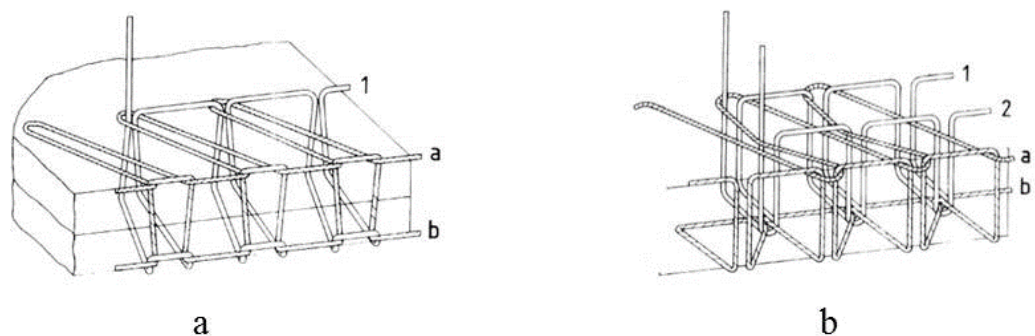


Figure 5.6 - Overlock stitch; (a) stitch type 505; (b) Stitch type 506 (BS 3870-1).

(d) Stitch class 600, Cover stitch

This stitch class is called a cover stitch or a flatlock stitch, formed by one or more sets of thread. It consists of three types: 602, 605 and 607 as show in Figure 5.7, which are used for knits, elastics, binding, lingerie, decoration, etc. The first set of thread is a needle thread, the second one is a top cover thread, and the third one is a bottom cover thread. Threads of two sets can be observed from either side.

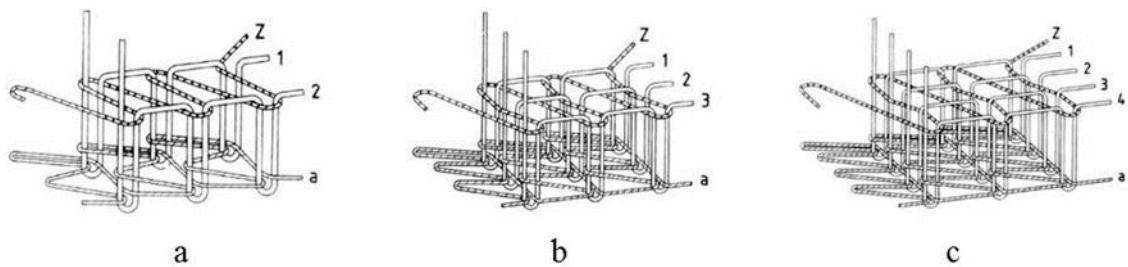


Figure 5.7 - Covering chain stitch; (a) Stitch type 602; (b) Stitch type 605 and (c) Stitch type 607 (BS 3870-1).

### 5.2.2 Materials

The stretch sensor is formed by using conductive thread and is constructed using stretchable fabrics which as already mentioned, allowing the stitches to be flexible, unobtrusive, and elastic. Fabric C, Table 5.1, as already revealed; single jersey made of Nylon 4.44 tex two-ply with Spandex 7.78 tex and weight of 260 g/m<sup>2</sup> is used as a fabric-substrate based sensor.

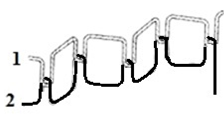

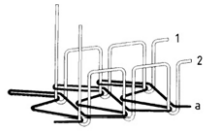
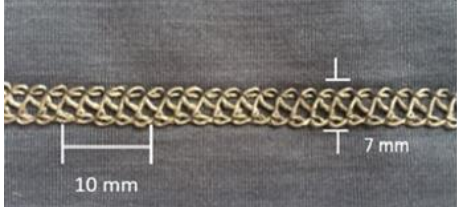
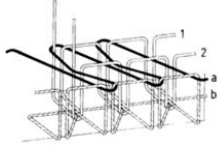

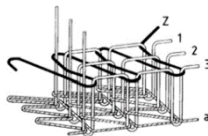

The experimental samples were sewn by stitching along the wale direction of the fabric using silver plated nylon conductive thread 117/1/ two-ply and 235/34 four-ply. These threads were selected for their proven good conductivity and stability. The properties of these threads are reported in detail in Chapter 3. Seven samples 50mm x 250 mm in size and four stitch types-304 (Zigzag stitch), 406 (2-needle multi-thread chain stitch, rear side), 506 (4-threads overlock stitch), and 605 (3-needles covering chain stitch) were constructed.

### 5.2.3 Experimental sample

Preliminary tests indicated that the stitch density of the assembly must follow commercial norms to achieve acceptable sewability with the conductive thread. Hence for the consistency of testing, three of the four stitch types with the same dimensions (5 stitches per cm and 7mm wide) were used. Stitch type 304, because of its design required different dimensions; 11 stitches per cm and 3mm wide, as shown in Table 5.2, the conductive thread being indicated by the black line in the stitch structure.

Throughout the experiment, stitch structure 304 was sewn by the PAFF® creative 4.5 sewing and embroidery machine. It could only be realised with silver plated nylon conductive thread 117/17 two-ply (33 tex). The silver-plated nylon conductive thread 234/34 four-ply (92 tex) causes fabric distortion due to this particular stitch geometry and for needing higher tension.

Table 5.2 - The experimental stitch structure for sensor design.

Stitch Type	Stitch Structure	Stitches per 10mm	Stitch Width (mm)	Close-Up of the Stitched Samples
304		11	3	
406		5	7	
506		5	7	
605		5	7	

#### 5.2.4 Experimental procedure

Sensor performance was evaluated by measuring their conductive properties, caused by the resistance changes in response to deformations that occur during stretching and relaxing. The measurement of extension and recovery cycles is performed in order for the performance of a sensor to be characterised. Figure 5.8 shows the experimental apparatus and set up. The sensor samples were clamped between the jaws of the tensile tester (Instron 3345) and the two ends of the sensors were connected to digital multimeter probes (DMM Agilent U1273A/U1273AX, Agilent Technologies, Inc. Santa Clara, CA 95051 USA). These probes were used together with logging the Agilent GUI Data Logger software controlled by a PC to record the variation of the electrical resistance response which was initially measured during extension and recovery cycles, at a sampling rate of 1 Hz. The jaws were electrically isolated from the fabric sensor with a layer of synthetic polymer rubber, so that only the resistance of the sensor itself would be measured by the multimeter. The jaws were set 150 mm apart and 250 mm long in the sensor direction (50mm is needed at either side of the sample for clamping, according to British Standard BS EN 14704-1:2005 test method, to determine the elasticity of the fabric).

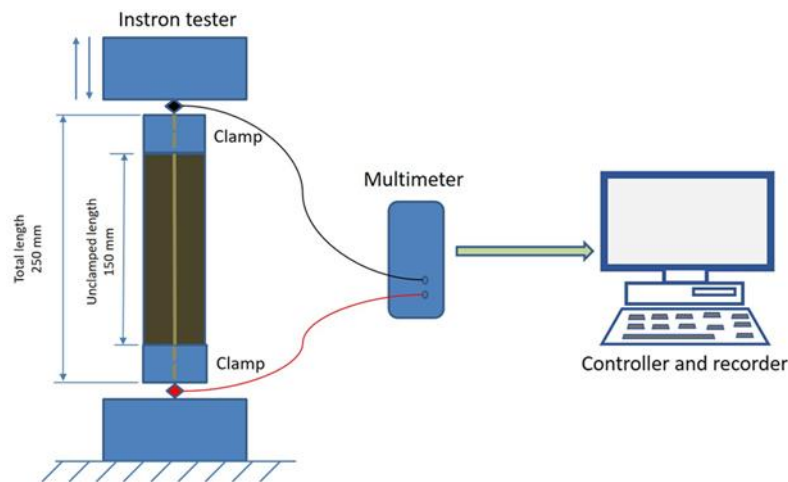


Figure 5.8 - Experimental setup.

Data from the tensile tester and multimeter were subsequently aligned and overlapped using digital timestamps. Each cyclic test is carried out at the rate of 200 mm/min and at 50% extension in 10 cycles. Further tests of 100 cycles were conducted in order for the repeatability of sensing performance of the sample sensor to be observed.

The experiment was carried out under standard atmospheric conditions of temperature and humidity at  $20^{\circ} \pm 2^{\circ}\text{C}$  and  $65\% \pm 2\%$  R.H. All samples were conditioned in the lab for 24 hours prior to testing, to achieve uniform temperature and humidity properties.

### 5.2.5 Data Analysis Procedure

In this section, the different sensor characteristics derived from the raw data is described, with reference to Figure 5.8, illustrating the sample clamping arrangement in the tensile tester jaws. The analysis of raw data from the stress/strain measurement was then conducted to convert extension and resistance into strain (%) and percentage resistance change (%), as shown below:

$$\varepsilon = \frac{\Delta l}{l}$$

$$\text{Resistance Change (\%)} = \frac{\Delta R}{R} \quad (1)$$

where  $\Delta l$  is the extension value from the tension tester and  $l$  is the unstretched gauge length taken from Figure 5.8 (150 mm). The calculation of the percentage resistance  $\Delta R$  change was more complex, since in this study, we are only interested in the percentage resistance change of the stretching portion of the sensor but not the portion within the jaws. The portion in the jaws provides a fixed additional resistance, known as the ‘resistance bias’. In the unstretched state, the assumption was that the sensor has an approximately uniform resistance per mm length. Thus, the resistance of the clamped portion (the resistance bias), is given by:

$$R_{bias} = (\text{proportion of length in clamps}) \times (\text{total unstretched resistance}) \quad (2)$$

The proportion of length in clamps is taken from Figure 5.8 as 0.4 (100/250mm), while the total unstretched resistance is different for each stitch and was taken as the resistance at time = 0 (the first data sample). The resistance bias is subtracted from all resistance data samples to give the resistance of the unclamped portion at any one time. To calculate the percentage resistance change, an ‘original’ or ‘baseline’ resistance is required. Figure 5.9 displays a typical plot of resistance vs time.

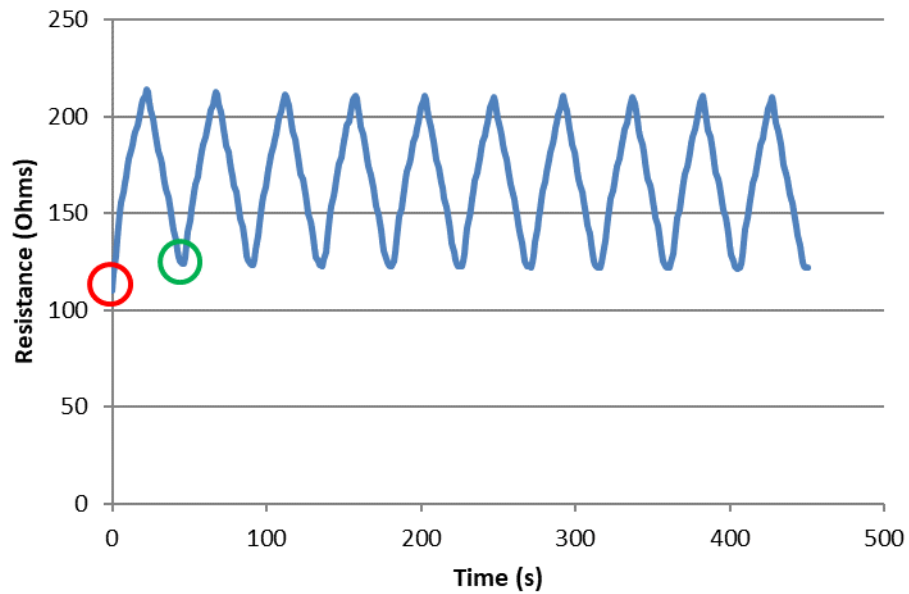


Figure 5.9 - Example of resistance vs time plot.

It is important to note that the unstretched resistance in the first cycle (circled in red) is substantially lower than that of subsequent cycles, where it becomes stabilised. As a result, the data does not take into account the first cycle of each sample. It is recommended to the end users that sensors are pre-stretched for the purpose of data accuracy from the beginning [79, 87]. Hence in the experiment, from now on, only data from the second cycle onwards is used (circled in green).

In this study, the aim is to find the values of working range and gauge factor for each stitch type. However, there is a possibility of some amount of variation between cycles, hence, data for a number of cycles were arranged on top of each other and averaged to find an assembly average. Ten cycles were used starting from the second cycle, as discussed. For example, the resistance at the start of each cycle was taken to be the average of the resistances at the start of cycles 2 through to 11. The second value of resistance was the average of the second sample of resistance for cycles 2 through to 11, and so on, until a complete averaged cycle was obtained. Strain was processed in a similar manner. An example of the percentage resistance change vs strain plot for this ensemble average can be seen in Figure 5.10.

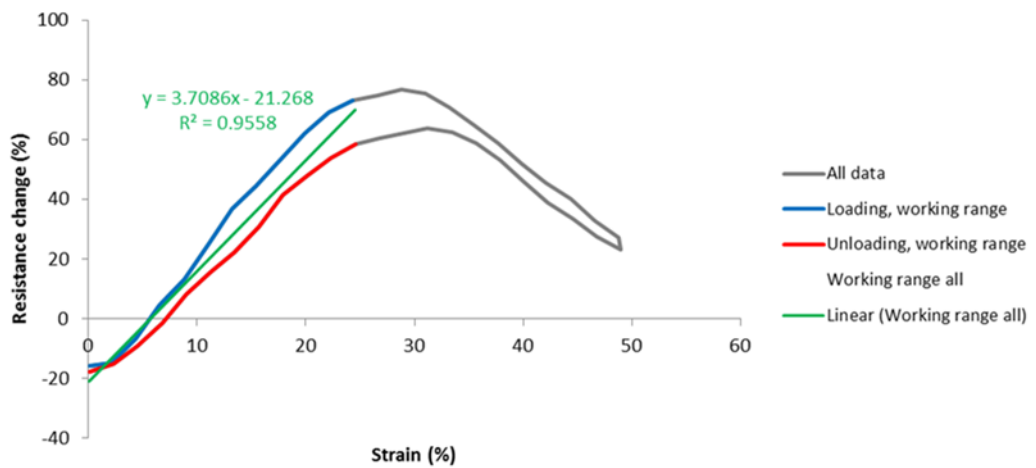


Figure 5.10 - Example of ensemble average over 10 cycles.

The grey curve is the ensemble average over 10 cycles for this particular stitch, which is past 25% of strain where the response appears to be highly non-monotonic and non-linear. Hence, the working range of this sensor lies within 0-25% strain. This is demonstrated on the graph as the blue and red lines, denoting the loading and unloading directions respectively. The line of best fit, marked in green, was fitted to the data within the working range, indicating a gauge factor of 3.71 in this case, and a coefficient of determination ( $R^2$ , in this case 0.94). The  $R^2$  is a measure of how well the data fits the line of best fit, indicating non-linearity, scatter and spread due to hysteresis.

Ultimately, the repeatability can be assessed by comparing resistance change vs strain in the graphs of the 2<sup>nd</sup> and 99<sup>th</sup> cycles, as shown in Figure 5.11. The second cycle was used for reasons disclosed earlier, and the 99<sup>th</sup> cycle was used because the 100<sup>th</sup> cycle presented some discontinuity, presumably due to some effect of the machine suddenly pausing. This graph revealed changes in characteristics such as gauge factor, hysteresis and unstretched resistance.

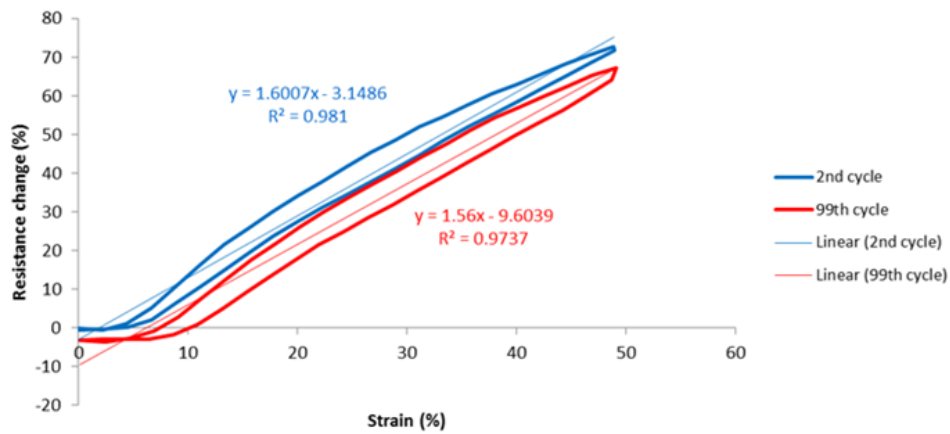


Figure 5.11 Example repeatability graph.

### 5.2.6 Experimental Results

In this study, the testing and evaluation of stitch stretch sensors was performed based on the theory and characterisation of a looped conductor stitch structure; both models of stretched and relaxed stitch structure's contact based phenomena was investigated. The measurement of samples was done to determine the relationship between electrical properties (resistance) and mechanical properties (strain-stress) of sensors. The electrical resistance was observed to increase when the fabric was stretched which is stated as resistance per unit length. When the sensor was in a relaxed state all the stitch threads are in contact with one another and the electrical resistance is low. As the sensor got stretched, the contact between each thread is reduced. The angle of stitch was then increased and its distance between each thread was observed to get longer. Subsequently, the increasing length was found to be proportional to an increase in electrical resistance. In contrast; when the sensor recovers back to its initial state, the sensor will become shortened, and hence its electrical resistance gets reduced, which is also in line with the deformation behaviour of the conductive path model which was presented in the literature [79].

To assist in explaining the sensor characteristics, close-up photos were also taken for visual inspection during stitch deformation. Table 5.3 displays close-up photographs of one typical sample of each stitch type, relaxed and stretched, the data of which is analysed further.



Table 5.3 - Close-up photographs of one sample of each stitch type, relaxed and stretched.





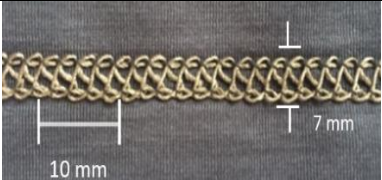






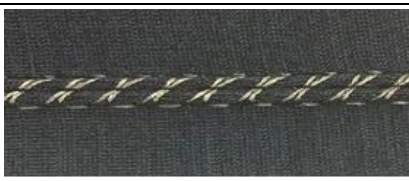
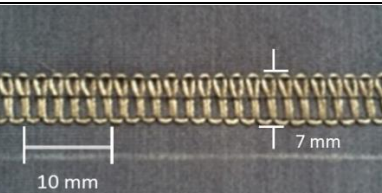
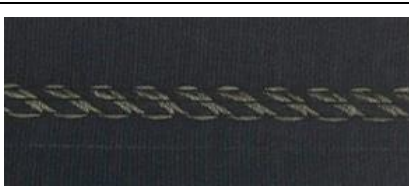
Stitch Type	Conductive Thread (Tex)	Relaxed State	Stretched State
304	two-ply 33		
406	two-ply 33		
	four-ply 92		
506	two-ply 33		
	four-ply 92		
605	two-ply 33		
	four-ply 92		

Figure 5.12 illustrates graphs of percentage resistance change vs strain for the various stitch types, averaged over all samples of each stitch type, and over the 2<sup>nd</sup> to 11<sup>th</sup> cycles. Data derived from these graphs is arranged in Table 5.4.

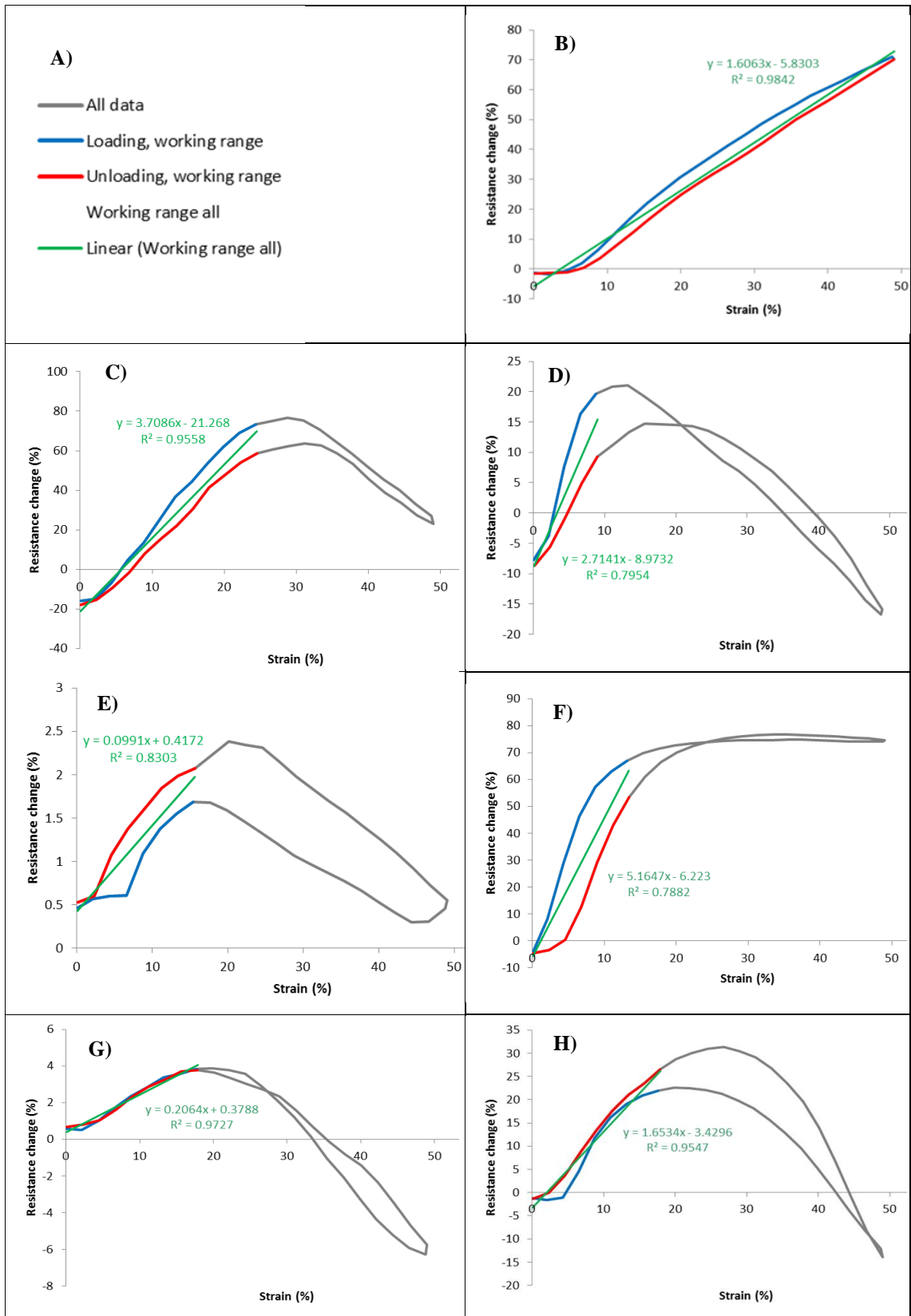


Figure 5.12 - Graphs of percentage resistance change vs. strain, assembly averages over the 2<sup>nd</sup> to 11<sup>th</sup> cycles. (a) Legend for all graphs; (b) 304: two-ply; (c) 406: two-ply; (d) 406: four-ply; (e) 506: two-ply; (f) 506: four-ply; (g) 605: two-ply; and (h) 605: four-ply. Note the different vertical axis scales. two-ply is thread 117/17, 33 tex and four-ply is thread 234/34, 92 tex.

Table 5.4 - Tabulated data from percentage resistance change vs. strain of the assembly from graph averages. Stitch two-ply uses 117/17 33 tex thread and four-ply uses 234/34 92 tex.

Stitch Thread type tex	Working Range (% strain)	Gauge Factor Over Working Range	Baseline Resistance ( $\Omega$ )	R <sup>2</sup> Overall Range	R <sup>2</sup> Over Working Range	Max Hysteresis Overall Range (% $\Delta R$ )
304 two-ply	0-50	1.61	125	0.98	0.98	6.25
406 two-ply	0-25	3.71	71.50	0.35	0.95	15.10
406 four-ply	0-8	2.71	55.60	0.25	0.79	11.40
506 two-ply	0-16	0.09	649	0.04	0.83	0.97
506 four-ply	0-12	5.16	46.70	0.60	0.78	33.60
605 two-ply	0-18	0.20	240	0.49	0.97	2.02
605 two-ply	0-18	1.65	39.30	0.02	0.95	11.10

The most noticeable aspect of the percentage resistance change vs strain in the graphs is the performance of the 304 two-ply stitch. It is highly linear, monotonic, and with a working range that appears to potentially extend past 50% extension. It also presents low hysteresis and a reasonable gauge factor. The high R<sup>2</sup> values also corroborate its good linearity.

Apart from the 304 two-ply and 506 four-ply, the other stitches adhere to a trend of increasing resistance followed by decreasing resistance, as the fabric is stretched. Thus, their working range is limited to a maximum of 8 to 25% (406 four-ply and two-ply respectively). This suggests that competing effects in the resistance may occur as a result of extension.

As previously described, one effect of extending the fabric is thought to open up contacts between adjacent lengths of conductive thread, hence increasing the conductive path (by moving the resistive lengths into series rather than parallel) and thus raising the resistance. In all stitches, the initial sensitivity of resistance to strain is low prior to it rapid increase

afterwards. The probable cause of this could be because few contacts are opened up before a certain level of strain is achieved.

Another factor, which might account for the resistance change which is in dimensions of the conductive thread itself, consequently altering the resistance per unit length. As previously stated, a conductor is increased in resistance as it is stretched, because of the conduction path is longer and its cross-sectional area is reduced. Even though the total length of the conductive thread is expected to increase as the fabric is stretched, in some case it could decrease, resulting in a reduction in sensor resistance. Figure 5.13 displays an example of fabric stretching with a stitch geometry that might result in a decrease in the overall conductive thread length.

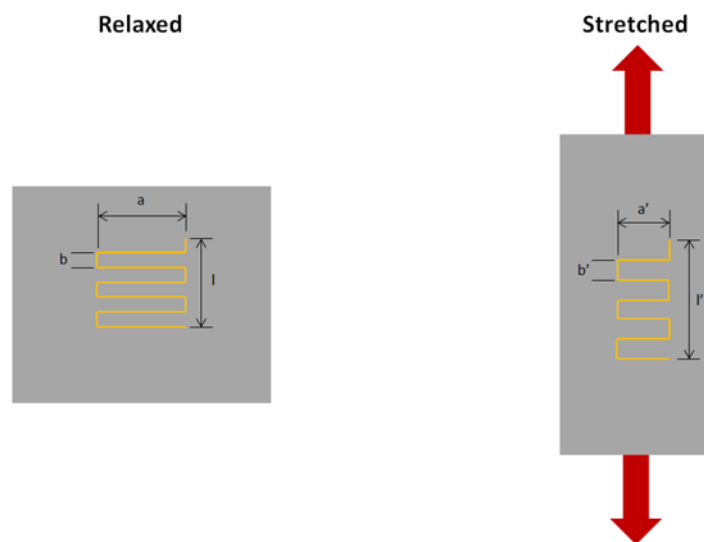


Figure 5.13 Conductive thread deformation

It is important to note that the main fabric is elongating as well as narrowing when it is stretched. This implies that any portions of conductive thread that are in the direction of the overall stretch are also being elongated, whereas any that are  $90^\circ$  to its length (i.e. lying across the fabric), will be shortening in length (compressing). In this stitch, there is more conductive thread length lying across the width than in the direction of stretch, therefore, overall the thread will be compressed, not stretched, hence reducing the sensor resistance. The tested stitch types were: 304 (used one thread type), 406 (used two thread types), 506 (used two thread types), and 605 (used two thread types).

Another explanation can be given if one examines the sewing thread tension performance when stretched on the tensile tester, shown in Chapter 3 (Figure 3.3), which leads to an increase in surface contact between conductive surfaces as the cross-section of the thread is expected to decrease under tension along its axis and improves in orientation along the direction of loading. Having said this, in this sensor, the sewing thread is not being stretched along its axis and hence any observation to that effect is difficult.

Another trend is that 4-ply compared to their 2-ply counterparts have lower resistances. This would be expected due to the increased cross sectional area in which case any conductor allows the current to flow through. Stitches 506 2-ply and 605 2-ply had particularly high baseline resistances of 649 and 240  $\Omega$  respectively. A higher baseline resistance, for a given gauge factor, indicates that changes in strain would generate larger changes in resistance. However, the high resistance sensors are also likely to have a much lower gauge factor (percent change of resistance to strain), so offsetting this advantage.

Large differences in the hysteresis can be observed across the full sample sensor range, but when considered as a proportion of the output of the sensors (easier to visually observe on the graphs), all sensors had a very similar hysteresis. Within the working range, stitch type 605 illustrated low hysteresis, again taken as a proportion of their output, while stitch type 506 showed the worst (highest) hysteresis. The 605 sensors also had good  $R^2$  values within their working range, indicating low hysteresis and high linearity.

Figure 5.14 shows graphs of percentage resistance change vs. strain of stitches between the 2<sup>nd</sup> and 99<sup>th</sup> cycles. Data derived from these graphs are tabulated in Tables 5.5 and 5.6.

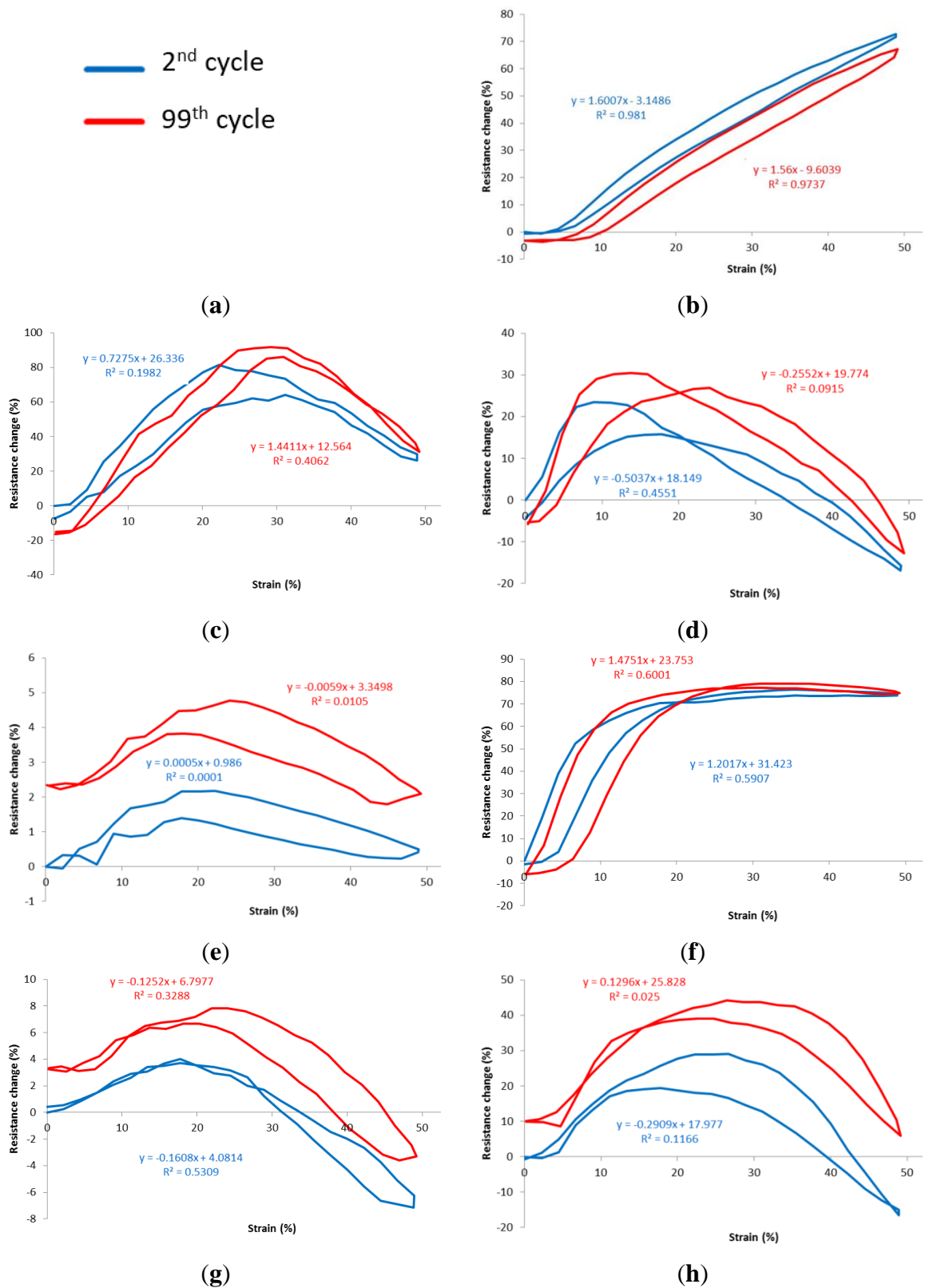


Figure 5.14 - Graphs of percentage resistance change vs. strain, for the 2<sup>nd</sup> and 99<sup>th</sup> cycles. (a) Legend for all graphs; (b) 304: two-ply; (c) 406: two-ply; (d) 406: four-ply; (e) 506: two-ply; (f) 506: four-ply; (g) 605: two-ply; and (h) 605: four-ply. Note the different vertical axis scales. two-ply is thread 117/17, 33 tex and four-ply is thread 234/34, 92 tex.

Table 5.5 - Change in gauge factor from 2<sup>nd</sup> to 99<sup>th</sup> cycles. Calculated across the entire extension.

Stitch Type Thread Type	G.F. 2 <sup>nd</sup> Cycle	G.F. 99 <sup>th</sup> Cycle	G.F. Drift	Percentage G.F. Drift (%)
304 two-ply	1.60	1.56	-0.04	-2.54
406 two-ply	0.72	1.44	0.71	98.10
406 four-ply	-0.50	-0.25	0.24	-49.30
506 two-ply	0.00	-0.00	-0.00	-1280
506 four-ply	1.20	1.48	0.27	22.80
605 two-ply	-0.16	-0.12	0.03	-22.10
605 four-ply	-0.29	0.13	0.42	-145

Table 5.6 - Change in relaxed percentage resistance change and R<sup>2</sup> values from 2<sup>nd</sup> to 99<sup>th</sup> cycles. Calculated across entire extension.

Stitch Type Thread Type	Relaxed $\Delta R$ 2 <sup>nd</sup> Cycle (Baseline) (%)	Relaxed $\Delta R$ 99 <sup>th</sup> Cycle (%)	Relaxed $\Delta R$ Drift	R <sup>2</sup> 2 <sup>nd</sup> Cycle	R <sup>2</sup> 99 <sup>th</sup> Cycle	Drift in R <sup>2</sup>
304 two-ply	0	-3.25	-3.25	0.98	0.97	-0.00
406 two-ply	0	-15.20	-15.20	0.19	0.40	0.20
406 four-ply	0	-5.70	-5.70	0.45	0.09	-0.36
506 two-ply	0	2.33	2.33	0.00	0.01	0.01
506 four-ply	0	-5.68	-5.68	0.59	0.60	0.00
605 two-ply	0	3.23	3.23	0.53	0.32	-0.20
605 four-ply	0	9.88	9.88	0.11	0.02	-0.09

Five out of seven sensor stitches show an increase in overall resistance between cycles 2 to 99. It was observed that the resistance in the relaxed state increases after each stretch cycle. Different types of stitches are affected by this phenomenon in varying degrees. This is because the path of conductivity is increased by differing volumes according to how much contact was made between loops before and after stretching.

It should be noted that other textile sensors could have similar gauge factors, but their working range and other performance properties are very different [26]. The most uniform stitch result was stitch type 304 which is due to its loop contact being broken gradually. The least uniform result was stitch type 605, which is due to its loop contact being broken suddenly. This phenomenon may be reduced in all sensor types by using

a greater stitch density, so improving contact and making the subsequent contact breakage more gradual. When we tried to alter the stitch density however sewability issues kicked in which gave less room to increase/reduce in the stitch density necessitating to keep to a commercial optimum.

### **5.3 Summary of the Results and Conclusions**

In this research, textile-based strain sensors that use different types of stitch structures, geometries and compositions were investigated. The effects on the sensor performance properties associated with the change in resistance have been examined for a number of different stitch geometries. All sensors show a significantly varying degree of resistance depending on their stitch structure. It has been shown that stitch pattern type has a significant effect on cyclic conductivity and resistance.

More specifically in this study it was found that stitch type 304 2-ply was the best performing stitch for use as a sensor. It features exceptionally high working range (potentially well past 50%) and linearity ( $R^2$  is 0.98), low hysteresis (6.25%  $\Delta R$ ), good gauge factor (1.61), and baseline resistance (125  $\Omega$ ) as well as good repeatability (drift in  $R^2$  is -0.00).

The innovative approach of this chapter is based upon the use of existing textile processes to produce a realistic wearable sensor. Sensors that use stitch techniques have the benefit of unconstrained placement on garments, ease of construction and layout of sensor design. High performance, low cost and comfort contributes to ideal sensor stitch design. This sensor was integrated in a sports bra in the following chapter 6, illustrating how respiration, as an example of body movement, can be measured. The development of more user-friendly interfaces will be required to make the collected data easily understood by the end user. However, this is outside the current investigation.



## **Chapter 6 – Sensor Integration in a Wearable Sport Bra for Well Being Monitoring**

The integration of wearable devices onto clothing worn on the body has become reality in the recent times. New methods and techniques in the field of wearable sensors which help to promote wellbeing as well as to prevent illness are being developed so they can become garments of everyday use. In this chapter, we show how these garments can be designed with the sensors being part of this design process, as a wholistic approach, so that these sensors are an integral part of the design and manufacture of a garment; in this case a sports bra. A lady's garment has been chosen since it is more challenging in design and implementation with shape as well as body movement in mind. To that end, two Smart Sports Bras (SSBs) were designed, with the textile electrodes forming part of the SSBs by trying out two methods of manufacturing: sewing and knitting, and with the stretch sensor placed in a strategic position on these bras to measure respiration, in this instance as an example, however it can be placed along the arm or the leg to measure movement as well.

Based on the previous experimental results in chapters three, four, and five, the threads and fabrics demonstrating optimum performance (Silver plated nylon conductive thread 234/34 4-ply and silver plated nylon conductive fabric, MedTex™ P-130) were selected to construct the electrodes and the interconnection lines within the garments and the stretch sensor, so the sensors are not attached but knitted in the design of these sports bras. In this research, two garments were produced using the most common method for garment production – the cut and sew method (CSM) and the knitting method (KM). These SSBs were designed to detect ECG signals as well as respiration using the textile sensor itself, which can demonstrate how a wearable garment can benefit from using these types of textile sensors.

In this chapter, the design and production of the SSBs and the ECG measurement are described, and subsequently the performance of the SSBs is assessed systematically while it is worn under various body movements – such as walking, sitting, arm waving. Further to this, in the same design, the stretch sensor is integrated to the SSB in conjunction with the textile based electrodes for health, fitness and well being monitoring.

## **6.1 Wearable Requirement and Electronic Garment Concept**

Electronic Garment Concept is generally used in this thesis to describe the design and making of an electronic monitoring sensor system that is worn next to the skin. Flexibility, functionality, aesthetics and fashion, and customisation are also built into this electronic garment concept. The fact that an electronic garment can be worn continuously means that any changes of user's data can be tracked and sent to a physician, trainer or doctor indicating forthcoming health issues [141], and in well-being situations the user can assess their well-being and improve their performance.

The basic requirement for any wearable system is ease of use, even for those with impaired movement ability, meaning that the electronic devices should be of low weight, minimal in size, being wireless and have very low power consumption (low energy) for continuous use [142]. The electronic devices and their associated interconnection are manufactured into the garments, and are dependent on the available space and design with a strong focus on being comfortable and requiring no maintenance. Washability was also a criteria in this design concept but its testing is left to be completed in future research. Therefore, the challenge of the Electronic Garment Concept is to design electrodes and stretch sensors which are part of a garment that can provide sensing and control functions which will allow long term monitoring over a wide variety of everyday activities.

## **6.2 Designing of the wearable Sport Bra**

The ease of use for the wearer and the effectiveness of the garment as a reliable wearable sensor depends upon the design, the materials and the manufacturing process used. In this study, the combined requirements of the incorporated electronics; the electrodes, data collection device, the stretch sensor and the connecting conductive threads, are taken into account. Sports bras are the main type of active wear which has to have a unique functional design that allows for dynamic breast support, good fit and comfort. Sports bras are regarded as high performance garments as they are designed to control excessive breast movement, so eliminating discomfort for the wearer. Sports bras are characterised as being either of a compression, encapsulation or combination type [143] as shown in Figure 6.1. Compression bras usually come in the form of a pullover without having an inbuilt cup shape, so they apply flattening of the breasts and thus holding them firmly to avoid bounce and excessive movement, as shown in Figure 6.1(a). Encapsulation sports bras are designed with inbuilt cups which support each breast individually and provide an

overall breast shape as compared to compression sports bras, show in Figure 6.1(b). Combination sport bras cater for both encapsulation and compression [144] as shown in Figure 6.1(c). Preliminary trials have shown that the compression bra was the most effective bra in reducing breast displacement [145, 146] and has good performance on bust stability [147].

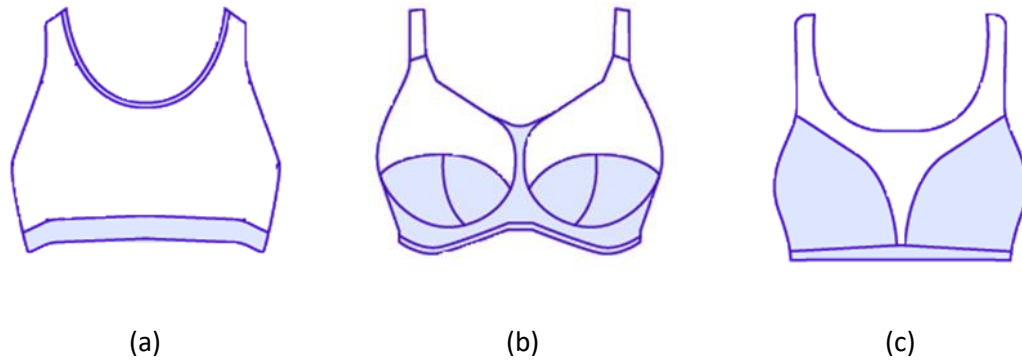


Figure 6.1 - Sport bras designs. (a) compression (b) encapsulation, (c) combination.

Gemperle et al. [148] suggest that wearable sensor garments should be worn in areas of the body where movement is minimal in comparison to the rest of the body. Therefore, the selection of a compression sport bra design type as a sensor garment for continuous monitoring of ECG and respiration is ideal in meeting the needs of the wearer as well as being optimum for collecting vital signals.

### 6.3 Designing a Smart Sport bra with Electrodes

#### 6.3.1 *Electrode design*

For the best performance and comfort, in this research, a smart garment was designed and made with pleasing aesthetics, based on experimental ECG data and stretch sensor data. Two manufacturing methods, cut and sew method (CSM) and knitting method (KM) were used and the garment performance was compared. Both methods incorporated textile electrodes suitable for ECG sensing and a stitch sensor suitable for respiration. Two materials were used; a silver plated nylon conductive knitted fabric and a silver-plated conductive fabric made of conductive thread, as reported in Chapter 3.

### (a) Fabric electrodes

The fabric electrodes were designed to use silver plated nylon conductive fabric, MedTex™ P-130. Cut and sew method is used to create this electrode which is incorporated into the single jersey's fabric-base as shown in Figure 6.2.



Figure 6.2 - The Electrode manufactured using CSM with conductive knitted fabric.

### (b) Knitted Electrode

The knitted electrodes were made of 234/34 four ply, silver plated nylon which present low values of electrical impedance as demonstrated in the assessment of textile-based electrodes development in the chapter 3. The knitted electrode is designed to be surrounded and supported by a knitted net structure, around the electrode area - as shown in Figure 6.3, This novel electrode supporting idea is discussed further below. Shima SWG091 N2, 15 gauge computerised flat-bed knitting machine is used to manufacture the electrode, the details of which can be seen in Appendix D.

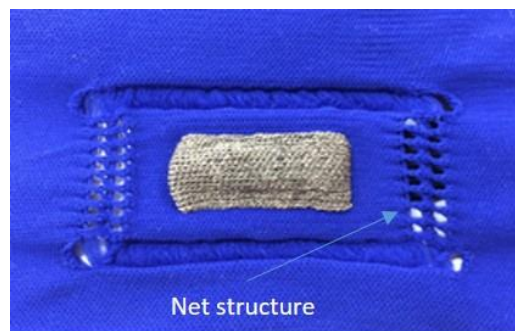


Figure 6.3 - The electrode manufactured using KM with conductive thread.

This net design technique enables electrodes to acquire stable electronic signals with minimum movement. To test this, two supporting electrode designs were compared – one with (Figure 6.4 a) and another without the net structure support (Figure 6.4b ). The design of net structure can assist in providing stability to the electrodes in relation to body movement and hence it reduces motion artefacts. Tests were carried out in order to assess how the different electrode parameters effect the sensor performance.

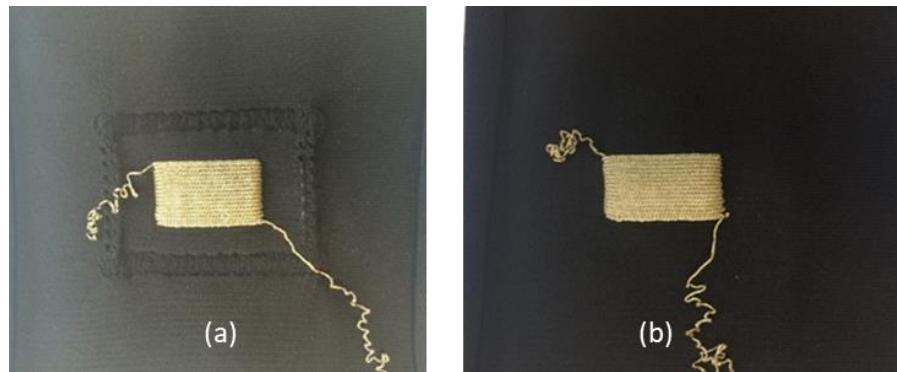


Figure 6.4 - Two types of knitted electrode designs, (a) plain knitted electrode and (b) a net electrode.

The most representative movement is the amount that the electrode could move or rotate along the body plane of the wearer. This can be captured by measuring the shear value of the two electrodes. The KES shear instrument (Figure 6.5a) was used and the experimental set up of both fabrics are show in Figure 6.5b. The graphs (Figure 6.6) are clearly illustrating the optimum design that stops body movement. The experimental results are presented with both electrode designs and baseline drift. The baseline resistance was influenced by fabric movement.



Figure 6.5 - Shear measurement, (a) KES shear instrument (b) shear experimental set up.

Our experimental results show the resistance baseline drift effect of the electrode when it is moving. The plain electrode structure resistance shows more fluctuation compared to electrode with the net structure which presents less noise and more stable performance in the dynamic wearing state of the garment, as shown in Figure 6.6.

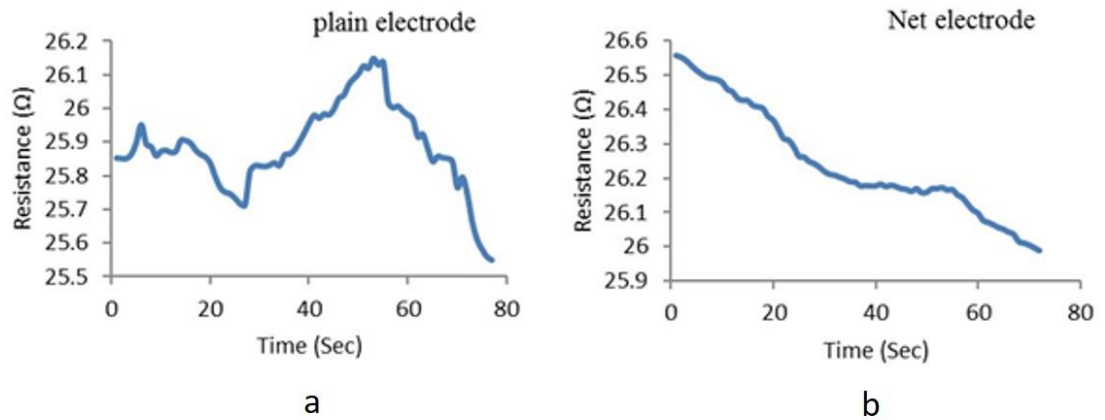


Figure 6.6 - Baseline drift of the electrode with (a) net structure, (b) plain structure.

The electrode surrounded by the net structure is showing higher stability than the plain electrode structure, because as you see in Figure 6.7 and 6.8 when comparing the shear characteristics of those electrode samples, the net electrode sample has lower shear rigidity  $G = 0.825 \text{ gf/cm. deg}$  than the plain electrode sample  $G = 1.050 \text{ gf/cm. deg}$  and acts as a “shock absorber” in the plane of the electrode attached to our body. The net electrode is affected less by the rotational forces of the body as we move our hands upwards causing the fabric to shear. The net structure also has better recovery at 2HG at  $3.8 \text{ gf/cm}$  and 2HG5  $4.2 \text{ gf/cm}$  against the plain electrode at  $4.7 \text{ gf/cm}$  and  $5.2 \text{ gf/cm}$  respectively.

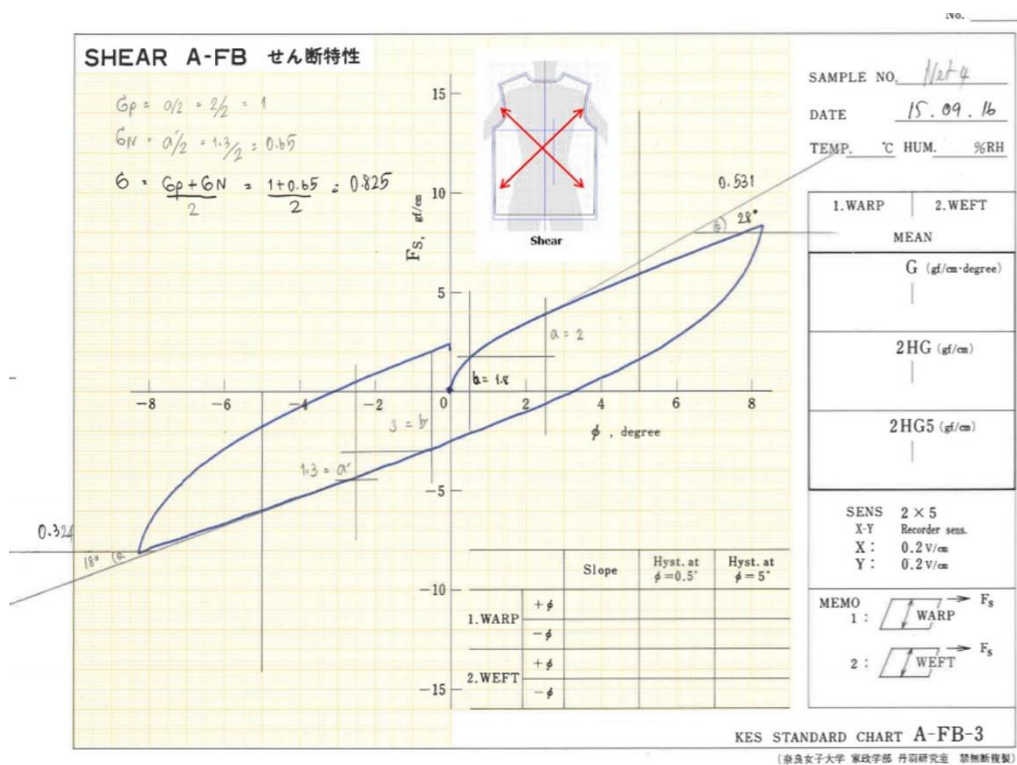


Figure 6.7 - The shear of the net structure fabric, indicating low shear rigidity  $G$  and good Hysteresis  $HG$ .

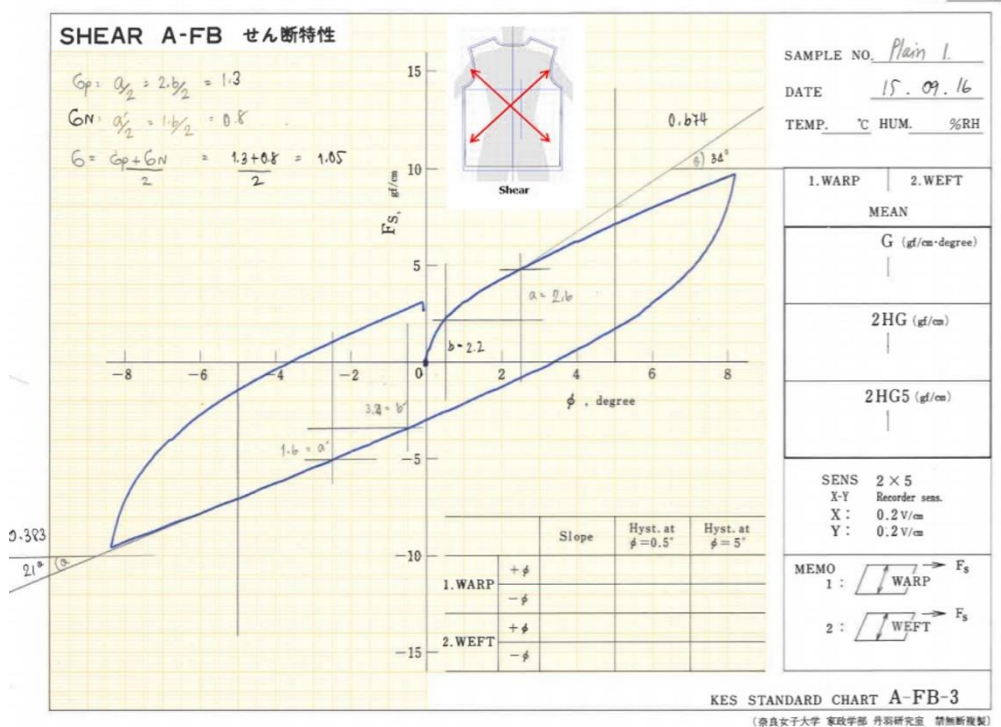


Figure 6.8 - The shear of the plain structure fabric, indicating higher shear rigidity  $G$  than the net structure fabric.

Table 6.1- Tear properties of Net and Plain fabric structures

Fabric electrode sample	G (gf/cm. deg)	2HG (gf/cm)	2HG5 (gf/cm)
Net structure	0.825	3.8	4.2
Plain structure	1.050	4.7	5.2

### 6.3.2 Smart Sport Bra Design

A SSB of a tight-fit compression bra type is designed and produced, bearing in mind the reduction of breast movement [149] and minimisation of motion artefacts [142]. The racerback shoulder straps create a Y-shape to provide good support for high impact workouts and stability of the electrode to skin contact. The prototype process of bra design and development is presented in Appendix E. Polyamide was used to produce the SSBs. The knitted structure of the SSB's enhances the fabrics ability for local compression, thus reducing artefacts caused by body movements, whilst making it easy to wear; a snap popper tape is used on the side of the bra.

The garments are designed as modular units, meaning that the ECG circuit box is easily detached and re-attached whenever the need arises. Metal snaps are used to connect the ECG device. The garment design is shown in Figure 6.9.

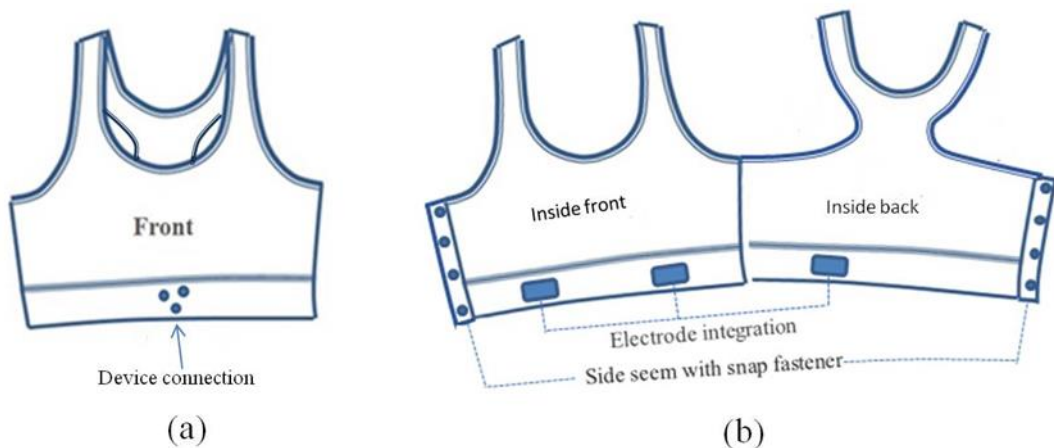


Figure 6.9 - Garment information design for ECG measurement.



### (a) Electrodes Position

The positioning of the three electrodes was determined after carrying out experiments as detailed in Chapter 4. The results of those experiments show that lead placement B (Back Horizontal Formation shown in Figure 4.11b) gave the best results. The electrodes are sited around the lower chest band, using a three-electrode configuration and are of a rectangular shape (size 20mm x 40mm) which has shown a good performance.

### (b) Electrode Interconnection

The method of interconnection of the electrodes within the garment is important in achieving a good functionality as well as ease and comfort of use. Traditionally, hard wires have been used to transport electrical signals, but in this research, textile-based conductive yarn is used. Textile based wiring by conductive yarns has the distinct advantage over traditional wiring in that it is much more flexible being part of the garment itself and hence more comfortable, unobtrusive and practical to wear as well as being more reliable in its connectivity over hard wiring, capable of washing and easier cleaning.

In this approach, circuit path and electrode connections are stitched using conductive threads. The “textile wiring” in this garment is formed in a zig-zag pattern which has the advantage of being used in any direction either horizontally or vertically and it has good elastic properties, avoiding breakages and falling apart. The interconnection path is secured to the ECG device via snap fasteners as shown in Figure 6.10.

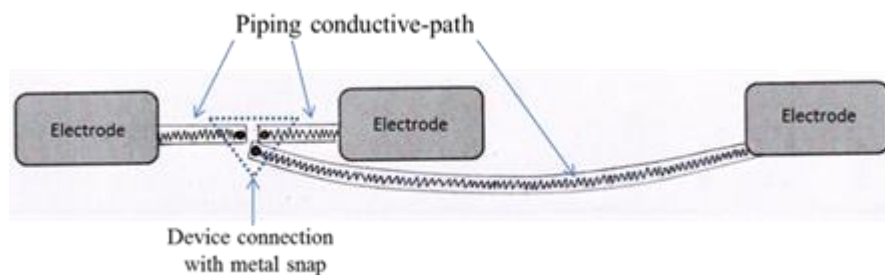


Figure 6.10 - Electrode's interconnections in zigzag formation line of SSBs.

The electrical interconnection used in the cut and sew SSB is made by the silver plated nylon thread 117/17 two-ply, already discussed, and the electrical interconnection used in the knitted SSB is made by the silver plated nylon thread 234/34 four-ply, also already discussed. The silver plated thread does not come with any form of insulation; hence, elastic fabric piping is used to cover the interconnection line and hence form a reliable insulation, as shown in Figure 6.8.

### 6.3.3 Garment production

#### (a) Cut and sew method (CSM) of SSB

The fabric used to make CSM-SSB is weft knitted fabrics with Nylon/Spandex in single jersey structure, which is widely used for body fit garments. Due to the ability of this fabric to stay close to the body of the wearer even during moving, it is excellent for integrating sensors as it enables those sensors to maintain uniform contact with the wearers body skin. The basic parameters of the fabric are shown in Table 6.2.

Table 6.2 - Specifications of the experimental single jersey fabrics.

Nylon Yarn count (Tex)	Spandex Yarn count (Tex)	Content Nylon/Spandex (%)	Weight g/m <sup>2</sup>	Thickness mm.	Yarn density per cm	
					Courses	Wale
4.44 / two-ply	7.78	75/25	260	0.55	20	39

A lady's typical size 10 bra design has been chosen for constructing the garment prototypes in this research. The design information was detailed in the garment specification sheet, in detail in Appendix F.1, which shows the basic pattern description and information of the garment. Along with the SSB body blocks, sport bra patterns are drafted and cut according to the working drawings of the garment patterns, as detailed in Appendix F.2. The completed CSM-SSB design is shown in Figure 6.11. The garment assembly and production of the CSM-SSBs are shown in Appendices G.1 and G.2.



Figure 6.11- CSM-SSB, (a) outer front. (b) inside front and back.

**(b) Knitted method (KM) of SSB**

The knitted structure has the advantage of being a close fit to the body with excellent support in different levels of body movement. It enhances the signal performance by maintaining stable and uniform contact between the sensor and skin. In this approach the KM-SSB with a net supporting structure was designed and made. The net structure is located next to the electrode area and around the garment body between the top and lower chest band, as shown in Figure 6.12. The information of the garment specification is presented in Appendix F.3 and the design diagram and final knitted pattern of KM-SSB, and the software devised in the Shima Seiki's, SWG091 N2 15 gauge knitting machine are presented in Appendix F.4.

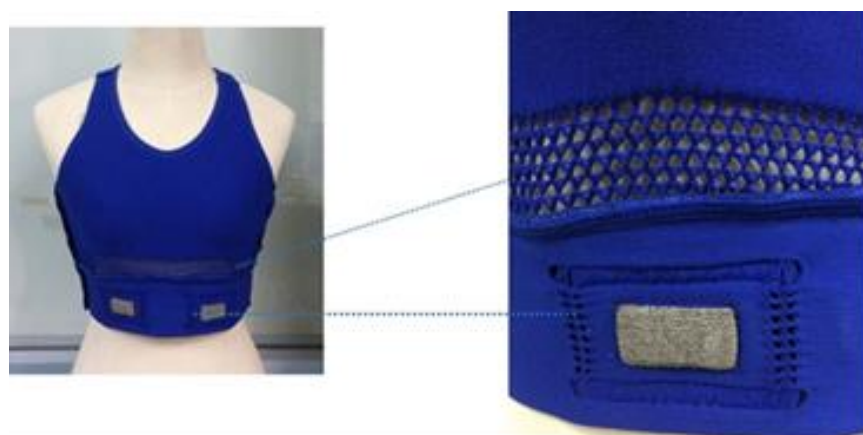


Figure 6.12 - Net structure design on the knitted sport bra.

The KM bra is knitted with Nylon in a single jersey structure. A Shima Seiki 15 gauge seamless knitting machine, was used and the Intarsia technique was chosen to reconnect the electrodes allowing the specific conductive yarn to be inserted into a specific area of the intarsia within the garment. The complete KM-SSB design is shown in Figure 6.13. The interconnection of electrodes to the ECG device is made with a zigzag stitch using silver plated nylon conductive thread 234/34 four-ply and linked with the connection point as shown in Figure 6.10. Weft insertion was tried prior to using a zig zag stitch but it had two problems; it could not be insulated unless a new yarn is developed which is something that we will be developing in future research and its stretching ability was also not guaranteed. Hence the zig zag approach was developed. The garment assembly and production of the KM-SSBs are shown in Appendices G.1 and G.2.



Figure 6.13 - KM-SSB. (a) outer front. (b) inside front and back.

#### 6.4 Evaluation of SSBs using real ECG measurement

A test is conducted, and the measurement of real ECG signals was taken. The two SSB's containing their three electrodes were worn by a healthy female subject, with no history of cardiac disease. Commercial gel ECG electrodes (3M, 2228, Minnesota, USA) were also used to compare the results given by the two SSB's. The ECG data collection device used in this garment is a Low Energy Wireless Device developed by Luo and Stylios [21].

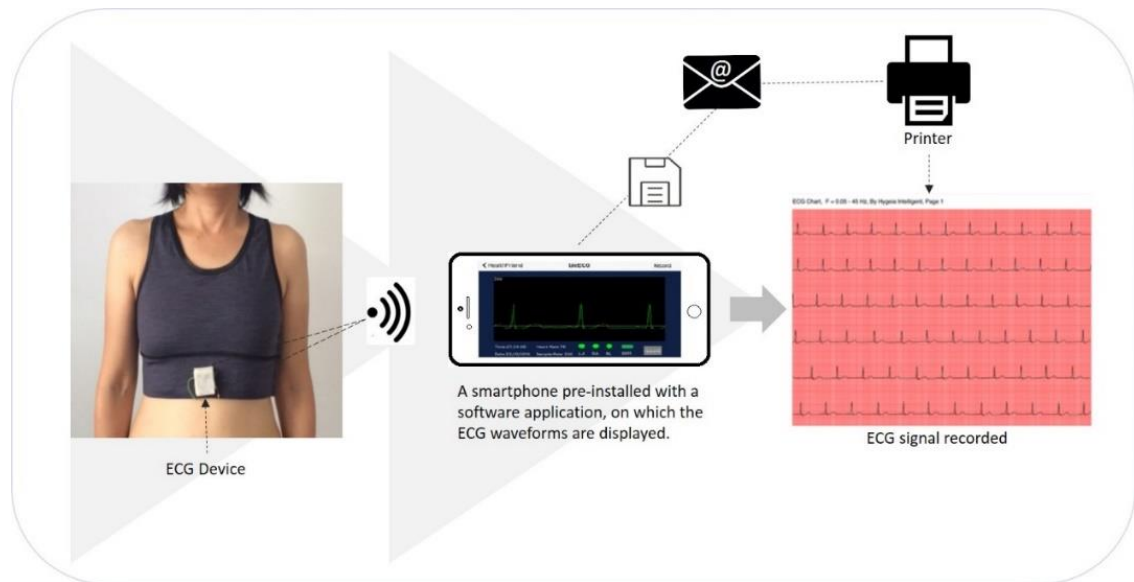


Figure 6.14 -The ECG system and measurement.

#### 6.4.1 Experimental procedure

The signals gathered by the SSB's electrodes are sent to the ECG device contained within the garment which in turn wirelessly transmits data to a smart phone on which a pre-installed app carries out analysis and shows the processed data in the form of PQRST waveform with corresponding values as shown in Figure 6.14. The electrodes were fixed onto the selected locations around the respective body position with a pressure of 4kPa. Figure 6.15 shows the pre-set activity carried out by the subject during the experiments, such as sitting (Figure 6.15a), walking on a flat ground (Figure 6.15b), and arm movements (Figure 6.15c), the duration of each activity was 20 seconds.

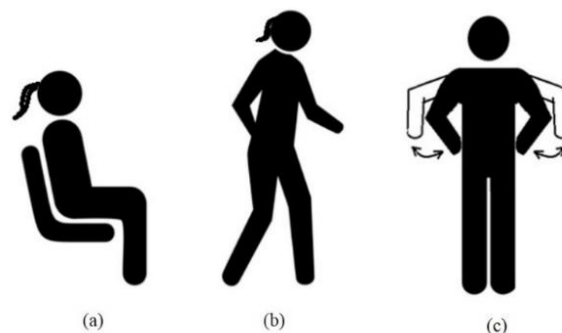


Figure 6.15 - The ECG measurement activities (a) sit position, (b) walk and (c) Arm movement.

### 6.4.2 Experimental results

Figures 6.16- 6.18 show the ECG signals recorded in the three body activities using the two garment designs with the textile electrodes and also with the gel commercial wet electrodes for comparison of performance during end use. The results from the two SSB's compared to the commercial gel ECG, show that the SSBs give reliable and consistent readings, with the textile while the gel ECG shows more consistent results when the subject is static, as expected.

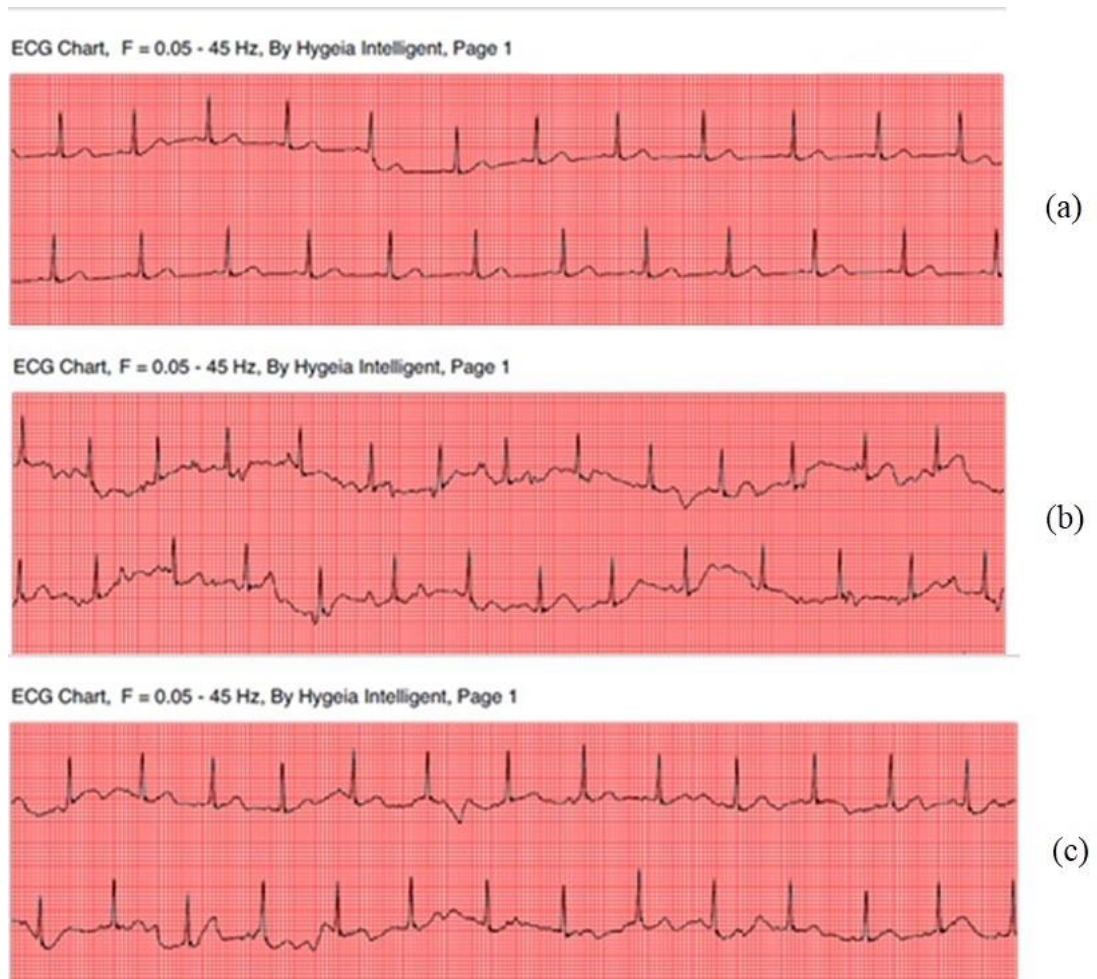


Figure 6.16 - ECG recorded from Cut & Sew SSB in the position of, (a) Sitting, (b) Walking, (c) Arm moving position.

ECG Chart, F = 0.05 - 45 Hz, By Hygeia Intelligent, Page 1



(a)

ECG Chart, F = 0.05 - 45 Hz, By Hygeia Intelligent, Page 1



(b)

ECG Chart, F = 0.05 - 45 Hz, By Hygeia Intelligent, Page 1



(c)

Figure 6.17 - ECG recorded from knitted SSB in the position of, (a) sitting, (b) walking, (c) arm moving position.

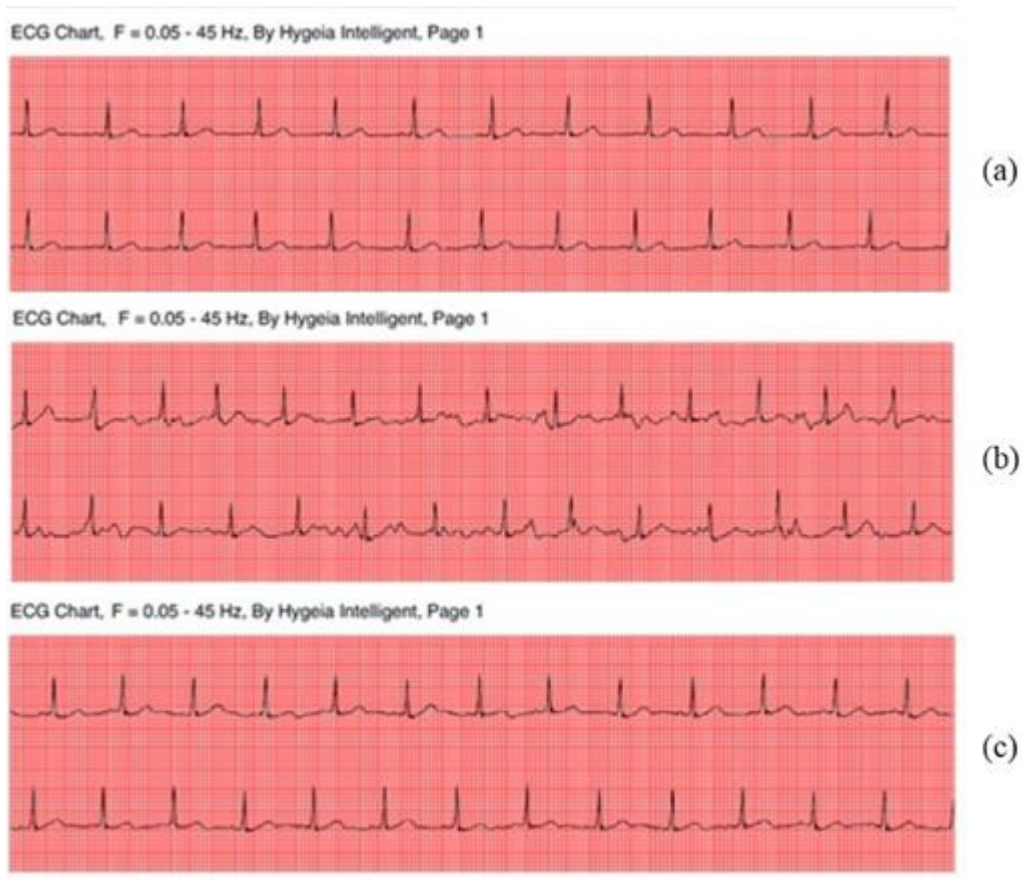


Figure 6.18 - ECG recorded from commercial electrode in the position of, (a) sitting, (b) walking and, (c) arm moving.

The ECG charts from Figure 6.16 show that the signal from the SSB of the CSM construction displays some baseline drift when the subject is moving (walking and arm moving). High frequency noise is also present in this SSB than in the knitted SSB or the conventional gel ECG. This is caused by motion artefacts due to the skin-electrode impedance [150] being disturbed. It has been considered that these electrodes maybe affected by respiration and also by vertical movement of the upper body during walking and jogging [149]. The results show, Figure 6.17, that the SSB in the KM construction produces the best performance of ECG signals and they are as reliable and consistent as those of the commercial gel-based ECG (Figure 6.18). The SSB in the KM knitted construction also has the benefit of the net structure around the electrode, acting as shock absorbing against body movement, and fitted with a net strip around the body (Figure 6.12) which reduces the chest displacement and so it enables it to remain in good contact with the body skin while the user is moving. This allows the electrodes to stay relatively still while maintaining good, undisturbed contact with the body skin and hence avoiding



signal contamination noise by body movement. Moreover, the body-fabric characteristic of KM-SSB is stiffer and has less stretchable fabric than the CSM bra's which, due to it being very soft and of stretchy nature, cannot support the wearers breasts during movement [151].

According to the results presented in all SSBs, the textile electrode works well and is able to give clear and accurate recording of ECG signals. The ECG signal from the textile electrode and garment assembly demonstrated a level of frequency noise and baseline drift that was not significant to adversely affect the accuracy of the recorded ECG. Therefore, the results show that the design of the SSB is suitable and enhances the performance of the textile electrodes, rendering this wearable garment suitable for good quality ECG monitoring.

## **6.5 Integration of stitch stretch sensor for respiration monitoring**

Unlike the electrodes that need placing at specific positions in the body in order to monitor the ECGs condition, the stitch stretch sensor can be placed anywhere that a body posture, a limb function, movement or respiration need monitoring. To illustrate the ability of integration it was decided to attach the stitch stretch sensor to a position in order to measure respiration as an example since ECG and respiration are clinically monitored together.

### **6.5.1 *Respiration measurement***

There are a number of methods to assess general respiratory condition [152-154]. Respiration rate can be determined by directly measuring the movement of air transferred into and out of the lungs, and it can also be measured indirectly by measuring the change in chest volume [121] as shown in Figure 6.19. Indirect measurement usually involves the assignment of movement and displacement of the upper abdomen and the rib cage [122, 155]. The respiration volume can be calculated by knowing the change in circumference of both of these locations. Strain-gauge respirometry [156, 157] is one method of indirect measurement that measures changes in the circumference of the body compartments. In practice, respiration rate is determined by monitoring the expansion and contraction of the rib cage over time for sports, well-being and medical purposes. Placement of the sensors at the upper abdomen and rib cage allows to monitor breathing

patterns, e.g. shallow breathing versus deep abdominal breathing or irregular disturbed breathing.

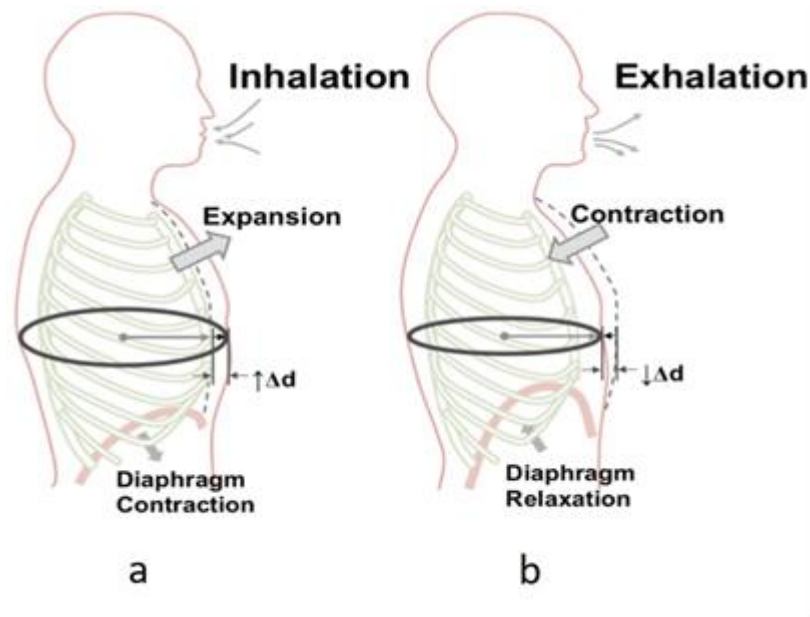


Figure 6.19 - Abdominal circumference changes of respiration: a) inhalation and b) exhalation phase [121].

### 6.5.2 Respiration sensor mounting and design

The textile-based sensor was developed using a stitch structure reported in Chapter 5. As the material is stretched, the electrical resistance of the conductive thread stitch increases, as already presented in Chapter 5. This influence can be used to detect joint movement and also to measure respiration rates. For efficient monitoring of respiration rate and depth, the sensor is mounted at the upper position of the abdomen with an associated signal processing unit [158]. In order to maximise the signal quality, the stitch stretch sensor was located at the front chest band of the bra, which closely follows the movements of the upper abdomen, making it capable of monitoring the respiration of the wearer. The design of the sensor is shown in Figure 6.20. The garment assembly and production of the Respiration-SSBs are shown in Appendix G.3.

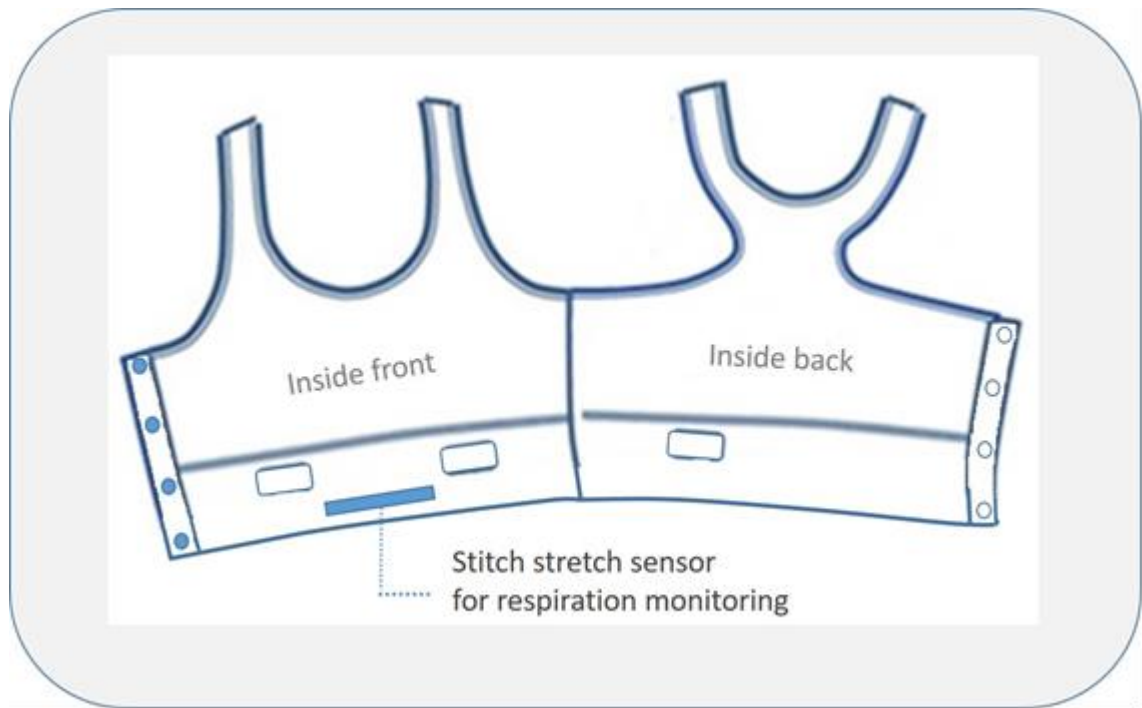


Figure 6.20 - Design feature of SSB for respiration monitoring.

The SSB system for respiratory monitoring based on conductive textile stretch sensors was constructed. The stitch stretch sensor is fabricated from stitch type 304 (Lock stitch, zigzag) which has already shown the optimum electronic function is from this sensor's performance, in laboratory tests, (in chapter 5) with a working range of 50%, a hysteresis of 6.25%  $\Delta R$ , and a good linearity of  $R^2$  is 0.984, a gauge factor of 1.61, and acceptable repeatability. Therefore this sensor was selected to create the respiration-sensing bra. The design aim of the respiration sensor is to achieve clear and reliable signal accuracy, wearer comfort, durable construction with an aesthetically pleasing appearance.

To preserve the sensor properties experienced in the laboratory, the sensor length of 150mm (the same size as the experimental sample) was stitched onto the chest band with two stitch lines, when the garment is relaxed so that no pre-stretch is applied on the sensor. In this prototype, the conductive path enables transmission of breathing information from the stretch sensor to the data collection device using conductive thread (Silver plated nylon 117/17 two-ply), as shown in Figure 6.21. Elastic fabric piping is used to cover the conductive path to prevent electrical interference. The data collection device is a modular unit contained in the same hardware box as in the ECG device. It is placed in the front of bra and can be removed for laundering.

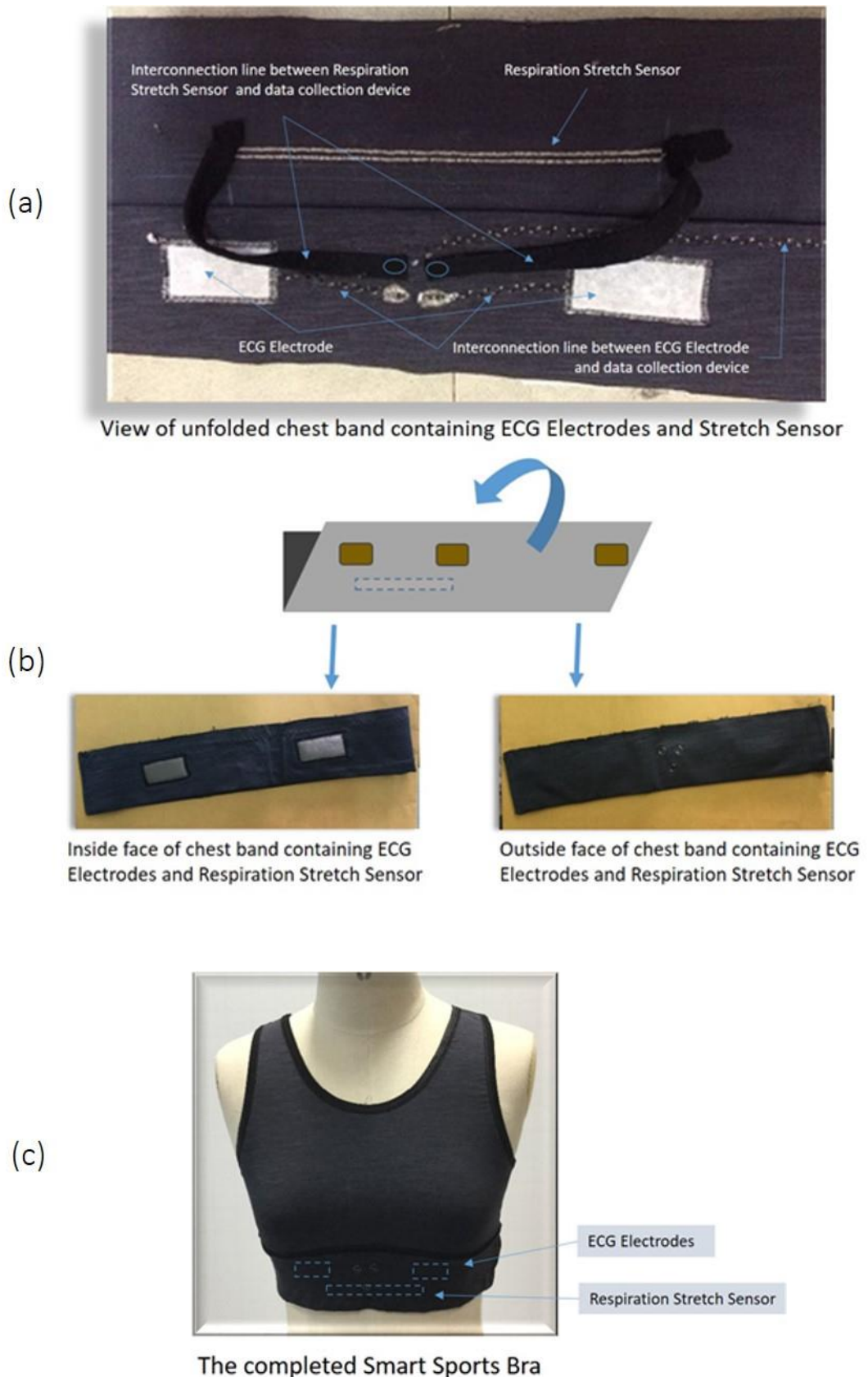


Figure 6.21- Fabrication of stitch stretch sensor for respiration monitoring, (a) ECG electrode and respiration stitch sensor position, (b) inside and outside of chest band, (c) the completed Smart Sport Bra.

Figure 6.22 shows a typical output of a respiration signal using the hardware platform device. The periodicity of breathing as well as the depth depicted in the amplitude of the signal are clearly seen. Further studies will explore the data more and also how it could be used for respiration health monitoring.

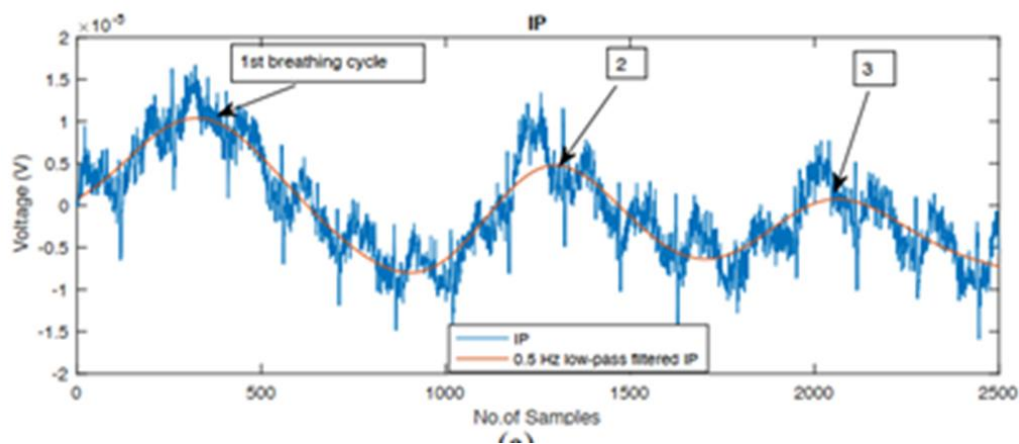


Figure 6.22 - A typical respiration signal at rest.

The garment shows that a low-cost sensor garments such as SSB could be mass-produced using sewing/whole knitting techniques commonly employed in the textile industry. The SSB features the optimum performing materials and stitch patterns in both the electrodes and the stitch stretch sensor, which are then integrated into the ideal design of bra for this purpose. Future work will focus on an assessment of the performance of the SSB for monitoring other body signals.

## 6.6 Summary of the Results and Conclusions

This research has demonstrated the design integration and applicability of textile-based sensors for health and fitness monitoring. The research demonstrates that the design and materials of the electrode-holding garment is as critical as the design of the E-sensors (electrode and stretch sensor) themselves. The garment must have the required characteristics to ensure that the electrode remains stable throughout periods of user movement and relaxation, to achieve accurate and uniform signal reading. The garment design and material chosen to be used in conjunction with the optimum electrode design was established after extensive investigation. The material (nylon/spandex in single jersey) was chosen for its excellent elasticity, body conformity and user comfort. The design (Y shaped racerback with net structure added between the lower and upper portion) was arrived at after detailed experiments, described in Appendix E. The garment design

technique which incorporates the electrodes into the SSBs and particularly the net “shock absorbing” structure has proved effective for producing stable electronic signals, whilst being comfortable and easy to wear.

The textile electrodes were compared with conventional gel electrodes under real user experience and the results recorded and presented. The experimental results show that the two-electrodes in the SSBs processed with CSM and KM can reliably measure ECG signals during body movement. It was shown that there was negligible baseline drift and low-frequency noise from both SSBs and the results are comparable to the standard ECG waveform signal from the commercial gel electrode. The findings also show that the SSB with a net supporting structure design provides better ECG signal stability, due to the higher hysteresis values which indicates higher shock absorbing of the fabric surrounding the electrode as the body moves and hence improving position stability and contact area between electrode and the body skin. Even though the textile electrodes do not use any conductive gel, their performance in real ECG monitoring coupled with the effective design and material properties of the garment gives comparable ECG measurements to gel-based electrodes, even under body movement conditions for which the gel commercial electrodes are not designed to have.

The work also shows how a stitch stretch sensor can be effectively integrated to the same SSB capable of measuring, but not limited to, respiration which can provide vital well-being signals of the wearer. To this effect breathing periodicity and depth of the amplitude can easily be monitored and problems such as sleep apnea easily detected. It means that the same, easy to wear garment, can be used to reliably and uniformly monitor ECG signals and respiration over long periods while remaining comfortable and allowing free movement.

The sensors in these garments maybe further improved by knitting all their parts in the machine, however this will require the development of specific yarns to overcome insulation needs and to have specific stretching properties.

## Chapter 7 – Summary and Conclusion

This research has investigated, developed and implemented wearable E-sensors for continuous monitoring of vital physiological signals; Soft, textile dry electrodes for ECG monitoring and stitch type stretch-sensors for monitoring movement. These E-sensors have been designed in a novel sports bra SSB wearable garment, showing how the garment design process is optimised by working at the design/technology interface to produce an unobtrusive, effective, comfortable high performance garment with high aesthetic and performance functionality.

The study has focused on electrodes and stretch sensors, regarding them as two areas of importance for advancing wearable technology and particularly continuous monitoring without the adverse effects of noise due to body movement. Investigations of material properties and performance was conducted before designing and establishing the actual sensors and optimising their performance. The study went on to design a wearable sports bra with the sensors being part of the design and assessed for end user ECG and respiration performance.

Having surveyed the literature with respect to electrodes, we identified the need of optimising the material, its structure and the size/shape of textile electrodes so that they can be used for continuous ECG monitoring. And for stretch sensor movement monitoring (respiration), aspects of sensor structure, signal stability and repeatability, accuracy and sensitivity have been investigated. Initially, a study regarding the conductive thread behavior was performed by measuring the electrical resistance properties when length and tension are altered. The silver-plated nylon 117/17 two-ply and silver-plated nylon 234/34 four-ply threads have shown good conductivity performance with their baseline resistance being  $215\Omega$  and  $23\Omega$  respectively. Tensile measurement in five-cycle experiments revealed the influence of tension on electrical resistance. When the thread is strained the fibers change their orientation and they are forced to compact and straighten, increasing the electrical resistance of both threads to  $440\Omega$  and  $69\Omega$  respectively, as shown in Figure 3.4.

The conductivity of fabrics was investigated for the development of dry electrodes. Five types of conductive fabric, Table 3.3, being light-weight, soft, and sewable were studied. The silver coating used in the conductive fabric is user friendly in that it does not cause skin irritation and has natural protection against bacteria.

Electrodes were made up to investigate their skin-impedance behaviour, as the structure and impedance of the human skin plays a key role in the electrode-skin interface. A skin dummy made of agar was devised in order to exclude the large influence from variation in skin properties on the results; this skin simulation model has good stability and repeatability, so the same skin properties can be repeated over time. The contact impedance of the five electrodes under investigation were between  $450\Omega$  and  $5.2k\Omega$ , with the best performing being by the MedTex™ P-130 (electrode 1), which is made of single jersey knitted fabric. This fabric has a large amount of silver coated area, providing good skin/electrode contact, high conductivity and low impedance  $450\Omega$ . The performance of electrode 1 is followed by electrode 5 made from silver plated conductive thread 234/34 4-ply with  $500\Omega$  impedance. These results have shown that the skin/electrode interface needs time to stabilise and show uniform and reliable results. The results have also shown that the knitted electrodes have better contact impedance than woven electrodes due to their property of being more flexible and so following the curvature of the body more closely.

The measurement of electrical signal transmission values of the two-best performing conductive fabric electrodes (electrode 1 and 5) were investigated and compared with commercial gel-electrodes. The signal characteristics of those electrodes have shown uniform and better than commercial electrodes electrical transmission. The fabric electrodes have shown no offset against the commercial gel electrode which is showed an offset of  $0.2V$ . between the measured signals and the reference signal (Table 3.6). This phenomenon can be attributed to the relaxation mechanism occurring in the electrolyte component of the polymer material in the gel. It was established that electrodes 1 and 5 are suitable for electrode use and that they can replace commercial gel electrodes, provided that their properties are carefully engineered and assessed. The added advantage here being that although the wet electrode cannot be used for continuous monitoring, the dry electrode can and in fact it gets better with extensive use due to sweating creating a more conductive contact between electrode and skin [151].

When considering the skin electrodes, not only the contact impedance of the electrode is of importance, but also the impedance at the electrode interface from its physical properties; size and shape. Therefore, the different physical characteristics in the mechanical interaction of textile electrodes were further investigated in various sizes, shapes, positions and pressures. Our studies have shown that the skin-electrode impedance can be reduced by increasing the size of the electrode. ECG measurements



obtained from three pairs of dry textile electrodes and one pair of commercial gel electrodes show that small-size electrodes generate more noise than larger electrodes due to their high skin-electrode impedance and that by increasing the electrode size to 20x40 mm, the quality of ECG signal is as good as that of the gel electrode.

Our investigations went on to find the effect of electrode position, and the results have shown that different electrode positions led to large differences in the average impedance value and a high variation in skin impedance can occur even between two positions on the same body that are close to each other, as seen in Figure 4.3. This research also shows that a skin/electrode stabilisation period of three minutes should be performed before electrodes are used to record any signals, in order to minimize electrode imbalance. The textile electrodes achieve good contact with the skin by utilising holding pressure, but of course this cannot be increased beyond the comfortable limits of the end user. When our work examined the holding electrode pressures ranging from 0.7 kPa (5mmHg) to 6 kPa (45 mmHg), it has found that 4 kPa (30 mmHg) is the optimum electrode-holding pressure to achieve body comfort and low skin-electrode impedance.

Finally the optimum electrode size and position on the body for ECG monitoring was then investigated (Section 4.2). It was found that the number of three electrodes could produce a medical grade ECG measurement/monitoring and that their optimum positioning is the electrodes in the back horizontal formation, as in Figure 4.10b. It is also important to note that the electrodes are positioned under the breast where minimal muscle movement is experienced. This type of dry electrodes can be used for ECG, heartbeat and EEG wearable devices.

An E-textile stretch sensor has then been investigated to enable movement monitoring. The elastic property of a stitch used in garment production is considered not only due to its response to mechanical movement change with the body but also because it can be part of the garment and/or of the ease of applying it anywhere in the garment. Hence conductive sewing threads have been investigated to develop a reliable E-textile sensor by stitching.

Preliminary the research examined the fabric properties in relationship to elasticity and recovery of six fabrics substrates that would hold the stitch, (Table 5.1) and it was found that a single jersey nylon (two-ply, 4.44 tex) with 25% Spandex (7.78 tex) is a good substrate with excellent stretch and recovery properties (93%).

Different types of stitch configurations, Stitch type 304, 406, 506, and 605 (Table 5.2) have been tested and evaluated based on the theory and characteristics of the conductive loop structure method in both stretched and relaxed stitch formation. It has been explained that when the sensor gets stretched the contact between each thread is reduced. The angle of stitch is increased and the distance between each thread gets longer. Subsequently, the electrical resistance in the conductive thread increases as the conductive path increases by being stretched. This increase in resistance is in direct proportion to the degree to which the thread is stretched or elongated. This property, along with the characteristic of the electrical resistance change being almost instantaneous, makes conductive thread an ideal candidate for use in a stretch sensor. It was found that stitch type 304 2-ply was the best performing stitch for use in this sensor. It features exceptionally good working range (potentially well past 50%) and linearity ( $R^2$  is 0.98), low hysteresis (6.25%  $\Delta R$ ), good gauge factor (1.61), and baseline resistance ( $125\Omega$ ), as well as good repeatability (drift in  $R^2$  is -0.00). This sensor is also comfortable to wear, easy to design and cost effective. The intention was to develop these sensors for garments that could be laundered or dry cleaned, some preliminary tests suggested likewise but this question will be answered thoroughly in further research.

Having now established two E-Textile sensors; a dry electrode and a stitch stretch sensor, their integrated design in a wearable vest was further investigated. The research proposes new perspectives for consideration in terms of garment-integration design, usability, functional form and the user's interaction, in which the sensors are part of the initial design of the garment. And because of this, aspects of holding pressure and minimisation of noise by body movement are all taken care by the garment design process- like saying that the garment is the sensor itself and that the two aspects; the garment and the sensors are not separate. To that effect two wearable SMART Sports Bras were designed and made up using cut and sew as well as knitted methods.

For ECG monitoring, the Nylon/spandex (4.44 Tex two-ply/7.78 Tex) in single jersey was found to have excellent elasticity and body comfort and the close fitting compression bra design with racer back (Y shape) was chosen (Appendix E). This design allows for a wide spectrum of body movement while retaining close contact with the skin. When electrodes and stretch sensors are incorporated into the SSBs, the natural characteristics of the bra structure assist in keeping stable and uniform contact between the skin and the sensor. To further help the stability of the electrodes, a novel knitted net structure was designed and made to hold the electrodes within the fabric of the bra, by reducing its

hysteresis around the local area of the electrode –acting as a shock absorber. This worked well because the bra/skin movement is very small anyway, due to the close fitting and flexible nature of the bra, so the net structure was able to cope with the amount of movement experienced, leaving the electrode in a stable position. This has further been shown in actual ECG measurement where a greater ECG signal stability is due to improving the contact between the electrode and the skin and avoiding body movement noise. The sports bra has been further optimized under a modular system in which an ECG device (Figure 4.11 ) can be easily snapped onto the garment and removed or replaced, making it ideal for washing. Finally, real ECG tests were undertaken using a software app pre-installed on the phone, in which the ECG waveforms are displayed showing that the quality of the ECG signal is comparable to the standard medical ECG waveform and that the textile electrode used goes beyond the performance of the commercial gel electrode, because now they can be used for continuous ECG monitoring whilst sitting, moving, climbing or running, (Section 6.4).

In this bra design the stretch sensor could be positioned anywhere for the monitoring of movement and as an example it was decided to use it to monitor breathing (Section 6.5). The sensor is positioned across the chest for respiration monitoring, which is a vital body function compatible with the ECG monitoring. The two ECG electrodes are placed along the 5th intercostal space on the right and left mid-clavicular, and the third one placed at the scapular line in the back. Typical traces can be used alone or in combination with the ECG to improve well-being, heart condition or to monitor breathing after exercising or sleep apnea. In fact, with the appropriate garment design, this stretch sensor can be positioned to measure muscle and joint movement anywhere in the body.

The materials, methods and techniques of this research project can be applied and adapted for products and applications in other wearable technology end uses. This study has been already disseminated by producing 3 refereed journal papers, one invited conference paper and two further publications are at a preparation stage.

## **7.1 Further work.**

This research has shown that there are many avenues of further work that may be explored. Further exploration on the ability of the SSB, along with the sensor apparatus to undergo regular washing would be of great benefit in helping to make it even more user friendly.

With the development of insulated yarns of specific stretching properties completely whole garments can be designed and developed.

The example design of the stitch stretch sensor being used for respiration measurement is just one of many possible applications. Further work exploring data collection of movement in other parts of the body such as knee, elbow, ankle etc. shows great potential.

The textile based electrodes that resulted from the research can be used in many additional scenarios, such as muscle measurement, EEG data collection, temperature and blood pressure monitoring.

Wearable textile sensors for extreme environments is another area of importance along of course with the focused medical rehabilitation narrowing which will allow for not needing hospitalisation. Further work on the stability of the electrodes and stretch sensor in changing environments would be beneficial to extend the range of usability of these devices.

Exploring other garments for men, for children, for the elderly and for extreme environments are areas of further interest. Venturing to miniturising all of these and to perhaps integrate them into micro/nano structures maybe another way of new and exciting research.

## REFERENCES

1. Tao, X., *Smart fibres, fabrics and clothing: fundamentals and applications*. 2001: Elsevier.
2. Stoppa, M. and A.J.s. Chiolerio, *Wearable electronics and smart textiles: A critical review*. 2014. **14**(7): p. 11957-11992.
3. Hughes-Riley, T., T. Dias, and C.J.F. Cork, *A historical review of the development of electronic textiles*. 2018. **6**(2): p. 34.
4. Suh, M., et al., *Critical review on smart clothing product development*. 2010. **6**(4).
5. Meoli, D., et al., *Interactive electronic textile development: A review of technologies*. 2002. **2**(2): p. 1-12.
6. Park, S., K. Mackenzie, and S. Jayaraman. *The wearable motherboard: A framework for personalized mobile information processing (PMIP)*. in *proceedings of the 39th annual design automation conference*. 2002.
7. Randell, C.J.T.T.I., *Computerised clothing will benefit textile manufacturers*. 2001. **10**(7): p. 3-28.
8. Berglin, L.T.H., *Smart Textiles and Wearable Technologies A study of smart textiles in fashion and clothing*. 2013.
9. Marzano, S., *New nomads: An exploration of wearable electronics by Philips*. 2000: 010 Publ.
10. Paradiso, R., et al., *WEALTHY-a wearable healthcare system: new frontier on e-textile*. 2005: p. 105-113.
11. Lymberis, A., D.J.W.e.s.f.p.h.m.s.o.t.a. De Rossi, and f. challenges, *Myheart: Fighting cardiovascular disease by preventive lifestyle and early diagnosis*. 2004. **108**: p. 36-42.
12. Narbonneau, F., et al. *OFSETH: Smart medical textile for continuous monitoring of respiratory motions under magnetic resonance imaging*. in *2009 Annual International Conference of the IEEE Engineering in Medicine and Biology Society*. 2009. IEEE.
13. Curone, D., et al., *Smart garments for emergency operators: the ProeTEX project*. 2010. **14**(3): p. 694-701.
14. Paradiso, R. and D. De Rossi. *Advances in textile technologies for unobtrusive monitoring of vital parameters and movements*. in *2006 International Conference of the IEEE Engineering in Medicine and Biology Society*. 2006. IEEE.
15. Mitchell, E., et al. *Breathing feedback system with wearable textile sensors*. in *2010 International Conference on Body Sensor Networks*. 2010. IEEE.
16. Guo, L., et al., *Design of a garment-based sensing system for breathing monitoring*. 2013. **83**(5): p. 499-509.
17. Pacelli, M., G. Loriga, and R. Paradiso. *Flat knitted sensors for respiration monitoring*. in *2007 IEEE international symposium on industrial electronics*. 2007. IEEE.
18. Coyle, S., et al., *BIOTEX—Biosensing textiles for personalised healthcare management*. 2010. **14**(2): p. 364-370.
19. Parthiban, M., M. Srikrishnan, and M.S. Viju, *Optical Fibers for Smart clothing & technical textile applications*.
20. Stylios, G.K. and D.Y. Yang. *The Concept of Mood Changing Garments Made From Luminescent Woven Fabrics and Flexible Photovoltaics "MoodWear"*. in *Advances in Science and Technology*. 2013. Trans Tech Publ.
21. George K Stylios, L.L., *A Novel Wearable Low Energy Mini Size ECG ANT Node for Health Monitoring*. Ege-meditex, international Congress on Healthcare and Medical Textile, Izmir, Turkey, 2012.

22. Jakubas, A., E. Łada-Tondyra, and M. Nowak. *Textile sensors used in smart clothing to monitor the vital functions of young children*. in *2017 Progress in Applied Electrical Engineering (PAEE)*. 2017. IEEE.
23. Molinaro, N., et al. *Wearable textile based on silver plated knitted sensor for respiratory rate monitoring*. in *2018 40th Annual International Conference of the IEEE Engineering in Medicine and Biology Society (EMBC)*. 2018. IEEE.
24. Di Tocco, J., et al. *A wearable system for respiratory and pace monitoring in running activities: A feasibility study*. in *2020 IEEE International Workshop on Metrology for Industry 4.0 & IoT*. 2020. IEEE.
25. The Engineering and Physical Sciences Research Council, E. *UK Research and Innovation*. 1994 [cited 2021 15 May ]; Available from: <https://epsrc.ukri.org/about/>.
26. Atalay, O., W.R. Kennon, and M.D.J.S. Husain, *Textile-based weft knitted strain sensors: Effect of fabric parameters on sensor properties*. 2013. **13**(8): p. 11114-11127.
27. Rattfält, L., et al., *Electrical characteristics of conductive yarns and textile electrodes for medical applications*. 2007. **45**(12): p. 1251-1257.
28. Hughes, J. and F.J.S. Iida, *Multi-functional soft strain sensors for wearable physiological monitoring*. 2018. **18**(11): p. 3822.
29. Carvalho, H., et al. *Health monitoring using textile sensors and electrodes: An overview and integration of technologies*. in *2014 IEEE international symposium on medical measurements and applications (MeMeA)*. 2014. IEEE.
30. Yapici, M.K., et al., *Graphene-clad textile electrodes for electrocardiogram monitoring*. 2015. **221**: p. 1469-1474.
31. Guo, L., et al. *'Disappearing Sensor'-Textile Based Sensor for Monitoring Breathing*. in *2011 International Conference on Control, Automation and Systems Engineering (CASE)*. 2011. IEEE.
32. Pacelli, M., et al. *Sensing fabrics for monitoring physiological and biomechanical variables: E-textile solutions*. in *2006 3rd IEEE/EMBS International Summer School on Medical Devices and Biosensors*. 2006. IEEE.
33. Li, H., et al., *Wearable sensors in intelligent clothing for measuring human body temperature based on optical fiber Bragg grating*. 2012. **20**(11): p. 11740-11752.
34. Vallozzi, L., et al. *Wearable textile GPS antenna for integration in protective garments*. in *Proceedings of the Fourth European Conference on Antennas and Propagation*. 2010. IEEE.
35. Mitschke, C., M. Öhmichen, and T.L.J.A.S. Milani, *A single gyroscope can be used to accurately determine peak eversion velocity during locomotion at different speeds and in various shoes*. 2017. **7**(7): p. 659.
36. Oliveira, A., et al. *A Textile Embedded Wearable Device for Movement Disorders Quantification*. in *2020 42nd Annual International Conference of the IEEE Engineering in Medicine & Biology Society (EMBC)*. 2020. IEEE.
37. IDTechEx. *E-Textiles & Smart Clothing 2021-2031: Technologies, Markets and Players*. 2021 [cited 2021 30 July]; Available from: <https://www.idtechex.com/en/research-report/e-textiles-and-smart-clothing-2021-2031-technologies-markets-and-players/828>.
38. Ismar, E., et al., *Futuristic clothes: Electronic textiles and wearable technologies*. 2020. **4**(7): p. 1900092.
39. Van Langenhove, L., R. Puers, and D.J.T.f.p. Matthys, *Intelligent textiles for protection*. 2005: p. 176-195.
40. Shyr, T.-W., et al., *A textile-based wearable sensing device designed for monitoring the flexion angle of elbow and knee movements*. 2014. **14**(3): p. 4050-4059.

41. Paradiso, R., G. Loriga, and N.J.I.t.o.I.T.i.b. Taccini, *A wearable health care system based on knitted integrated sensors*. 2005. **9**(3): p. 337-344.
42. Arquilla, K., A.K. Webb, and A.P.J.S. Anderson, *Textile electrocardiogram (ECG) electrodes for wearable health monitoring*. 2020. **20**(4): p. 1013.
43. Cheng, J., et al., *Designing sensitive wearable capacitive sensors for activity recognition*. 2013. **13**(10): p. 3935-3947.
44. Cho, G., et al., *Performance evaluation of textile-based electrodes and motion sensors for smart clothing*. 2011. **11**(12): p. 3183-3193.
45. Hatamie, A., et al., *Textile based chemical and physical sensors for healthcare monitoring*. 2020. **167**(3): p. 037546.
46. Popovic, Z., P. Momenroodaki, and R.J.I.C.M. Scheeler, *Toward wearable wireless thermometers for internal body temperature measurements*. 2014. **52**(10): p. 118-125.
47. Boano, C.A., et al. *Accurate temperature measurements for medical research using body sensor networks*. in *2011 14th IEEE International Symposium on Object/Component/Service-Oriented Real-Time Distributed Computing Workshops*. 2011. IEEE.
48. Carpi, F. and D.J.I.t.o.I.T.i.b. De Rossi, *Electroactive polymer-based devices for e-textiles in biomedicine*. 2005. **9**(3): p. 295-318.
49. Brady, S., et al., *Body sensor network based on soft polymer sensors and wireless communications*. 2007.
50. Zhao, C., et al., *A thread-based wearable sweat nanobiosensor*. 2021: p. 113270.
51. Wu, K.-f., C.-h. Chan, and Y.-t. Zhang. *Contactless and cuffless monitoring of blood pressure on a chair using e-textile materials*. in *2006 3rd IEEE/EMBS International Summer School on Medical Devices and Biosensors*. 2006. IEEE.
52. Pailles-Friedman, R.J.A.M.T., *Electronics and Fabrics: The Development of Garment-Based Wearables*. 2018. **3**(10): p. 1700307.
53. Lymberis, A. and R. Paradiso. *Smart fabrics and interactive textile enabling wearable personal applications: R&D state of the art and future challenges*. in *2008 30th Annual International Conference of the IEEE Engineering in Medicine and Biology Society*. 2008. IEEE.
54. Neuman, M.R.J.M.i.a. and design, *Biopotential electrodes*. 1998. **4**: p. 189-240.
55. Button, V.L.D.S.N., *Chapter 2 - Electrodes for Biopotential Recording and Tissue Stimulation*, in *Principles of Measurement and Transduction of Biomedical Variables*, V.L.D.S.N. Button, Editor. 2015, Academic Press: Oxford. p. 25-76.
56. Ödman, S., et al., *Movement-induced potentials in surface electrodes*. 1982. **20**(2): p. 159-166.
57. Tam, H. and J.G.J.I.T.o.B.E. Webster, *Minimizing electrode motion artifact by skin abrasion*. 1977(2): p. 134-139.
58. Meziane, N., et al., *Dry electrodes for electrocardiography*. 2013. **34**(9): p. R47.
59. Xu, P., H. Zhang, and X.J.T.P. Tao, *Textile-structured electrodes for electrocardiogram*. 2008. **40**(4): p. 183-213.
60. Einthoven, W.J.A.f.d.g.P.d.M.u.d.T., *Die galvanometrische Registrierung des menschlichen Elektrokardiogramms, zugleich eine Beurtheilung der Anwendung des Capillar-Elektrometers in der Physiologie*. 1903. **99**(9): p. 472-480.
61. Ishijima, M.J.M., B. Engineering, and Computing, *Cardiopulmonary monitoring by textile electrodes without subject-awareness of being monitored*. 1997. **35**(6): p. 685-690.
62. Hoffmann, K.-P. and R. Ruff. *Flexible dry surface-electrodes for ECG long-term monitoring*. in *2007 29th Annual International Conference of the IEEE Engineering in Medicine and Biology Society*. 2007. IEEE.

63. Baek, J.-Y., et al., *Flexible polymeric dry electrodes for the long-term monitoring of ECG*. 2008. **143**(2): p. 423-429.
64. Pola, T. and J. Vanhala. *Textile electrodes in ECG measurement*. in *2007 3rd International Conference on Intelligent Sensors, Sensor Networks and Information*. 2007. IEEE.
65. Pylatiuk, C., et al. *Comparison of surface EMG monitoring electrodes for long-term use in rehabilitation device control*. in *2009 IEEE International Conference on Rehabilitation Robotics*. 2009. IEEE.
66. Yamagami, M., et al., *Assessment of dry epidermal electrodes for long-term electromyography measurements*. 2018. **18**(4): p. 1269.
67. Scilingo, E.P., et al., *Performance evaluation of sensing fabrics for monitoring physiological and biomechanical variables*. 2005. **9**(3): p. 345-352.
68. Chi, Y.M., T.-P. Jung, and G.J.I.r.i.b.e. Cauwenberghs, *Dry-contact and noncontact biopotential electrodes: Methodological review*. 2010. **3**: p. 106-119.
69. Huhta, J.C. and J.G.J.I.T.o.B.E. Webster, *60-Hz interference in electrocardiography*. 1973(2): p. 91-101.
70. Reilly, J.P., et al., *Electrical stimulation and electropathology*. 1992: Cambridge University Press.
71. de Talhouet, H. and J.G.J.P.M. Webster, *The origin of skin-stretch-caused motion artifacts under electrodes*. 1996. **17**(2): p. 81.
72. Medrano, G., et al. *Skin electrode impedance of textile electrodes for bioimpedance spectroscopy*. in *13th International Conference on Electrical Bioimpedance and the 8th Conference on Electrical Impedance Tomography*. 2007. Springer.
73. Searle, A. and L.J.P.m. Kirkup, *A direct comparison of wet, dry and insulating bioelectric recording electrodes*. 2000. **21**(2): p. 271.
74. Ankhili, A., et al., *Washable and reliable textile electrodes embedded into underwear fabric for electrocardiography (ECG) monitoring*. 2018. **11**(2): p. 256.
75. Thirunavukkarasu, S. and D. Kaliyamurthie, *Management of streaming body sensor data through wireless transmission for medical information systems*. *International Journal of Innovative Research in Computer and Communication Engineering*. **2**(8).
76. Suh, M., *Wearable sensors for athletes*, in *Electronic Textiles*. 2015, Elsevier. p. 257-273.
77. Cochrane, C., et al., *Design and development of a flexible strain sensor for textile structures based on a conductive polymer composite*. 2007. **7**(4): p. 473-492.
78. Metcalf, C.D., et al., *Fabric-based strain sensors for measuring movement in wearable telemonitoring applications*. 2009.
79. Gioberto, G. and L. Dunne. *Theory and characterization of a top-thread coverstitched stretch sensor*. in *2012 IEEE International Conference on Systems, Man, and Cybernetics (SMC)*. 2012. IEEE.
80. Jeong, J., et al. *Wearable respiratory rate monitoring using piezo-resistive fabric sensor*. in *World congress on medical physics and biomedical engineering, september 7-12, 2009, munich, germany*. 2009. Springer.
81. Totaro, M., et al., *Soft smart garments for lower limb joint position analysis*. 2017. **17**(10): p. 2314.
82. Gioberto, G. *Garment-integrated wearable sensing for knee joint monitoring*. in *Proceedings of the 2014 ACM International Symposium on Wearable Computers: Adjunct Program*. 2014.
83. Atalay, O.J.M., *Textile-based, interdigital, capacitive, soft-strain sensor for wearable applications*. 2018. **11**(5): p. 768.



84. Guo, L. and L. Berglin. *Test and evaluation of textile based stretch sensors*. in *AUTEX 2009 World Textile Conference, Izmir, Turkey 2009*. 2009.
85. Suh, J.-H., et al. *Finger motion detection glove toward human-machine interface*. in *2015 IEEE SENSORS*. 2015. IEEE.
86. Yamada, T., et al., *A stretchable carbon nanotube strain sensor for human-motion detection*. 2011. **6**(5): p. 296.
87. Gioberto, G., C. Compton, and L.J.S.T.J. Dunne, *Machine-stitched E-textile stretch sensors*. 2016. **202**: p. 25-37.
88. Atalay, O. and W.R.J.S. Kennon, *Knitted strain sensors: Impact of design parameters on sensing properties*. 2014. **14**(3): p. 4712-4730.
89. Guo, L., L. Berglin, and H.J.N.T.J. Mattila, *Textile strain sensors characterization-sensitivity, linearity, stability and hysteresis*. 2010(2): p. 51-63.
90. Kannaian, T., et al., *Experimental investigations of woven textile tape as strain sensor*. 2015. **96**(2): p. 125-130.
91. Imran, M., A.J.S. Bhattacharyya, and A.A. Physical, *Thermal response of an on-chip assembly of RTD heaters, sputtered sample and microthermocouples*. 2005. **121**(2): p. 306-320.
92. Cochrane, C., V. Koncar, and M.J.W.t.A. Lewandowski, *Development of a flexible strain sensor for textile structures*. 2008: p. 67.
93. Munro, B.J., et al., *The intelligent knee sleeve: A wearable biofeedback device*. 2008. **131**(2): p. 541-547.
94. Guo, L., L. Berglin, and H.J.T.r.j. Mattila, *Improvement of electro-mechanical properties of strain sensors made of elastic-conductive hybrid yarns*. 2012. **82**(19): p. 1937-1947.
95. Ukkonen, L., L. Sydänheimo, and Y. Rahmat-Samii. *Sewed textile RFID tag and sensor antennas for on-body use*. in *2012 6th European Conference on Antennas and Propagation (EUCAP)*. 2012. IEEE.
96. Linz, T., et al. *Fully untegrated EKG shirt based on embroidered electrical interconnections with conductive yarn and miniaturized flexible electronics*. in *International Workshop on Wearable and Implantable Body Sensor Networks (BSN'06)*. 2006. IEEE.
97. Martínez-Estrada, M., et al., *Impact of conductive yarns on an embroidery textile moisture sensor*. 2019. **19**(5): p. 1004.
98. Jia, J., et al., *Conductive thread-based textile sensor for continuous perspiration level monitoring*. 2018. **18**(11): p. 3775.
99. Pakhchyan, S. *Conductive thread*. 2010 [cited 2021 10 May]; Available from: <https://www.kobakant.at/DIY/?p=379>.
100. Gilliland, S., et al. *The Textile Interface Swatchbook: Creating graphical user interface-like widgets with conductive embroidery*. in *International Symposium on Wearable Computers (ISWC) 2010*. 2010. IEEE.
101. Zeagler, C., et al. *Can i wash it? the effect of washing conductive materials used in making textile based wearable electronic interfaces*. in *Proceedings of the 2013 International Symposium on Wearable Computers*. 2013.
102. Marozas, V., et al., *A comparison of conductive textile-based and silver/silver chloride gel electrodes in exercise electrocardiogram recordings*. 2011. **44**(2): p. 189-194.
103. Gioberto, G., et al., *Overlock-stitched stretch sensors: Characterization and effect of fabric property*. 2013. **8**(3).
104. Gioberto, G., et al. *Detecting bends and fabric folds using stitched sensors*. in *Proceedings of the 2013 International Symposium on Wearable Computers*. 2013.
105. Mattmann, C., F. Clemens, and G.J.S. Tröster, *Sensor for measuring strain in textile*. 2008. **8**(6): p. 3719-3732.

106. Tiller, J.C., et al., *Designing surfaces that kill bacteria on contact*. 2001. **98**(11): p. 5981-5985.
107. Cömert, A., M. Honkala, and J.J.B.e.o. Hyttinen, *Effect of pressure and padding on motion artifact of textile electrodes*. 2013. **12**(1): p. 1-18.
108. Liu, Z., et al., *Progress on fabric electrodes used in biological signal acquisition*. 2015. **3**(03): p. 204.
109. Raicu, V., et al., *A quantitative approach to the dielectric properties of the skin*. 2000. **45**(2): p. L1.
110. Beckmann, L., et al., *Characterization of textile electrodes and conductors using standardized measurement setups*. 2010. **31**(2): p. 233.
111. Kwon, H.J., Y. Osada, and J.P.J.P.j. Gong, *Polyelectrolyte gels-fundamentals and applications*. 2006. **38**(12): p. 1211-1219.
112. Pal, K., et al., *Polymeric hydrogels: characterization and biomedical applications*. 2009. **12**(3): p. 197-220.
113. Sengwa, R., S. Choudhary, and S.J.E.P.L. Sankhla, *Low frequency dielectric relaxation processes and ionic conductivity of montmorillonite clay nanoparticles colloidal suspension in poly (vinyl pyrrolidone)-ethylene glycol blends*. 2008. **2**: p. 800-809.
114. Rosell, J., et al., *Skin impedance from 1 Hz to 1 MHz*. 1988. **35**(8): p. 649-651.
115. Puurtinen, M.M., et al. *Measurement of noise and impedance of dry and wet textile electrodes, and textile electrodes with hydrogel*. in *2006 international conference of the IEEE Engineering in Medicine and Biology Society*. 2006. IEEE.
116. Zhang, X., K. Yeung, and Y.J.T.R.J. Li, *Numerical simulation of 3D dynamic garment pressure*. 2002. **72**(3): p. 245-252.
117. Steijlen, A.S., et al., *A novel 12-lead electrocardiographic system for home use: development and usability testing*. 2018. **6**(7): p. e10126.
118. Crawford, J. and L.J.J.o.P.P. Doherty, *Recording a standard 12-lead ECG: filling in gaps in knowledge*. 2009. **1**(7): p. 271-278.
119. Kligfield, P., et al., *Recommendations for the standardization and interpretation of the electrocardiogram: part I: the electrocardiogram and its technology a scientific statement from the American Heart Association Electrocardiography and Arrhythmias Committee, Council on Clinical Cardiology; the American College of Cardiology Foundation; and the Heart Rhythm Society endorsed by the International Society for Computerized Electrocardiology*. 2007. **49**(10): p. 1109-1127.
120. Romero, I., et al. *Motion artifact reduction in ambulatory ECG monitoring: an integrated system approach*. in *Proceedings of the 2nd Conference on Wireless Health*. 2011.
121. Min, S.D., Y. Yun, and H.J.I.S.J. Shin, *Simplified structural textile respiration sensor based on capacitive pressure sensing method*. 2014. **14**(9): p. 3245-3251.
122. Konno, K. and J.J.J.o.a.p. Mead, *Measurement of the separate volume changes of rib cage and abdomen during breathing*. 1967. **22**(3): p. 407-422.
123. Kim, H.K., et al., *Characteristics of electrically conducting polymer-coated textiles*. 2003. **405**(1): p. 161-169.
124. Wu, J., et al., *Conducting polymer coated lycra*. 2005. **155**(3): p. 698-701.
125. Pacelli, M., et al., *Sensing threads and fabrics for monitoring body kinematic and vital signs*. 2001.
126. Oh, K.W., H.J. Park, and S.H.J.J.o.A.P.S. Kim, *Stretchable conductive fabric for electrotherapy*. 2003. **88**(5): p. 1225-1229.
127. Wijesiriwardana, R., T. Dias, and S. Mukhopadhyay. *Resistive fibre-meshed transducers*. in *Seventh IEEE International Symposium on Wearable Computers, 2003. Proceedings*. 2003. IEEE.

128. Farrington, J., et al. *Wearable sensor badge and sensor jacket for context awareness*. in *Digest of Papers. Third International Symposium on Wearable Computers*. 1999. IEEE.
129. Greenspan, B., et al., *Development and testing of a stitched stretch sensor with the potential to measure human movement*. 2018. **109**(11): p. 1493-1500.
130. Dupler, E. and L.E. Dunne. *Effects of the textile-sensor interface on stitched strain sensor performance*. in *Proceedings of the 23rd International Symposium on Wearable Computers*. 2019.
131. Alias, N.M., M. Ahmad, and N. Hamzaid. *Fabric-based sensor for applications in biomechanical pressure measurement*. in *International Conference on Movement, Health and Exercise*. 2016. Springer.
132. Babaarslan, O.J.T.R.J., *Method of producing a polyester/viscose core-spun yarn containing spandex using a modified ring spinning frame*. 2001. **71**(4): p. 367-371.
133. Scilingo, E.P., et al., *Strain-sensing fabrics for wearable kinaesthetic-like systems*. 2003. **3**(4): p. 460-467.
134. Campbell, T., et al., *Conducting polymer fabric strain gauges: A unique biomechanical monitoring device*. 2003: p. 48.
135. Campbell, T.E., et al., *Can fabric sensors monitor breast motion?* 2007. **40**(13): p. 3056-3059.
136. Lorussi, F., et al., *Wearable, redundant fabric-based sensor arrays for reconstruction of body segment posture*. 2004. **4**(6): p. 807-818.
137. Voyce, J., P. Dafniotis, and S. Towlson, *Elastic textiles*, in *Textiles in sport*. 2005, Elsevier. p. 204-230.
138. Ibrahim, S.J.T.R.J., *Mechanisms of stretch development in fabrics containing spandex yarns*. 1966. **36**(8): p. 696-706.
139. Eltahan, E.J.J.o.C., *Effect of lycra percentages and loop length on the physical and mechanical properties of single jersey knitted fabrics*. 2016. **2016**.
140. Gorjanc, D.Š., V.J.F. Bukosek, and T.i.E. Europe, *The behaviour of fabric with elastane yarn during stretching*. 2008. **16**(3): p. 63-68.
141. Fernández-Caramés, T.M. and P.J.E. Fraga-Lamas, *Towards the Internet of smart clothing: A review on IoT wearables and garments for creating intelligent connected e-textiles*. 2018. **7**(12): p. 405.
142. Ashok, L. and V. Kumar, *Electronics in Textiles and Clothing: Design, Products and Applications*. 2020: CRC PRESS.
143. Bowles, K.-A., et al., *Features of sports bras that deter their use by Australian women*. 2012. **15**(3): p. 195-200.
144. Scurr, J.C., J.L. White, and W.J.J.o.s.s. Hedger, *Supported and unsupported breast displacement in three dimensions across treadmill activity levels*. 2011. **29**(1): p. 55-61.
145. Zhou, J., W.J.J.o.F.B. Yu, and Informatics, *A study on biomechanical models of sports bra's shoulder straps*. 2013. **6**(4): p. 441-451.
146. Adriana, C. and F. BAYTAR, *Towards developing a method for identifying static compression levels of seamless sports bras using 3d body scanning*. 2016.
147. Zhang, L., J. Wang, and R. Han. *Influence Factors of Sports Bra Evaluation and Design Based on Large Size*. in *MATEC Web of Conferences*. 2016. EDP Sciences.
148. Gemperle, F., et al. *Design for wearability*. in *digest of papers. Second international symposium on wearable computers (cat. No. 98EX215)*. 1998. IEEE.
149. Steele, J.R., et al., *The Bionic Bra: Using electromaterials to sense and modify breast support to enhance active living*. 2018. **5**: p. 2055668318775905.

150. An, X. and G.K.J.M. Stylios, *A hybrid textile electrode for electrocardiogram (ECG) measurement and motion tracking*. 2018. **11**(10): p. 1887.
151. Lawson, L., D.J.C. Lorentzen, and T.R. Journal, *Selected sports bras: comparisons of comfort and support*. 1990. **8**(4): p. 55-60.
152. Miller, M.R., et al., *Standardisation of spirometry*. 2005. **26**(2): p. 319-338.
153. Mottram, C., *Ruppel's Manual of Pulmonary Function Testing-E-Book*. 2013: Elsevier Health Sciences.
154. Criée, C., et al., *Body plethysmography—its principles and clinical use*. 2011. **105**(7): p. 959-971.
155. Benito, S. and A. Net, *Pulmonary function in mechanically ventilated patients*. Vol. 13. 2012: Springer Science & Business Media.
156. Russell, R. and P.J.E.r.j. Helms, *Evaluation of three different techniques used to measure chest wall movements in children*. 1994. **7**(11): p. 2073-2076.
157. De Groote, A., et al., *Measurement of thoracoabdominal asynchrony: importance of sensor sensitivity to cross section deformations*. 2000. **88**(4): p. 1295-1302.
158. Zhao, Z., et al., *Machine-washable textile triboelectric nanogenerators for effective human respiratory monitoring through loom weaving of metallic yarns*. 2016. **28**(46): p. 10267-10274.

## Appendix A - The specification sheet of the electrode design.

SPECIFICATION SHEET				
Style: Fabric electrodes		Drescriptions : Electrode formation		Fabric :
Prototype No : 1		Category : Electrode		Consumption :
Date : August 2016				
SIZE SPECIFICATION (UNIT :mm.)			GARMENT MEASUREMENT	
	SIZE	S	M	L
A	Electrode width	15	15	20
B	Electrode length	15	30	40
C	Electrode hight	5	5	5
D	Electrode-base width	31	46	56
E	Electrode-base length	42	42	47
F	Electrode hight	5	5	5
DESIGN SKETCH				
ACCESSORY			SWATCH /COLOUR	
1	Silver plated nylon conductive fabric	1		
2	Non woven	1		
3	Textile filler	1		
4	Thermoplastic adhesive	1		
5	Metal snap Ø 10 mm	1		

**Appendix B** - Additional Results for the effect of electrode size on the skin-electrode impedance.

For investigating the optimum size of textile electrodes, three different electrode sizes have been made as shown in Table 4.2. The electrodes were made using the same conductive fabric (Electrode 1), as previously discussed, chapter 3. Pairs of identical electrodes were made for each of the three sizes, so there were six electrodes in total.

To exclude the variation in time-induced impedance, all three pairs of textile electrodes were placed on the skin concurrently and measured immediately. However, it is important to note that the different electrode positions still produce impedance disparities, causing the measurement results to not only reflect the difference in electrode properties, but also the skin position difference. In order for the influence of electrode position on the results of skin-electrode impedance to be understood and analysed, the three pairs of electrodes were attached on the same skin positions that had been measured in the first experiment (Only the skin positions 2, 4, and 6 have been used in this experiment, due to size limitation in accommodating the larger size electrodes). The experiment was conducted two times in two different groups of electrode position, as illustrated in Figure b.1. In electrode position group A, the large-, medium-, and small-size electrodes were attached to the skin positions 2, 4, and 6 respectively. In the electrode position group B, the large- and small-size electrodes switched positions, while the middle electrode is still placed in position 4. The three pairs of electrodes were placed together and precisely positioned on a piece of self-adhesive fabric in order for them to be placed on the skin concurrently and under the same electrode-holding pressure, as shown in Figure b.2. The measurement of skin-electrode impedances took place every 20 seconds for 30 minutes .

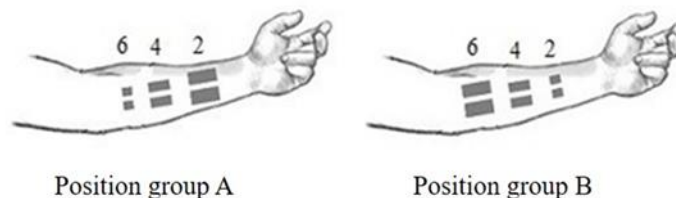


Figure b.1- Electrode size with electrode positions order, group A and B.

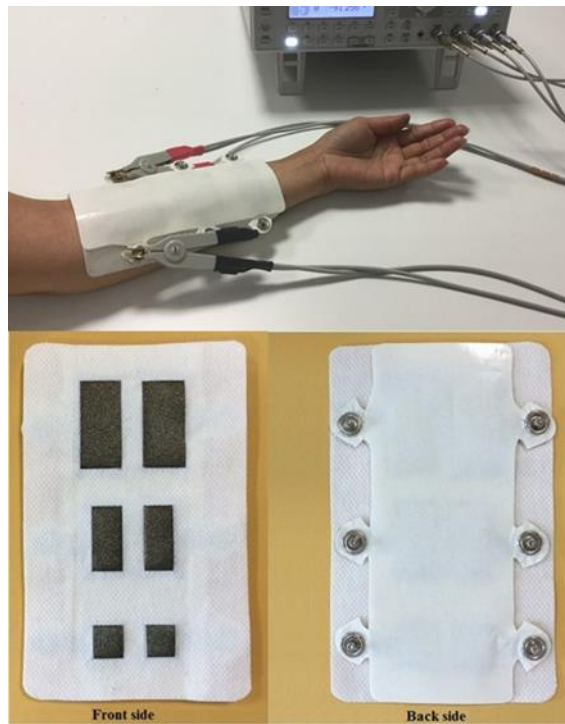


Figure b.2- Electrode size measurement and Assembled electrodes, front and back side.

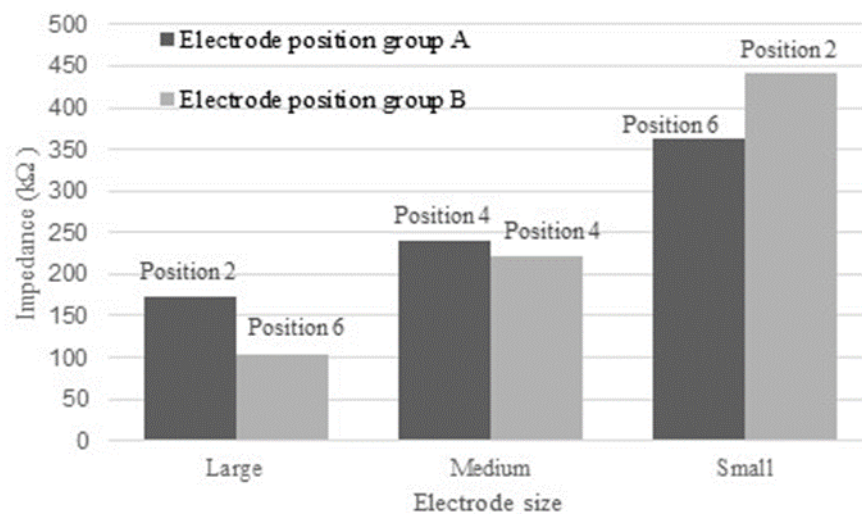


Figure b.3 -The skin-electrode impedance of different textile electrodes size at different electrode positions.

Figure b.3 displays the skin-electrode impedance data measured 30 minutes after the electrodes are placed on the skin. The results are consistent as the skin-electrode impedance decreases when the electrode size increases. It can also be seen that the electrode positions have a significant influence on the impedance magnitude. For both

large- and small-size electrodes, the skin-electrode impedance at position 2 is always higher than that at position 6. The impedance difference is nearly 72 k $\Omega$  and 78 k $\Omega$  for large-size and small-size electrodes respectively. These impedance differences can be explained by the effect of electrode position, shown in Figure 4.4(b), where the impedance in position 6 is much lower than position 2. For the medium sized electrodes, the impedance difference in position 4 can be described by the time-induced impedance variations, as the results from group A and group B were measured at different times. Nonetheless, the time induced impedance difference is only 17.8 K $\Omega$ , which is insignificant compared to the difference in the impedance caused by the electrode size and position. Hence, it is essential to consider the impact of the electrode size and position when measuring the skin electrode impedance.

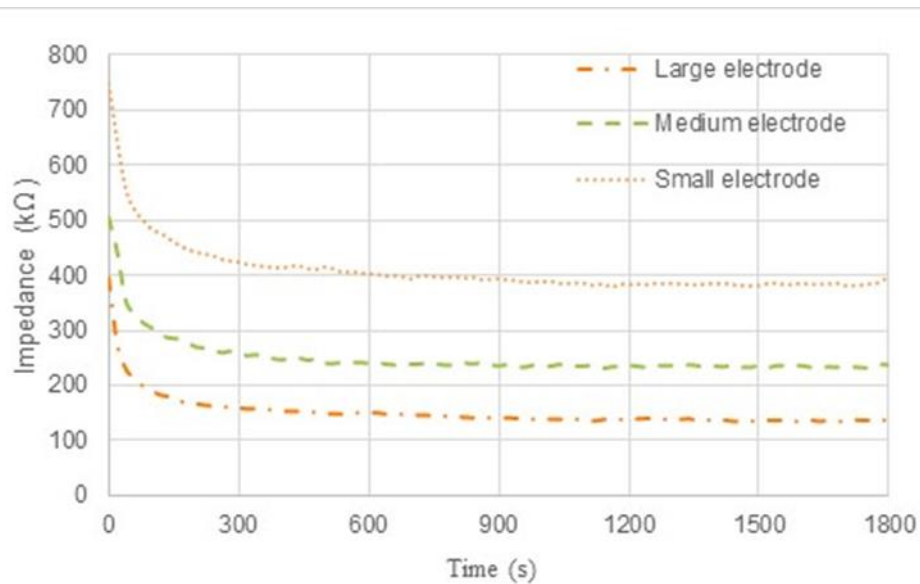


Figure b.4- Results of skin-electrode impedance at 100Hz against time of three sizes of electrode, large (20mmx40mm), medium (15mmx30 mm) and small (15mmx15 mm).

Figure b.4 shows the results of average impedance measured at two different electrode position groups. All impedance values are persistently decreasing within the first three minutes and then steadily become stable. The impedance of the small-size electrodes reduces from 747 k $\Omega$  to 448 k $\Omega$ , the medium-size electrode decreases from 506 k $\Omega$  to 280 k $\Omega$  and the large-size electrode reduces from 396 k $\Omega$  to 170 k $\Omega$ . The primary cause is the accumulated perspiration between the skin and the electrodes, which forms a conductive layer that builds up the electrical conductivity of human skin over time. A stabilization time of three minutes is required before performing any measurement, in

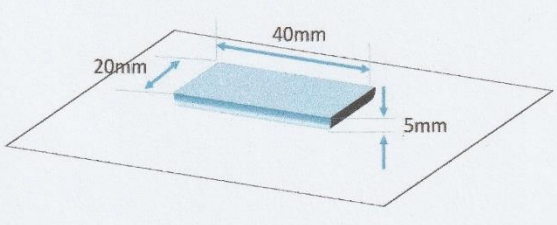


order for the impedance imbalance to be minimised and hence allowing the electrode to become stable. The large-sized textile electrode pair 20 x 40 mm has therefore given the lowest impedance values and hence it is the most suitable for signal recording.

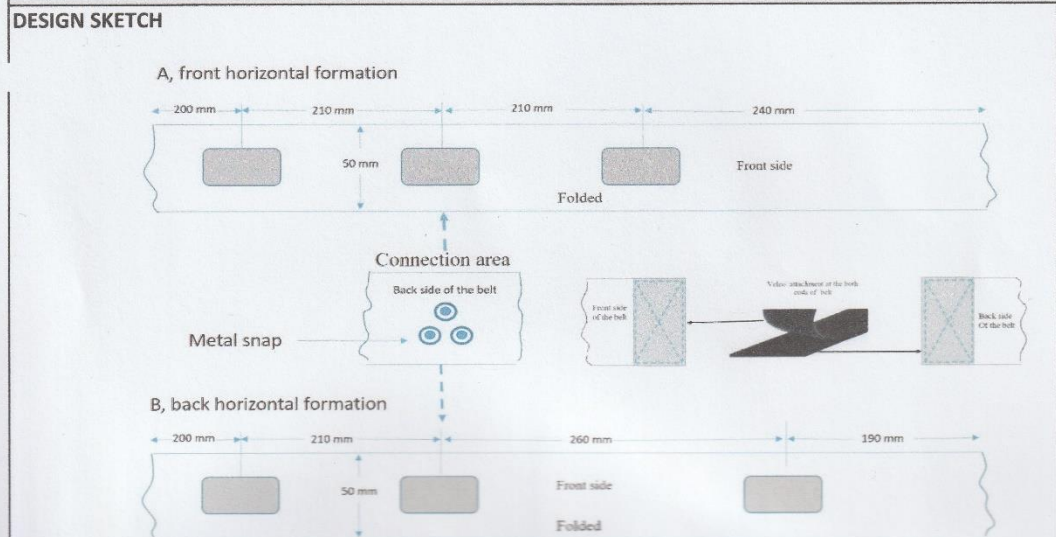
# Appendix C - The details of the two formations of the belt electrode.

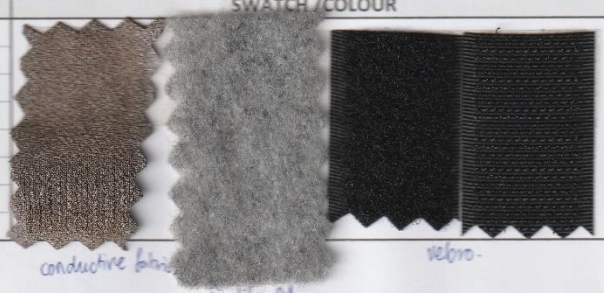
SPECIFICATION SHEET					
Style: Fabric electrodes			Descriptions : Electrode belt		Fabric : 165 mm for 3 electrodes.
Prototype No : 1 Electrode formation			Category : Belt		Consumption :
Date : August 2016					
SIZE SPECIFICATION		(UNIT :mm.)			
	SIZE		L		
A	Electrode width		20		
B	Electrode length		40		
C	Electrode high		5		

**GARMENT MEASUREMENT**



Electrode size



ACCESSORY		SWATCH /COLOUR		
1	Silver plated nylon conductive fabric CUT. 39 X 54mm 3			
2	Metal snap Ø 7 mm			
3	Textile filler 20x40mm			
4	Velco CUT 50 mm			

**Appendix D** - The computerised flat-bed knitting machine; Shima Seiki SWG091, N2 15 gauge.



## Appendix E - Garment Prototypes and design development of SSBs.

The final prototype used in the research was the result of 4 distinct stages of development. The first prototype (1) was made with cut and sew method and featured a cut and sew electrode. Motion artefact was noted to be beyond tolerable limits, so the second prototype (2) was produced using a knitted method, and featuring a knitted electrode with a surrounding net structure to limit the skin/electrode movement. In addition to this, a net structure (indicated in yellow) was added between the lower and upper portion of the bra to further reduce movement around the electrode area.

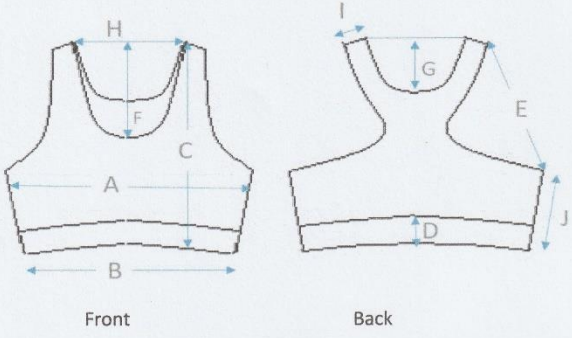
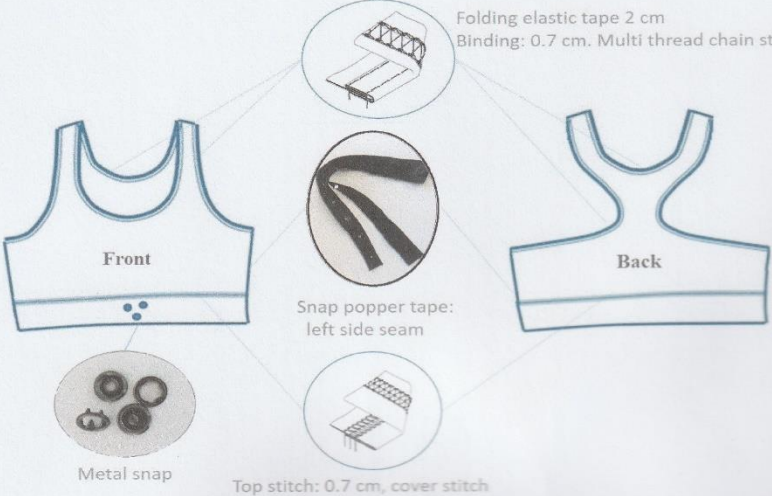
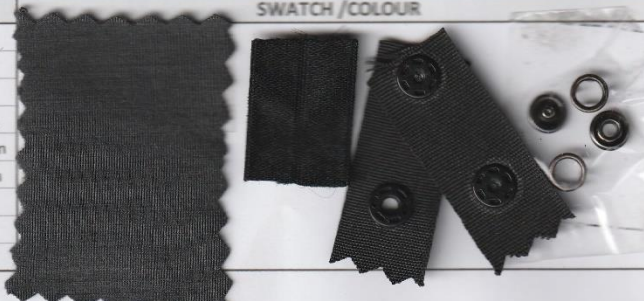
A further development was then made in the design of the bra itself with the adoption of a Y shape racerback (3) to replace the U shape racerback. This further improved the stability of the garment in relation to the body, so reducing the motion artefact experienced by the electrode.

The final development (4) was to change the position of the fastener (circled in yellow in the figure below) in the bra from the rear side. This was to facilitate ease of putting on and taking off the garment.



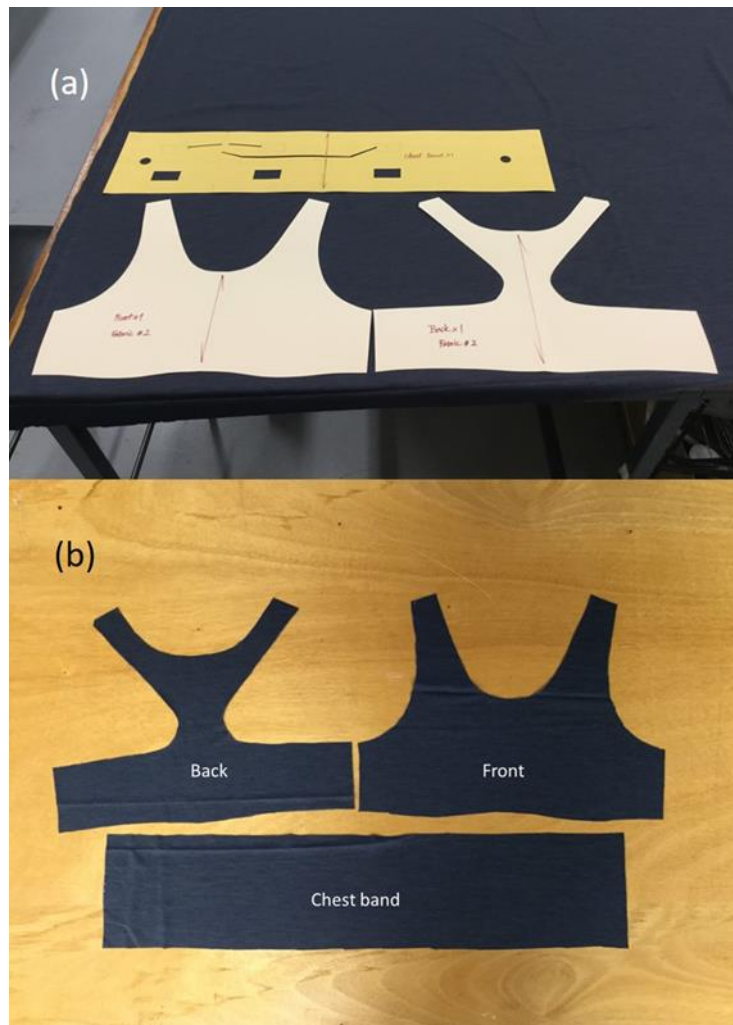
## Appendix F - The description and information of the SSBs.

### Appendix F.1- The specification sheet of the Cut & Sew method bra.

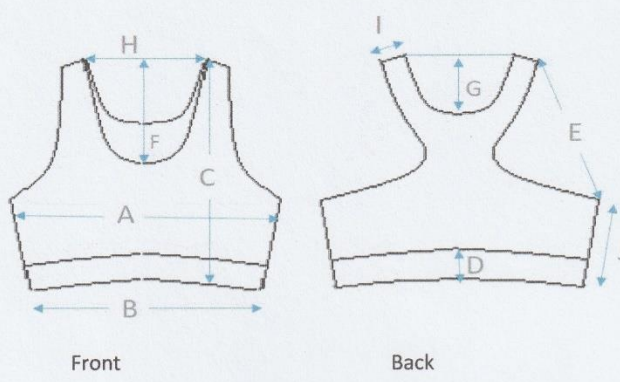

SPECIFICATION SHEET				
Style: Cut & Sew bra		Descriptions : Sport bra	Fabric :	
Prototype No : 1		Category : lady	Consumption :	
Date : August 2017				
SIZE SPECIFICATION (UNIT :mm.)		GARMENT MEASUREMENT		
	SIZE	10		
A	Chest (2.5 cm below armhole)	330		
B	Bottom	300		
C	Body length (HPS)	280		
D	Chest band high	80		
E	Armhole (cruve)	170		
F	Front neck drop	130		
G	Back neck drop	50		
H	Neck width	150		
I	Shoulder width	40		
J	Side seem	130		
				
<b>DESIGN SKETCH</b>				
				
ACCESSORY		SWATCH /COLOUR		
1	Nylon/ Spandex single jersey 40/2			
2	Single jersey lining			
3	silver plated nylon conductive knitted fabric			
3	Metal snap Ø 7 mm			3 set
4	Elastic folder tape width 20mm			112 cm
5	Snap popper tape			15 cm
6	Silver plated nylon conductive thread 117/17 2-ply			
7	Sewing thread: Grey	5		

Appendix F.2- Pattern construction of the Cut & Sew method bra.

A compression bra design has been devised to construct the SSBs in this project. A garment pattern can be formed by a two-dimensional block (a) and cutting process. The pattern cutting consists of front, back and chest bands(b).

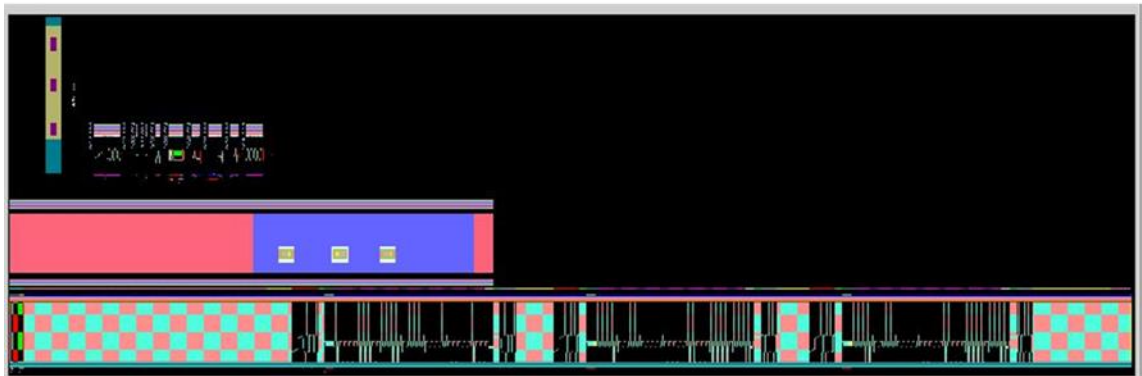
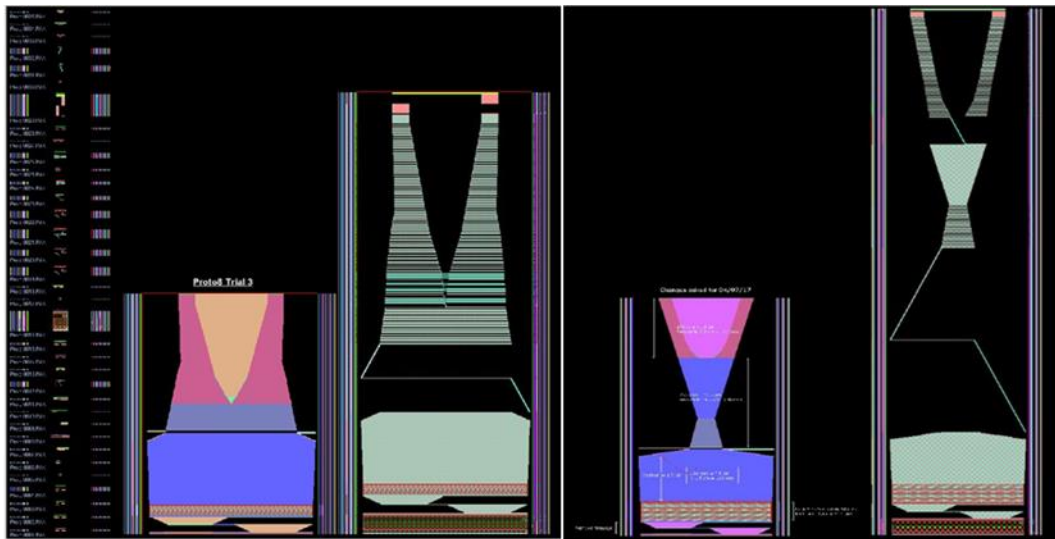


Appendix F.3 - The specification sheet of the Knitted method bra.

SPECIFICATION SHEET				
Style: Knitted Garment bra		Descriptions : Sport bra	Fabric :	
Prototype No : 1		Category : lady	Consumption :	
Date : August 2017				
SIZE SPECIFICATION (UNIT: mm.)		GARMENT MEASUREMENT		
SIZE		10		
A	Chest (2.5 cm below armhole)	330		
B	Bottom	300		
C	Body length (HPS)	280		
D	Chest band high	80		
E	Armhole (cruve)	170		
F	Front neck drop	130		
G	Back neck drop	50		
H	Neck width	150		
I	Shoulder width	40		
J	Side seem	130		
				
<b>DESIGN SKETCH</b>				
				
ACCESSORY		SWATCH /COLOUR		
1	Nylon 66			
2	Metal snap Ø 7 mm			3 set
3	Elastic folder tape width 20mm			112 cm
3	Snap popper tape			15 cm
4	Silver plated nylon conductive thread 234/34 4-ply			
5	Sewing thread: Blue	5		

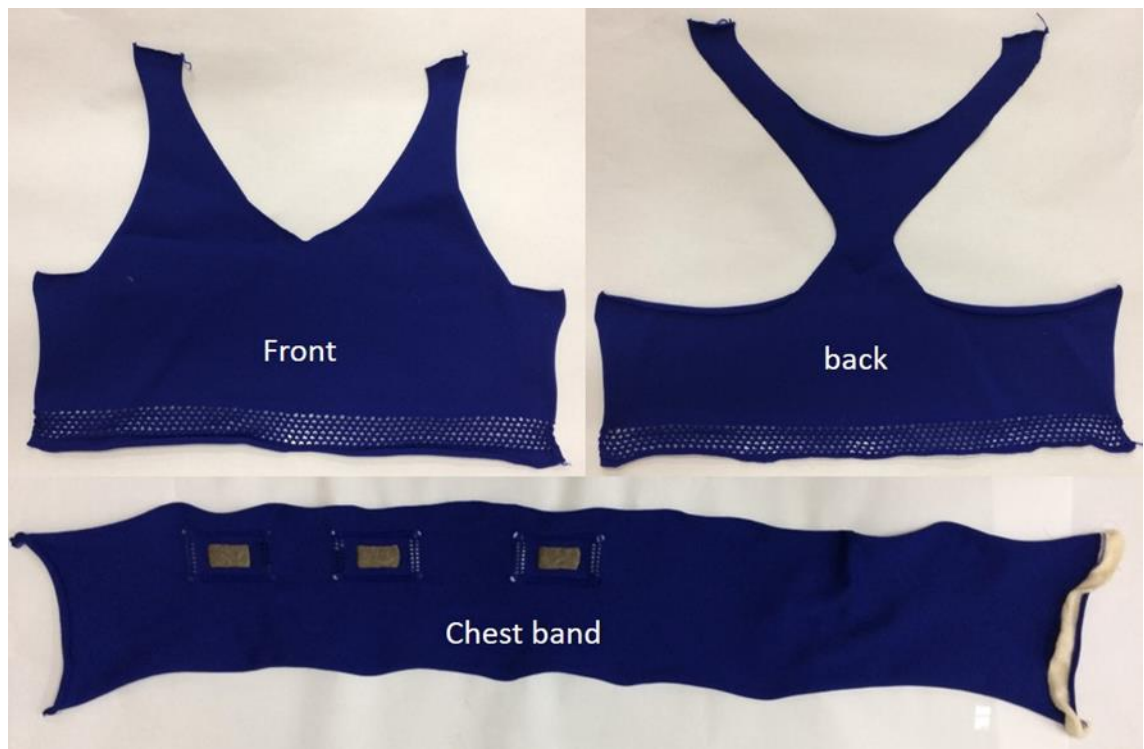
#### Appendix F.4 - Pattern construction of the Knitted Method.

The SSB Knitted Method is formed by using a Computerised flat-bed knitting machine; Shima Seiki SWG091 N2 15 gauge. The knitted electrode section is made using the Intarsia technique which allows the conductive yarn to be inserted into a specific area within the garment (Chest band). The design diagram of KM-SSB is from the software of Shima Seiki's, SWG091 N2 15 gauge knitting machine (Appendix C).



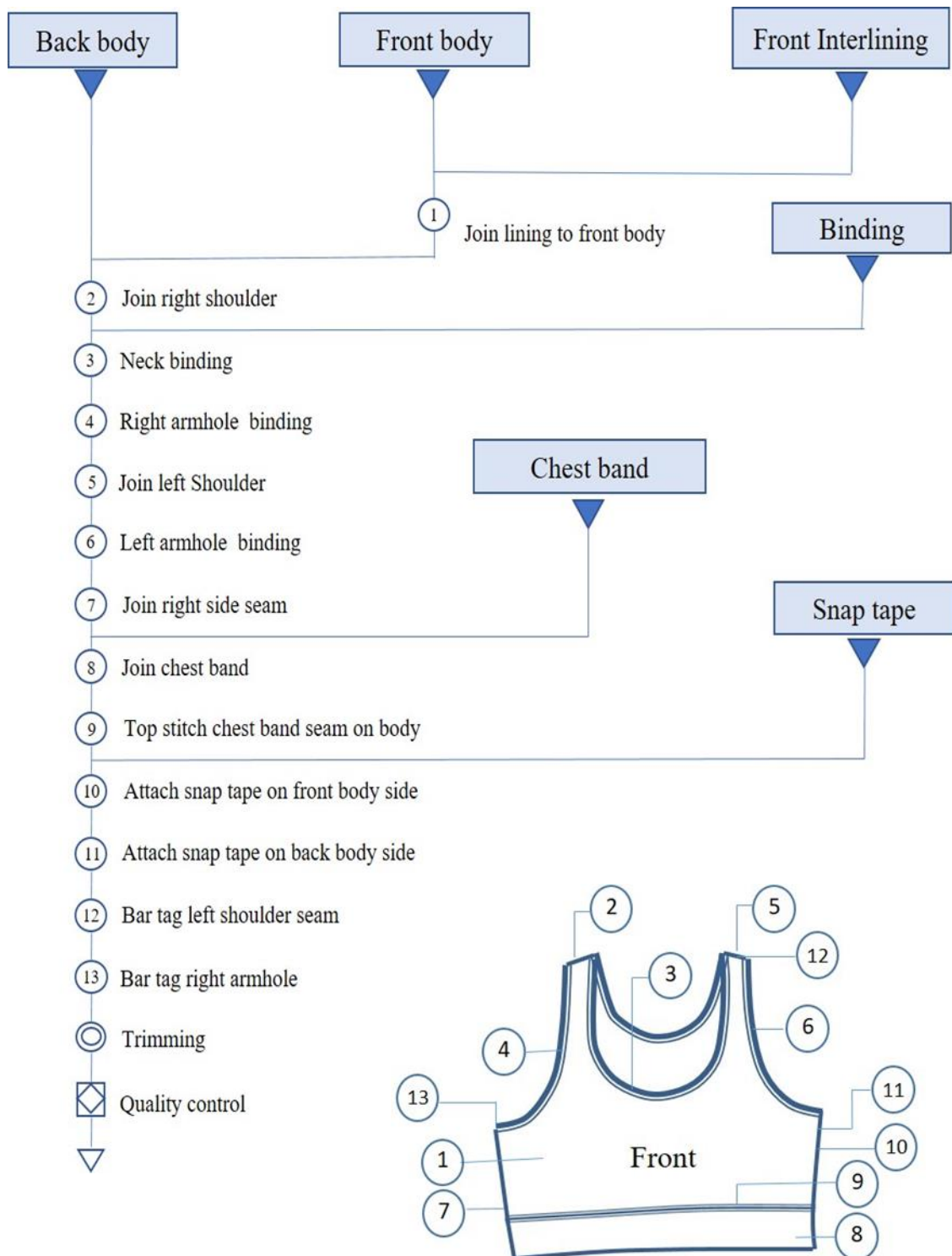


The final knitted pattern in back, front and chest band.

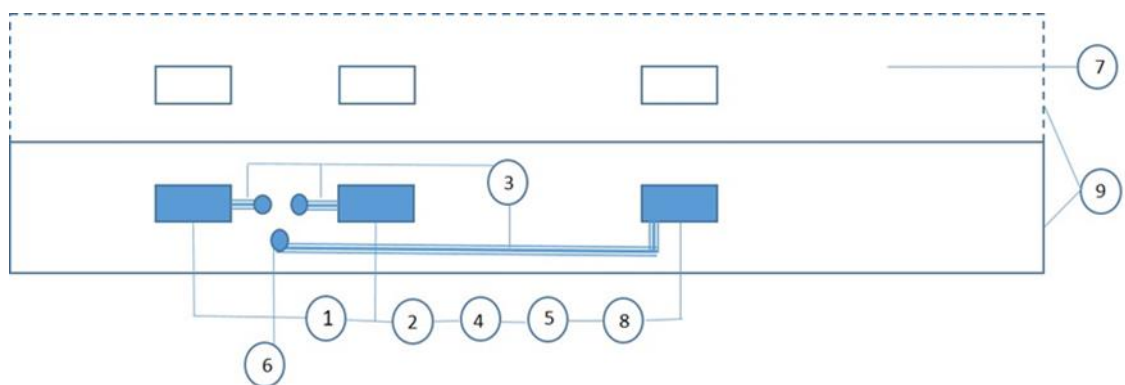
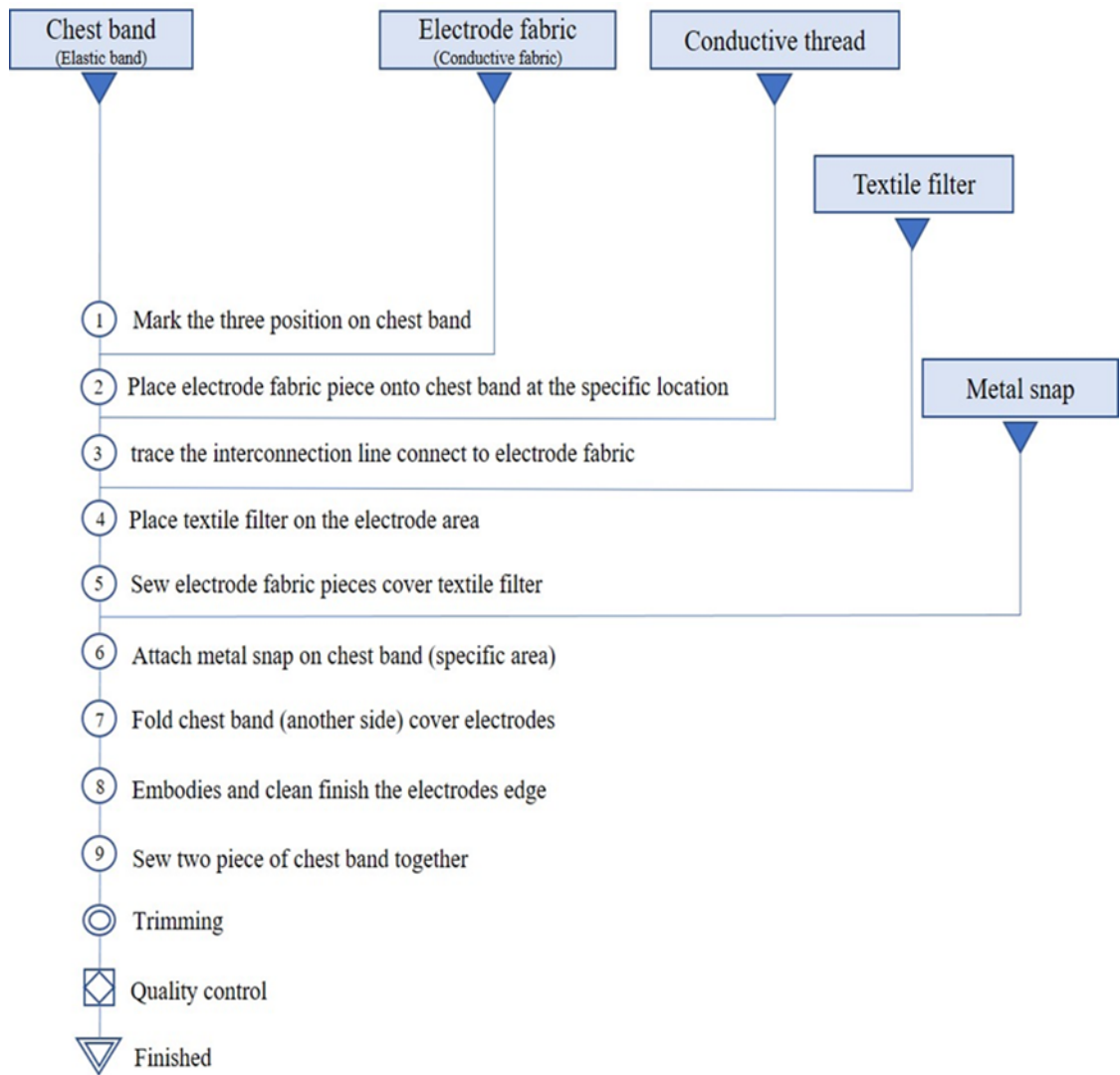


## Appendix G - Garment production of SSBs.

### Appendix G.1- Garment Production; Top body part.



Appendix G.2 - Garment Production; lower body part, chest band of fabric electrodes.



Appendix G.3- Garment Production; lower body part, chest band of respiration bra.

